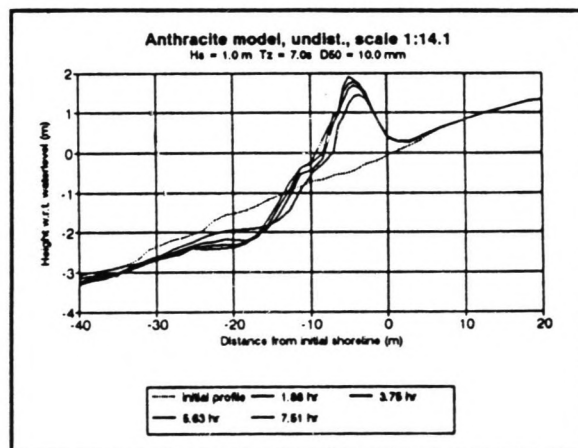
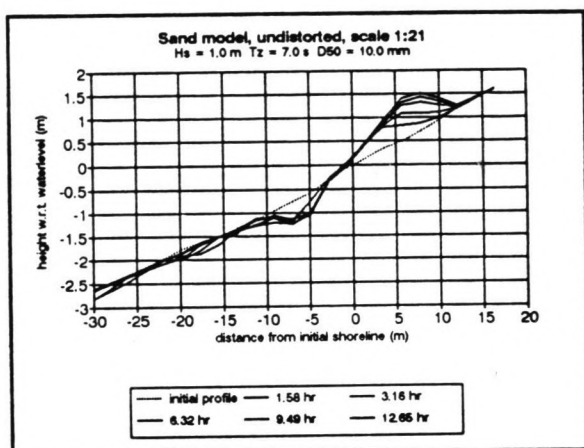


EVOLUTION OF BEACH PROFILES UNDER RANDOM WAVES

oktober 1993

C. M. Janssen



RIVER, ESTUARY AND COASTAL ENGINEERING

**EVOLUTION OF BEACH
PROFILES UNDER
RANDOM WAVES**

by

C. M. JANSSEN

Dissertation submitted for the degree of "Civiel Ingenieur" of the Delft University of Technology and for the International Diploma of Imperial College of Science, Technology and Medicine, where the project was performed as part of the MSc-course, attended through the ERASMUS exchange program.

Department of Civil Engineering

Imperial College of Science, Technology and Medicine

1993

SYNOPSIS

Cross-shore sediment transport is an important phenomenon in coastal engineering, which mainly accounts for the short-term changes in the coastline. To study on- and offshore transport the evolution of the beach profile is considered.

For investigation of the beach profile small-scale physical models are often used. A problem in using a physical model is the introduction of scale-effects resulting from the impossibility of scaling all parameters correctly. Many researchers therefore derived scaling laws which determine the relationship between the model scale and the scale of the other parameters. A literature review revealed that many of them give contradictory results.

A different problem in using physical models is that for small-scale models the required model grain diameter of the sediment becomes too small, which would introduce cohesive forces in the sediment. For this reason light-weight material is sometimes used as the beach material. However there are still doubts about the validity of the use of light-weight material.

In order to study the behaviour of light-weight material in physical models, experiments were performed using random waves in the large wave tank of the Hydraulics Laboratory. Both sand and anthracite were used as the model materials.

Although all the resulting beach profiles showed accretive conditions, characterized by the development of a berm at the beach and the deepening of a step in the breaker zone, differences between the profiles in the anthracite and sand models were very large.

Beach profiles were analyzed using different methods. The eigenfunction analysis turned out to be helpful only for the analysis of field data. In the other methods the relation between the characteristic features of the profile and the parameter H/wT was investigated. This parameter is assumed to be a criterion to differentiate between on- and offshore transport and represents the wave conditions and sediment characteristics for the evolution of the beach profile. In general the relation was rather poor and there is clearly a need for further theoretical and model studies.

ACKNOWLEDGEMENTS

I would like to thank Ir. K. Bezuijen and Prof. Ir. K. d'Angremond of the Delft University of Technology for their support and their help which made it possible to study for a year at Imperial College of Science and technology in London.

I am very grateful to Drs. G. de Graaf for her help in arranging an ERASMUS scholarship at Imperial College and I would like to thank ERASMUS for the grant, which allowed me to study at Imperial College for a year.

I also would like to thank the technicians of the Hydraulics Laboratory of the Civil Engineering Department of Imperial College, Mr. W. Bobinski, Mr. J. Audsley and Mr. J. Mires for all their help during the experiments.

I would like to thank particularly Prof. P. Holmes for his support and stimulating enthusiasm during this project.

CONTENTS

Synopsis.

Acknowledgements.

Contents.

List of symbols.

1 Introduction.

2 Literature survey.

2.1 Equilibrium beach profiles.

2.1.1 The type of profile.

2.1.1.1 Criteria based on wave height, wave length and grain diameter.

2.1.1.2 Criteria based on the fall velocity of the sediment.

2.1.1.3 The influence of the initial slope.

2.1.1.4 Criterion based on balancing powers.

2.1.1.5 The influence of random waves.

2.1.2 The shape of profile.

2.1.2.1 The " $h = Ay^m$ " model.

2.1.2.2 The beach slope as a representation of the beach profile.

2.1.3 Summary.

2.2 Scaling laws.

2.2.1 Empirical model laws.

2.2.2 Analytical model laws.

2.2.2.1 Linear scaling.

2.2.2.2 Preserving the dimensionless fall velocity parameter.

2.2.2.3 Different analytical scaling laws.

2.2.3 Scaling laws derived by preserving the criterion between erosive and accretive profiles.

2.2.4 Summary.

3 Experiments.

3.1 Comparison of the scaling laws.

3.1.1 The fall velocity as a representation of the sediment.

3.1.2 Comparison of model sediment diameters for different scaling laws.

3.2 Choice of the experiments.

3.2.1 Undistorted model experiments.

3.2.1.1 Wave conditions.

3.2.1.2 The dimensionless fall velocity parameter.

3.2.2 Distorted model experiments.

3.2.2.1 Distorted models according to Vellinga's law.

3.2.2.2 The dimensionless fall velocity parameter.

3.3 Description of the experiments.

3.3.1 Waves.

3.3.1.1 Wave generation.

3.3.1.2 Wave data collection and analysis.

3.3.2 Beach profiles.

3.3.2.1 Length of the beach and amount of sediment.

3.3.2.2 Duration of experiments.

3.3.2.3 Beach profile measurements.

4 Results.

4.1 General features.

4.1.1 The berm.

4.1.2 The step.

4.1.3 Shoreline advancement.

4.1.4 Differences between sand and anthracite models.

4.2 Analysis of beach profiles.

4.2.1 Method of empirical eigenfunctions.

4.2.1.1 Statistical method.

4.2.1.2 Analysis of data.

4.2.1.3 Discussion.

4.2.2 The beach slope as a representation of the profile.

4.2.2.1 First evaluation of the beach slopes.

4.2.2.2 Errors in measurement and calculation of H/wT and the mean beach slope.

4.2.2.3 Revised evaluation of the mean beach slopes.

4.2.2.4 Summary.

4.2.3 Analysis in terms of three characteristic points of the beach profile.

4.2.4 Summary.

5 Conclusions and recommendations.

References.

Appendix A	Sieve analysis.
Appendix B	Wave data.
Appendix C	Beach profile graphs.
Appendix D	Data on the berm and the step of the beach profile.
Appendix E	Data on the position of the shoreline.
Appendix F	Data on the mean beach slope.
Appendix G	Computer program for eigenfunction analysis and results.
Appendix H	Data on measurement errors in wave height and period.
Appendix I	Porosity of the sediment.

LIST OF SYMBOLS

A	$[m^{(1-m)}]$	Scale parameter depending on sediment characteristics.
A	$[m^2]$	Spatial correlation matrix.
a	$[-]$	Empirical parameter.
a_{ij}	$[m^2]$	Element of spatial correlation matrix.
B	$[m]$	Berm height.
B'	$[-]$	Dimensionless berm height.
B	$[m^2]$	Temporal correlation matrix.
b	$[-]$	Empirical parameter.
b_{ij}	$[m^2]$	Element of temporal correlation matrix.
C	$[-]$	Criterion number for the type of beach profile.
C_D	$[-]$	Drag coefficient.
c	$[m/s]$	Wave celerity.
c_g	$[m/s]$	Group celerity of the waves.
D	$[m]$	Grain diameter of the sediment.
$D1$	$[m]$	Largest diameter of a particle.
$D2$	$[m]$	Intermediate diameter of a particle.
$D3$	$[m]$	Smallest diameter of a particle.
D_{10}	$[m]$	10% undersize of the sediment diameter.
D_{50}	$[m]$	Mean diameter of the sediment.
D_{90}	$[m]$	90% undersize of the sediment diameter.
d	$[m]$	Water depth.
E	$[N/s]$	Energy flux of the waves.
e_n	$[-]$	Eigenvector or eigenfunction.
e_{1x}	$[-]$	Eigenvector corresponding to the largest eigenvalue.
f	$[Hz]$	Frequency of the waves.
g	$[m/s^2]$	Gravity acceleration.
H	$[m]$	Wave height.
H_0	$[m]$	Deep water wave height.
H_b	$[m]$	Breaker height.

H_s	[m]	Significant wave height.
h	[m]	Depth of the beach profile.
h_*	[m]	Depth of seaward limit of active motion.
h_*'	[m]	Dimensionless depth of seaward limit of active motion.
J	[-]	Percolation slope.
k	[-]	Parameter representing the permeability.
L	[m]	Wave length.
L_0	[m]	Deep water wave length.
l	[m]	Typical horizontal length.
m	[-]	Dimensionless exponent.
m_i	[-]	Initial slope.
m_e	[-]	Equilibrium slope.
n_i	[-]	Scale of parameter i (ratio of prototype to model value).
n_t	[-]	Number of beach profiles recorded.
n_x	[-]	Number of measurement points along the beach profile.
q	[m ² /s]	Volumetric sediment transport rate in per unit width.
Re	[-]	Reynolds number.
S	[m]	Height to which a particle is brought into suspension.
S	[m ² /s]	Spectral density.
T	[s]	Wave period.
T_z	[s]	Zero-crossing period.
t	[s]	Time.
t	[s]	Fall time of a sediment particle.
u	[m/s]	Horizontal velocity.
u_{max}	[m/s]	Maximum orbital velocity.
u_*	[m/s]	Threshold velocity of sediment motion.
v	[m/s]	Vertical velocity.
W_*	[m]	Seaward limit of active motion.
W_*'	[-]	Dimensionless limit of active motion.
w	[m/s]	Fall velocity of the sediment.
x	[m]	Distance from the shoreline.
y	[m]	Distance from the shoreline.

α	[-]	Amplitude constant in the Jonswap spectrum.
β	[-]	Proportionality parameter for height of particle suspension.
$\tan\beta$	[-]	Beach slope.
γ	[-]	Peak enhancement factor in the Jonswap spectrum.
γ'	[-]	Specific gravity.
Δ	[-]	Model distortion (ratio of horizontal to vertical scale).
Δy	[-]	Shoreline advancement (recession).
$\Delta y'$	[-]	Dimensionless shoreline advancement (recession).
δ_l	[-]	Scale factor.
θ_c	[-]	Critical Shields-parameter.
λ	[-]	Horizontal scale.
λ_n	[-]	Eigenvalue of a matrix.
λ_l	[-]	Largest eigenvalue of a matrix.
μ	[-]	Vertical scale.
ν	$[m^2/s]$	Kinematic viscosity.
ξ	[-]	Surf similarity parameter.
Π_{Q_s}	[-]	Dimensionless sediment transport rate.
π	[-]	Mathematical constant (3.141592654).
ρ	$[kg/m^3]$	Density of water.
ρ_s	$[kg/m^3]$	Density of the sediment.
τ_c	$[N/m^2]$	Critical bed shear stress.
ψ	$[s/m]$	Scale parameter.
ω	$[rad/s]$	Angular frequency of the waves.

Introduction.

Sediment transport in the coastal zone is of great interest in engineering practice. In the design of coastal structures it is important to know how much material is moved and in what direction. The same can be said for the management of an eroding beach.

Sediment transport is usually divided into two components: Alongshore transport and on-offshore transport. The former is accepted to account for the long-term changes of the coastline, while on-offshore transport is mainly influenced by the short-term events, although the two components obviously interact. These short-term events include erosion of the beach and the foreshore in storms with high and steep waves and the building up afterwards during periods of fairer weather and corresponding less steep waves.

The oscillatory motion due to the waves is the main factor in generating sediment transport. Relationships between wave conditions and the resulting sediment transport however are very difficult to establish. For the longshore component some theoretical and empirical formulae have been derived, although the magnitude of the sediment transport they predict may vary considerably.

The behaviour of on-offshore transport is even less well understood. This is a result of the large number of nearshore hydrodynamic processes involved, like wave breaking, mass transport, undertow, wave set-up and set-down and up- and downrush.

Formulae to predict the magnitude of on-offshore transport therefore do not exist. Research has been rather concentrated on the description of the beach profile which develops when subjected to certain wave conditions. Especially the equilibrium beach profile is an important characteristic. This is the profile which dissipates or reflects all the wave energy reaching it in such a way that no net sediment transport occurs anywhere along the profile.

In nature the equilibrium profile may never be achieved due to ever changing wave conditions and water level. Still, the investigation of this profile is important as it can give an indication of the amount of sand needed in artificial beach nourishment or of the performance of coastal defence structures.

To study the on-offshore transport and enhance the knowledge about the resulting beach profile, often physical models are used.

Data collection in a model is much easier and less expensive than in field studies. Also interpretation of field data can be more difficult due to too many variables in nature. In a physical model there is no need for simplifying assumptions or omitting any unknowns, as usually is seen in analytical or numerical models in order to solve the equations.

A major drawback of a physical model however is the introduction of scale-effects. These scale-effects are due to the smaller size of the model and the resulting changes in relative importance of various forces. The scale-effects must be well understood in order to make a representative model of the complex reality.

The most difficult parameter to scale down in a physical model, is the grain diameter of the sediment. This is a result of the cohesive effects of small sediment particles. To avoid the use of very small sediment particles, light-weight material is sometimes used in the model. There remains however a lot of uncertainty about the validity of using light-weight material in coastal movable-bed models.

In this project experiments were performed to study the evolution of beach profiles under random waves. As a model material both sand and anthracite were used in order to investigate the behaviour of light-weight material.

First a literature survey was performed on the different descriptions of equilibrium beach profiles, which were derived from field or laboratory studies. Also a review is presented about the different scaling laws, derived to establish the relation between the model scale and the scale of the parameters involved in sediment transport (chapter 2).

In chapter 3 the experiments performed in this project are described. The results of these experiments and the analysis of the data from the recorded beach profiles are discussed in chapter 4.

Chapter 5 presents the conclusions and recommendations, which arise from this project.

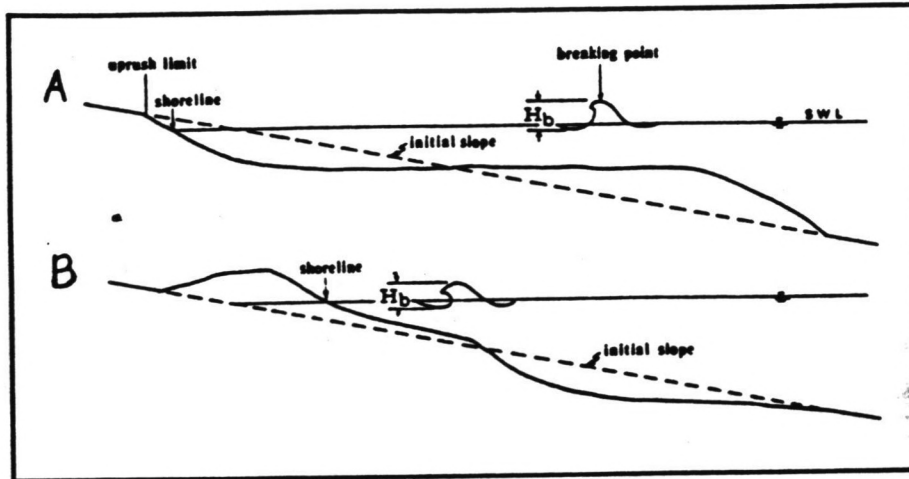


Figure 2.1 Definition sketch of bar (A) and step (B) profiles.

2 Literature survey.

2.1 Equilibrium beach profiles.

Beach profile evolution is directly related to the on-offshore sediment transport. Increase of the sediment transport causes erosion, while accretion takes place if the sediment transport becomes smaller. The magnitude of the sediment transport depends on the wave conditions.

A lot of research has been done to derive a relation between wave conditions and resulting beach profile. Most of this work has been concentrated on the description of the *type* of profile that developed. In addition some researchers have described the *shape* of the beach profile.

To make a distinction between erosive and accretive profiles, different criteria have been derived, containing wave and/or sediment characteristics. In the case of describing the shape of the profile an equation is established, giving the depth as function of distance offshore and wave and/or sediment characteristics.

2.1.1 The type of profile.

The type of profile is usually described in terms of a criterion which divides the profiles into erosive and accretive ones. This criterion depends on different variables corresponding to the wave and sediment characteristics.

2.1.1.1 Criteria based on wave height, wave length and grain diameter.

In the early stage two different equilibrium profiles were recognized: The "bar" (erosive, storm or winter) profile and the "step" (accretive, swell or summer) profile. The bar profile develops during storms, when high-energy waves erode the beach and the foreshore. The sediment removed is deposited beyond the breaker zone as a longshore bar. The step profile develops during periods with low-energy waves. These waves bring the sediment up the beach and the longshore bar is eroded creating a step offshore (see figure 2.1). The criterion for the development of one of these types of profiles depends on the wave height, the wavelength and the grain diameter.

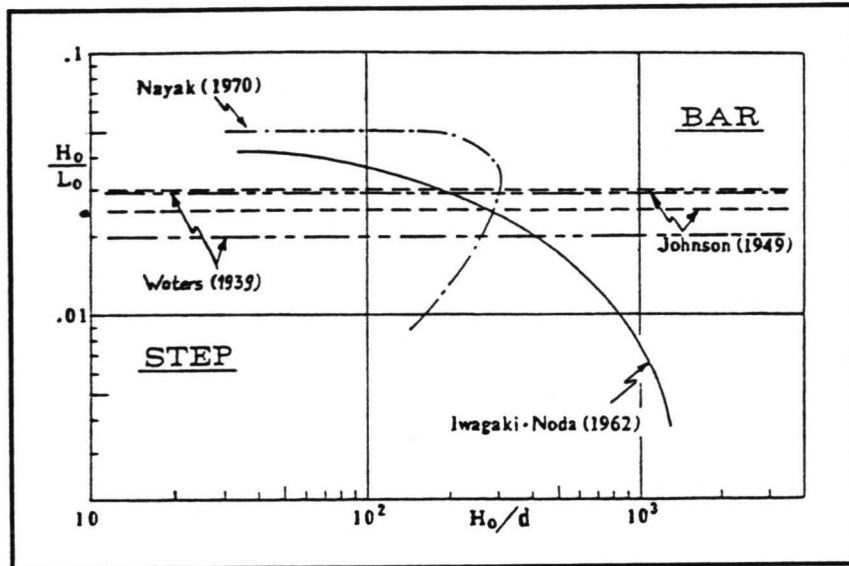


Figure 2.2 Criteria for bar or step profiles, according to different researchers.

Waters ('39) found a critical wave steepness, H_0/L_0 of 0.02 to 0.03. Smaller values of the wave steepness result in step profiles, while larger values than the critical one give bar profiles.

Johnson ('49) found that if the steepness is less than 0.025 a step profile will develop, while a bar profile is formed if H_0/L_0 is greater than 0.03.

Iwagaki & Noda ('62) included the grain size of the sediment into the criterion for profile type. They found that for:

and for	$H_0/D_{50} < 300$	the critical steepness is 0.025
	$H_0/D_{50} > 1000$	the critical steepness is 0.01.

Nayak ('70) included the specific gravity into the criterion for bar or step profiles. The four criteria, all derived from laboratory experiments are shown in figure 2.2 (modified from **Sunamura & Horikawa ('74)**).

2.1.1.2 Criteria based on the fall velocity of the sediment.

Dean ('73) found that the fall velocity is an important parameter in the criterion between erosive and accretive shores. The idea is that during the passage of a wave the sand grain is suspended to a height $S = \beta H$. If the fall time $t = S/w$ is smaller than half the wave period than the grain is transported onshore. Coarser grains therefore move onshore, while smaller sediment particles move seaward. The criterion found by Dean therefore becomes:

$$H/wT = C$$

If C is greater than 0.85 the sediment transport is offshore and if C is less than 0.85 the sediment transport is onshore.

The **Shore Protection Manual ('84)** recommends for the constant C a value of 1.0 rather than 0.85 for both laboratory and field data.

Kriebel, Dally & Dean ('86) evaluated Dean's criterion in a set of laboratory experiments and found an even higher value for C , of 2 to 2.5. They also raised doubts about the general validity for the recovery case.

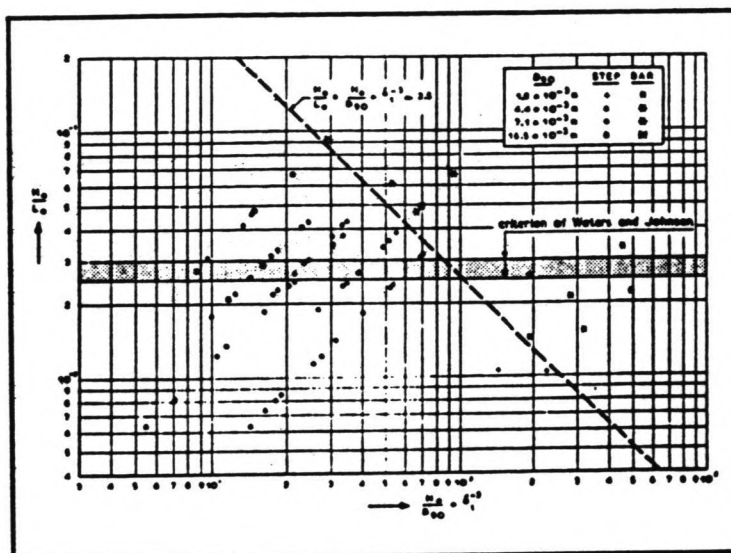


Figure 2.3 The criterion between bar and step profiles derived by Van Hijum ('74)

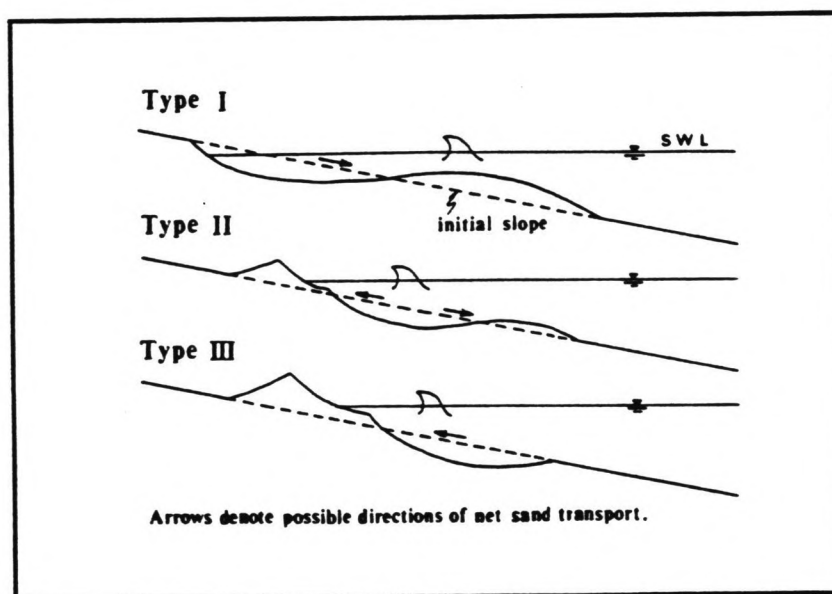


Figure 2.4 The beach profile types found by Sunamura & Horikawa ('74)

Allen ('85) evaluated the criterion of $H/wT = 1.0$. He showed that, for the 111 profiles considered, this criterion predicted 98% of the erosional beaches correctly, but only 45% of the accretive beaches. This agrees with the observations of Nairn ('90), who concluded that only 20 of the 30 tests he performed (numerically) were predicted correctly by Dean's criterion.

2.1.1.3 The influence of the initial slope.

Van Hijum ('74) investigated the equilibrium profiles of coarse material in small scale experiments. He only considered bed-load transport, because of the scale-effects (see later). Van Hijum identified two profiles: a step and a bar profile. The criterion for bar formation was found to be:

$$\frac{H_0^2}{L_0 * D_{90} * \delta_1^3} = 2.5$$

Where H_0 is the deep water wave height, L_0 is the deep water wave length and D is the sediment diameter. The subscript 90 means that 90% of the sediment (by weight) has a diameter smaller than D_{90} . δ_1 is a scale factor which is equal to 1 if D_{90} is larger than 6.0 mm and equal to $(D_{90}/0.006)^{1/2}$ if D_{90} is smaller than 6.0 mm. The criterion is shown in figure 2.3.

Van Hijum concluded from his measurements that the profile is independent on the initial slope.

Sunamura & Horikawa ('74) considered the initial slope of the model beach to be an important parameter for the development of equilibrium profiles. They found three different types of profiles (see figure 2.4):

- 1) Shoreline retrogression and sand accumulation offshore.
- 2) Shoreline advancement and piling up of sand offshore.
- 3) Shoreline progression but no sand deposition offshore.

The criterion for the development of the profiles depends on the wave steepness (H_0/L_0), the initial slope ($\tan \beta$) and the ratio of the grain size over the wavelength (D/L_0):

$$\frac{H_0/L_0}{\tan \beta^{-0.27} * (D/L_0)^{0.67}} = C$$

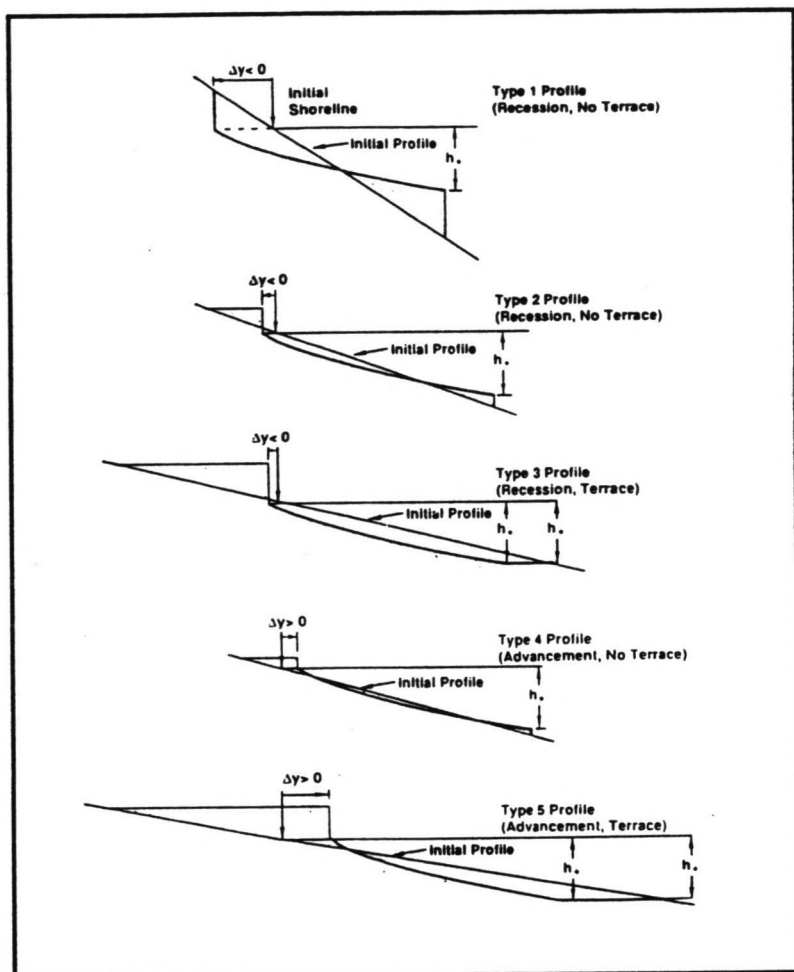


Figure 2.5 The beach profile types, found by Dean ('91).

If the constant, C is greater than 4 the profile is erosional and if C is less than 8 the profile is accretional.

Kriebel, Dally and Dean ('86) also found that the equilibrium profile depends on the initial profile. They concluded that for very steep profiles an equilibrium profile is not achieved unless the tests are run for a very long time.

Gourlay ('80) however, found that only very flat initial slopes affect the equilibrium profile. The reason for this is that some of the energy of the steep waves will be dissipated outside the surf zone, resulting in a different equilibrium profile than for steeper initial slopes.

Dean ('91) published a paper in which he distinguished five profile types (see figure 2.5). Development of the equilibrium profile depends on the wave and sediment characteristics and the initial profile of the model beach. For type 1 the initial slope is much steeper than the equilibrium slope, causing only seaward sediment transport. While for type 5 the initial slope is much flatter, resulting in only landward sediment transport. Depending on the dimensionless depth at the seaward limit of motion ($h_*' = h_*/(m_i * W_*)$) and the dimensionless berm height ($B' = B/(m_i * W_*)$) the type of profile which is formed can be found from figure 2.6. Here h_* is the breaking depth, which is equal to 1.28 times the breaker height, H_b , m_i is the initial slope, W_* is the seaward limit of active motion and B is the berm height. Figure 2.6 also gives values for the non-dimensional shoreline advancement, $\Delta y'$, which is equal to $\Delta y/W_*$, where Δy is the advancement of the shoreline.

Suh & Dalrymple ('88) derived an expression for the shoreline advancement. This expression reads:

$$\Delta y' = \frac{1}{2} \left(\frac{6}{5} h_*' - 1 \right)$$

Laboratory experiments showed good results for this relationship. However it was difficult to predict h_*/W_* , which can be interpreted as the equilibrium slope, m_e . It was assumed that the equilibrium slope is dependent of the dimensionless fall velocity parameter (H/wT) and therefore the shoreline advancement was expressed as a function of this parameter. The result is:

$$\frac{\Delta y'}{h_*'} = a + b m_i \left(\frac{H}{wT} \right)^{\frac{1}{2}}$$

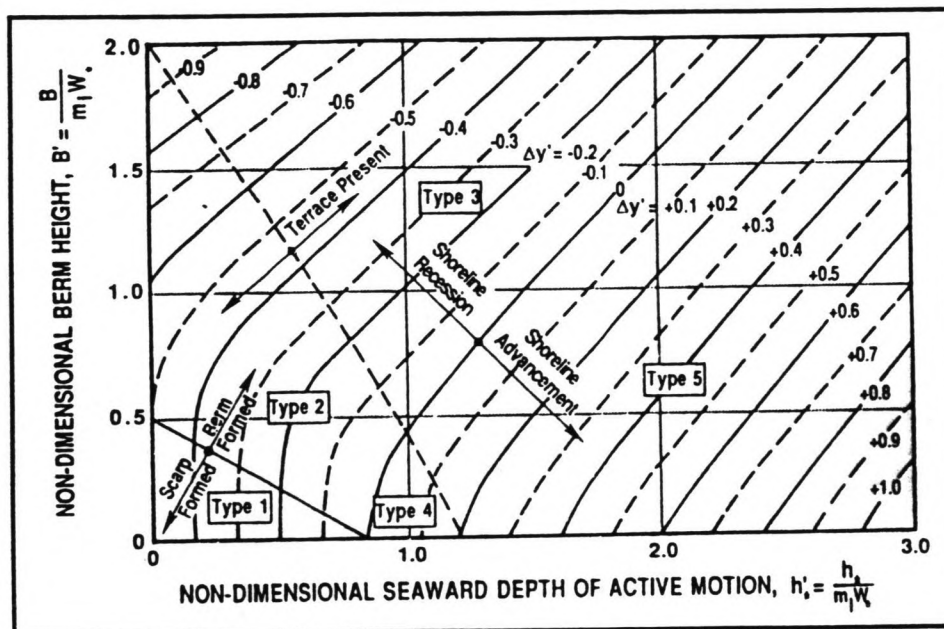


Figure 2.6 Distinction between the different profile types from Dean ('91), depending on the dimensionless berm height and the dimensionless depth at the seaward limit of motion.

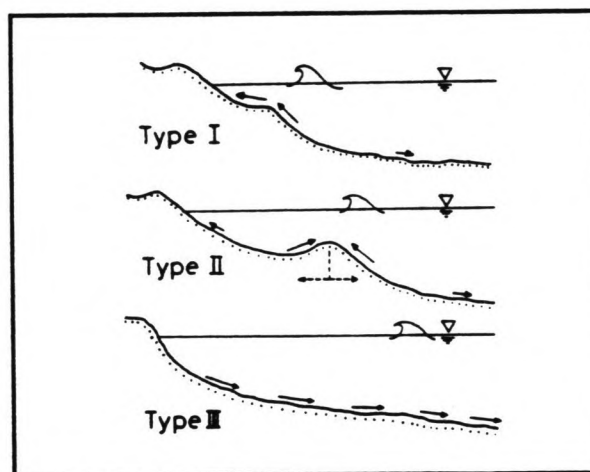


Figure 2.7 Classification of beach profiles, found by Hattori & Kawamata ('80). The arrows denote the direction of net sediment transport.

The values of the parameters a and b are derived empirically:

$$a = 1.02$$

$$b = -20.78$$

2.1.1.4 Criterion based on balancing powers.

Hattori & Kawamata ('80) based their criterion between accretive and erosive beaches on the following physical consideration: The net sediment transport attains a state of equilibrium if the power expended through the gravity force in suspending sand grains is balanced by the power due to the uplifting force, arising from the turbulence generated by breaking waves. From the laboratory experiments they found three different types of profile. An accretive, an erosional and an intermediate profile, characterised by a bar at the breaking position and sediment transport in both on- and offshore direction (see figure 2.7). The criterion to distinguish these profiles is:

$$\frac{H_0}{w(d_{50}) * T} \tan\beta - 0.5$$

The parameter T represents the wave period and $w(d_{50})$ is the fall velocity of a particle with a diameter equal to the mean diameter of the sediment. Although there is a mixed region for values of C between 0.3 and 0.7, in general the type of profile is accretive for $C < 0.5$ and erosive for $C > 0.5$.

2.1.1.5 The influence of random waves.

Most of the research on equilibrium profiles has been done using regular waves in the model. To be able to use these results in reality it is important to know how the randomness of the waves influences the equilibrium profile.

Nishi, Sato & Nakamura ('90) used two different concepts to investigate the difference between laboratory beach profiles due to regular and due to random waves.

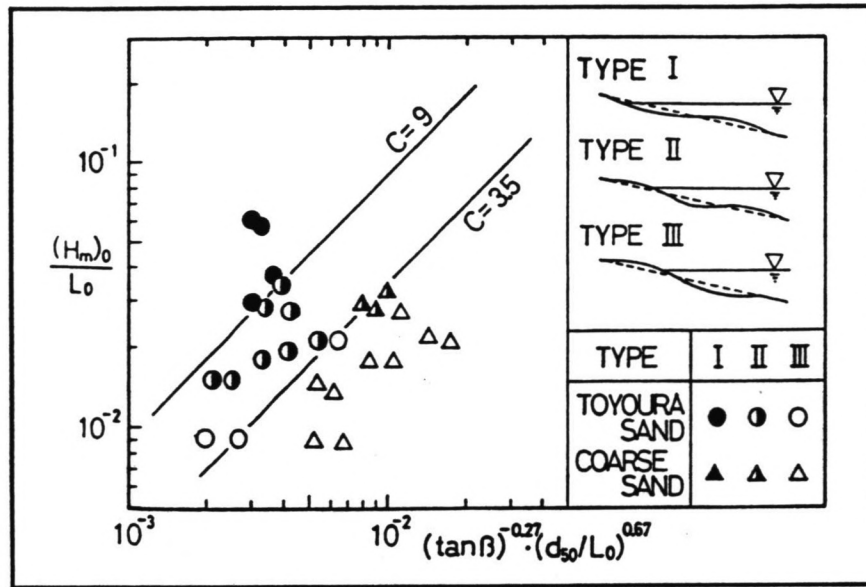


Figure 2.8 The criterion between accretive and erosive beaches for random waves, derived by Mimura et al ('88).

The first concept is that of same energy flux, which means the significant wave height is chosen such that the energy flux for the random waves is equal to the energy flux from the regular waves. The energy flux is equal to:

$$E = \frac{1}{8} \rho g H^2 c_g^2$$

Where E is the energy flux, ρ is the density of water, g is the gravity acceleration, H is the wave height and c_g is the group velocity of the waves. Nishi *et al* found that this concept does not result in an equivalent topography or equivalent beach profiles.

The second concept is that of same representative wave heights. They investigated the topography assuming the regular wave height to be equal to the significant wave height, then to the mean wave height and then to the average wave height of the highest 10% of the waves ($H_{1/10}$). None of these choices gave equivalent topographies for regular and random waves.

In general the random waves gave smoother profiles. The onshore beach profile changes were quite large in the case of random waves due to the presence of many large swash waves, although the shoreline changes were smaller. The position of a longshore bar was farther offshore and the berm height was higher. The reason for this is the higher probability of large wave run-up in random waves.

Mimura, Otsuka & Watanabe ('86) also considered beach transformation due to random waves. They investigated different important processes and tried to find a representative wave height in terms of the significant or the mean wave height. The experiments were performed at model scale.

The first process they considered is the macroscopic beach profile change. As a criterion for erosive or accretive beaches they used the criterion of Sunamura & Horikawa ('74) (see section 2.1.1.3). The best similarity with regular waves was found if the mean wave height was used as the representative wave height, although the progress of beach transformation was considerably slower for random waves. They found that if the criterion number, C , is larger than 3.5 the profile is erosional and if C is smaller than 9 the profile is accretional (see figure 2.8).

For the threshold of sand movement the significant wave height gave a better agreement than the mean wave height. This is because the smaller wave heights do not cause any motion at the bottom. As a result the sand grains are not transported by the smaller waves.

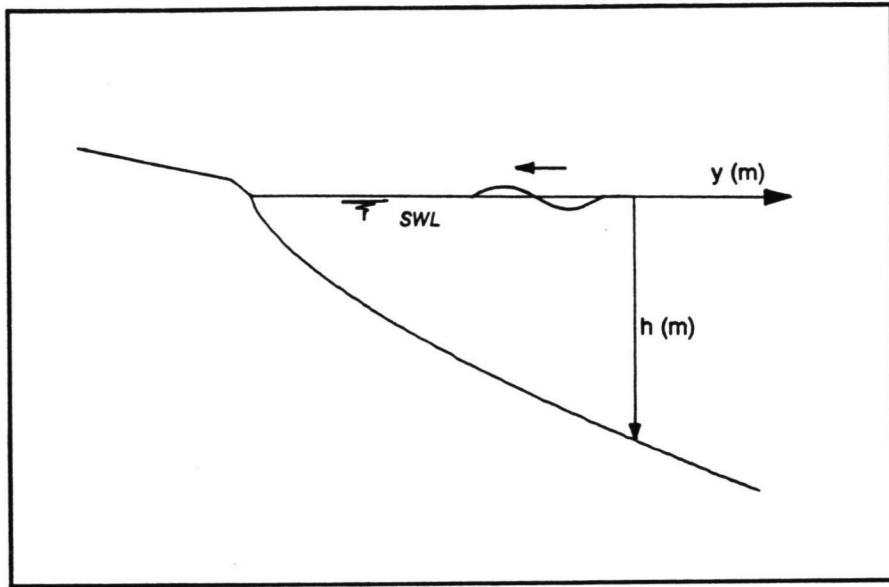


Figure 2.9 Definition sketch of the " $h = Ay^m$ " profile.

The characteristics of ripples were supposed to play an important role in the sediment transport. The relationship between ripple length and orbital diameter showed the best agreement between random and regular waves if the significant wave height was chosen as the representative wave height.

Finally, for the cross-shore sediment transport rate the mean and the significant wave heights gave similar results and no representative wave height could be specified.

2.1.2 The shape of profile.

In addition to the studies which describe the type of profile, some researchers have investigated the shape of the profile.

2.1.2.1 The " $h = Ay^m$ " model.

Bruun ('54) was the first who related the depth of the profile to the distance offshore. He analyzed beach profiles along the Danish North Sea Coast and Mission Bay, California. From these data he found that the equilibrium profile can be described by:

$$h = Ay^{\frac{2}{3}}$$

where h is the depth below Mean Water Level, y the distance from the shoreline and A a parameter depending on the sediment characteristics. A definition sketch of this profile is shown in figure 2.9.

Dean ('77) based the relation for the equilibrium profile on the physical consideration of uniform energy dissipation per unit volume of water and found the same expression as Bruun. Analysis of 502 beach profiles in the field resulted in the best fit for m of 0.67. Although the theoretical assumption only holds for the dissipative surf zone, Dean also includes a description of the nearshore zones.

The parameter A has been evaluated by **Moore ('82)**, who found that A is proportional to D^* . Using the fall velocity as a representation of the sediment size **Dean ('91)** showed that this results in:

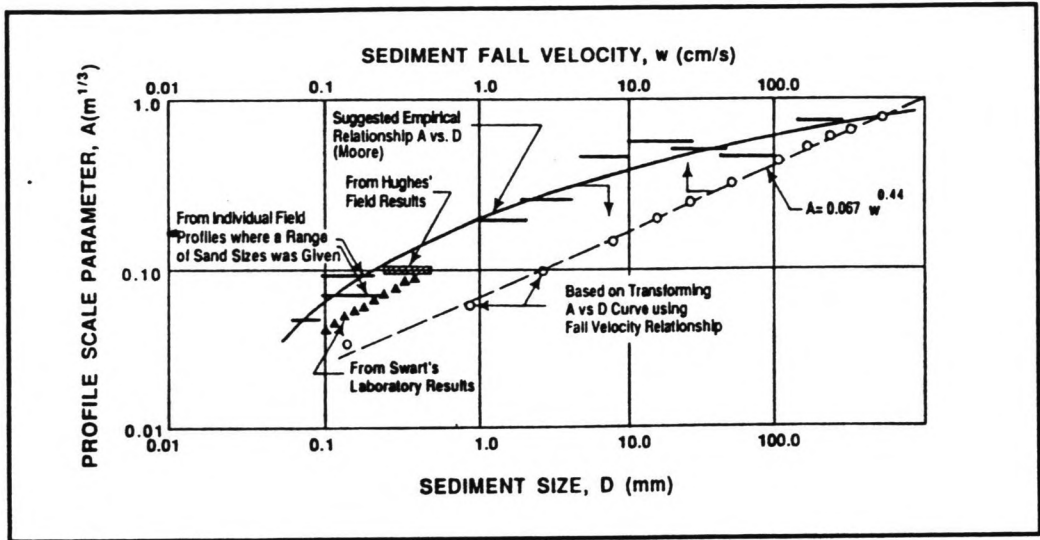


Figure 2.10 Relationship between the parameter A and the grain diameter, respectively fall velocity, according to Dean ('91).

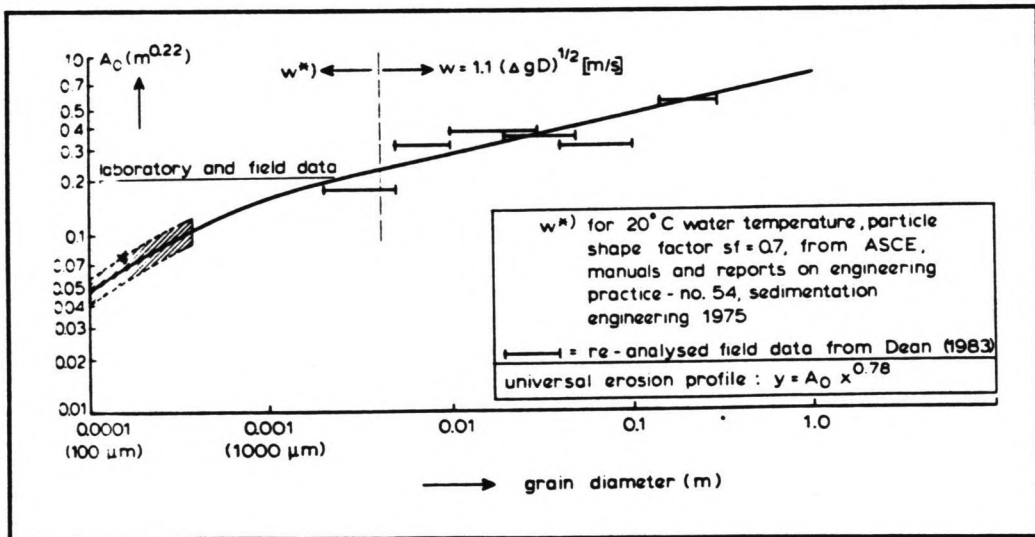


Figure 2.11 Relationship between the parameter A and the grain diameter, according to Vellinga ('82).

$$A = 0.067 w^{0.44}$$

where w is the fall velocity of the sediment. This relation is shown in figure 2.10.

Based on an extensive laboratory study on dune erosion which included full scale experiments in the large wave tank of the Delft Hydraulics Laboratory, **Vellinga ('84)** found that the profile can be described by:

$$h = 0.080 y^{0.78}$$

After including the wave conditions in terms of steepness and the sediment characteristics a more general relationship was found:

$$h = 0.70 * \left(\frac{H_0}{L_0}\right)^{0.17} * w^{0.44} * y^{0.78}$$

The variables are defined as before. The relation between the parameter A and the grain diameter for this profile is presented in figure 2.11.

Boon & Green ('88) evaluated the relationship found by Bruun and Dean for beach profiles along the Caribbean Sea. They concluded that the relationship $h = Ay^m$ is quite successful, although they found a value for m of 0.55 rather than 0.67. This could be caused by the different conditions in the Caribbean, which usually experiences fair weather waves of low energy and low steepness, while the tidal range is very small.

2.1.2.2 The beach slope as a representation of the beach profile.

Sunamura ('84) derived relations for the beach-face slope as a representation of the equilibrium profile. He found different expressions for laboratory and field data. These relationships read:

$$\tan\beta = \frac{0.013}{(H_b^2/gDT^2)} + 0.15$$

$$\tan\beta = \frac{0.12}{\sqrt{\frac{H_b}{(gD)^{0.5}T}}}$$

They are derived for laboratory and field data respectively. T is the wave period, H_b is the breaker height, D is the sediment diameter, g is the gravity acceleration and $\tan\beta$ is the beach-face slope.

Boon & Green used the parameter A to represent the beach slope by substituting $h = 1.0$ m into the equation $h = Ay^m$. This gives $\tan\beta_1 = A^{1/m}$. Comparison of the field data with the relationships derived by Sunamura gave the best agreement if $A^{1/m}$ was used as the beach slope. They concluded that the beach profiles could be satisfactorily described by $h = Ay^m$ with $m = 0.55$. The parameter A can be found from:

$$A^{\frac{1}{m}} = \frac{0.013}{H_b^2/gDT^2} + 0.12$$

2.1.3 Summary.

In section 2.1 equilibrium beach profiles are discussed. A distinction is made between the type of the profile and the shape of the profile.

The two types of profile are a "bar" or erosive profile and a "step" or accretive profile. Criteria are presented which determine the type of profile, expected to develop, depending on the wave conditions and the sediment characteristics.

The most well-known criterion is Dean's number or the dimensionless fall velocity parameter, H/wT . Either a "bar" or a "step" profile is developed if the value of H/wT is larger, respectively smaller than the critical one. The magnitude of the critical value is uncertain and varies between 0.85 and 2.5 according to different researchers.

Other criteria include the wave steepness, the grain diameter, related to the wave height or the wave length and the beach slope. It remains unclear if the type of profile, observed in laboratory experiments, is affected by the initial slope.

Only little research has been done on beach profile evolution due to random waves. In general beach profiles under random waves are smoother and the evolution time is longer, than in the case of regular waves.

In addition to the type of profile, descriptions of the shape of profile have been studied.

A well-known description of the shape of the equilibrium beach profile, mainly based on field data is: $h = A y^{(2/3)}$, where h is the depth of the profile, y is the distance offshore and A is a parameter characterizing the sediment. This relationship shows reasonable agreement with beach profiles in the field. However, agreement with profiles observed in laboratory experiments is less satisfying. The disadvantage of this model is the exclusion of wave conditions for the description of the profile.

An alternative way of describing the profile is by using the beach slope as a representation of the shape of the profile. In this case sediment characteristics as well as wave conditions are used to describe the profile.

2.2 Scaling laws.

Physical models play an important role in both research and practical cases related to onshore and offshore sediment transport and the resulting beach profiles. In order to build a representative model all the important parameters involved in sediment transport should be scaled down correctly. This however is not possible as can be shown in the following way:

Sediment transport can be described as a function of various dimensionless parameters

$$\Pi_Q = \varphi\left(\frac{u_* D}{\nu}, \frac{u_*^2}{\gamma' g D}, \frac{\rho_s}{\rho}, \frac{l}{d}, \frac{u}{\sqrt{gd}}, \frac{H}{wT}\right)$$

Where Π_{Q_s} is the dimensionless sediment transport rate, u_c is the critical velocity of sediment motion, D is the sediment diameter, ν is the viscosity of water, ρ is the density of water, ρ_s is the density of the sediment, $\gamma' = (\rho_s - \rho) / \rho$, g is the gravity acceleration, u is the horizontal velocity, d is the water depth, l is a horizontal length, H is the wave height, T is the wave period and w is the fall velocity of the sediment. The fall velocity depends among other parameters on the shape factor of the particles. This is a factor which represents the degree of particle angularity.

Correct modelling of the sediment transport requires the same value of these dimensionless parameters in model and prototype. The problem now is that not all the variables can be scaled down. It is impossible to scale gravity. Also the fluid properties are not to scale if water is used in the model. The density, viscosity and surface tension of the fluid are therefore the same in model and prototype. As an example it can be shown that this leads to contradicting requirements for the size of the grain diameter in the model. Preservation of ρ_s/ρ requires the use of the same material in the model. This means that the scale of the submerged weight (γ_s) is equal to 1. Substitution into the expression for the densimetric Froude number this gives:

$$n_D = n_u^2$$

Where n_i is the ratio of the prototype value of the parameter i to the model value. Because the scale of the viscosity is equal to one, preservation of the Reynolds number gives:

$$n_D = n_u$$

Another problem with physical models is that the scaling of the grain diameter can change the properties of the sediment. If the diameter becomes too small the sediment becomes cohesive.

For these reasons many researchers have derived scaling laws such that the profiles in the model are similar to those in the prototype. Some of the model laws are purely empirical, others are derived from a more analytical point of view, requiring similitude of important parameters in model and prototype.

2.2.1 Empirical model laws.

Noda ('72) derived different scaling laws by considering seven basic conditions of similitude for the physical processes involved in sediment transport. Because Noda considered equilibrium beach profiles, the time scale of beach evolution is not taken into account. To evaluate these laws, Noda conducted experiments, using the same sand size in the model as in the prototype. The experiments however show no geometric similarity and Noda concluded that scaling laws are impossible for the same sand in model and prototype.

He derived a model law directly from experimental data, using 14 different materials and 22 different grain sizes. The relationships between the horizontal and vertical scale and the scale of material size and density are as follows:

$$n^D n_{\gamma'}^{1.85} = \mu^{0.55}$$

$$\lambda = \mu^{1.32} n_{\gamma'}^{-0.386}$$

Where λ is the horizontal and μ the vertical scale. n_i is the scale of the parameter i , which is equal to the ratio of the prototype value of the parameter i over the model value. D is the sediment diameter and $\gamma' = (\rho_s - \rho)/\rho$, where ρ_s is the density of the sediment and ρ is the density of water. This model law is presented graphically in figure 2.12.

Noda recommended the use of sand, as it is inexpensive and has the correct shape factor. To avoid cohesive effects the minimum possible size is 0.1 mm. As a result it may be necessary to use light-weight material. The specific weight of this material should be larger than 1.3. Below this value the material characteristics cause dampening of the wave heights.

Although Noda found good agreement between prototype and model profiles **Collins & Chestnut ('75)** carried out wave tank studies to evaluate these relationships and concluded that the model law failed the verification test in that the shape of offshore and inshore zones was not reproduced and the movement of the shoreline was not correctly predicted. The slope of the foreshore was correctly predicted in three of the four runs. **Hallermeier ('85)** also considered Noda's scaling laws and suggested that discrepancies may result from the fact that Noda only considered shore-accretive situations. Besides, the experiments used as "prototype" are small-scale laboratory tests with the vertical scale being only 1:4.

Another empirical model law was derived by Vellinga ('82). He used experiments of dune erosion during storm events, conducted by Van de Graaff ('77). These experiments consisted of series of two-dimensional tests with vertical scales of 1:150, 1:84, 1:47 and 1:26 and two different types of sand. From these scale series Vellinga found the following relations:

$$n_t = \sqrt{\mu}$$

$$\frac{\lambda}{\mu} = \left(\frac{\mu}{n_w^2}\right)^{0.28}$$

Where λ is the horizontal scale, μ is the vertical scale, n_t is the time scale and n_w is the scale of the fall velocity of the sediment particle. The time is scaled according to Froude's criterion: The Froude number in the model must be equal to the Froude number in the prototype.

The scaling laws derived by Vellinga preserve the wave steepness (H_0/L_0) and the dimensionless fall velocity parameter (H/wT), introduced by Dean ('73). Both parameters are considered important in the development of beach-profiles.

The gap in the scale series between $\mu = 26$ and $\mu = 1$ was considered to be still quite large and scale-effects could be present. Therefore Vellinga performed experiments with smaller sand. Because of the preservation of (H/wT) this is equivalent to experiments with higher waves (Vellinga '78).

At this time it became possible to perform experiments at a large scale in the large wave flume of the Delft Hydraulics Laboratory. Erosion quantities from tests with $\mu = 5$ confirmed the relationships found earlier, although erosion profiles for models with the same sediment were not fully satisfactory. A better agreement was found if finer sand was used in the model which agrees with the observations from Noda.

2.2.2 Analytical model laws.

The model laws described so far were all purely empirical. Many model laws, though, are derived analytically, based on physical considerations. These scaling laws are discussed in the next sections.

2.2.2.1 Linear scaling.

Van Hijum ('74) considered the scale effects for the development of equilibrium profiles of coarse material. To investigate these Van Hijum used linear scaling of sediment and a time scale modelled according to Froude. Because Van Hijum stated that it is only possible to scale down the mechanism of bed load, preservation of the Shields parameter is required. He considered the assumption of only bed-load transport reasonable for gravel. The model law based on these requirements is:

$$n_H = n_L = n_h = n_D = n_v^2 = n_c^2 = n_T^2 = \lambda = \mu$$

$$n \left(\frac{v^2}{\gamma' g D} \right) = 1$$

If the first relation is substituted into the second one, the latter becomes:

$$n_{\gamma'} = 1$$

The same material must thus be used in prototype and model. Experiments show that models scaled down according to these relations respond to scale if D_{90} is greater than 6.0 mm. The only variable not effected by the scaling is the height of wave run-up above still water level. From this observation Van Hijum concluded that scale-effects are restricted to the transport mechanism and do not play a role in porosity or roughness.

2.2.2.2 Preserving the dimensionless fall velocity parameter.

As mentioned before the dimensionless fall velocity H/wT is supposed to be an important parameter for the development of beach profiles. Dalrymple & Thompson ('76) were among the first who derived scaling laws requiring preservation of this parameter. These seven model laws are summarized in table 2.1.

Experiments conducted by Dalrymple & Thompson used the same sediment as in the prototype ($n_D = 1$). This restricts the verification to model laws #3, #5, #6 and #7. Despite the very small scaling used ($\mu = 2$) the differences are large. The best results gave scaling law #7.

Three of the seven proposed scaling laws were not tested, but Dalrymple & Thompson expected that model law #1 (see table 2.1) will give the best results, as this one includes the most important assumptions.

For a representative model they recommended geometric similarity, preservation of wave steepness and dimensionless fall velocity and use of same material in the model as in the prototype to avoid alien effects of light-weight material.

Table 2.1 Summary of model laws derived by Dalrymple & Thompson.

Law	n_γ	n_{D50}	n_T	λ	Note
#1	1	$\mu^{0.25}$	$\mu^{0.5}$	μ	Preserves Froude number, H_0 , L_0 , geometric similarity, Stokes fall velocity
#2	$\mu^{1.5}$	$\mu^{-0.5}$	$\mu^{0.5}$	μ	Preserves bed particle Reynolds number, densimetric Froude number, H_0/L_0
#3	1	1	μ	$\mu^{1.5}$	Assumes laminar boundary layer. Preserves bed shear stress, Froude number.
#4	$\mu^{-0.1875}$	$\mu^{0.063}$	$\mu^{1.0625}$	$\mu^{1.5625}$	Assumes turbulent boundary layer.
#5	1	1	μ	$\mu^{1.5}$	Preserves Froude number.
#6	1	1	μ	μ^2	Preserves bed particle Reynolds number, bed shear stress.
#7	1	1	μ	μ	Preserves geometric similarity, H_0/L_0 .

Noda ('78) also found that models scaled down preserving (H/wT) gave better similarity than linear scaling.

He considered the dimensionless depth of equilibrium profiles (h/L_0) to be a function of the following dimensionless parameters:

$$\frac{l}{L_0}, \frac{H_0}{L_0}, \frac{H_0}{D}, \frac{D * \sqrt{gH_0}}{v}, \frac{\rho}{\rho_s}, \tan\beta$$

where l is the horizontal distance, H_0 is the deep water wave height, L_0 is the deep water wave length, D is the sediment diameter, g is the gravity acceleration, γ is the viscosity of water, ρ_s is the density of the sediment, ρ is the density of water and $\tan\beta$ is the beach slope.

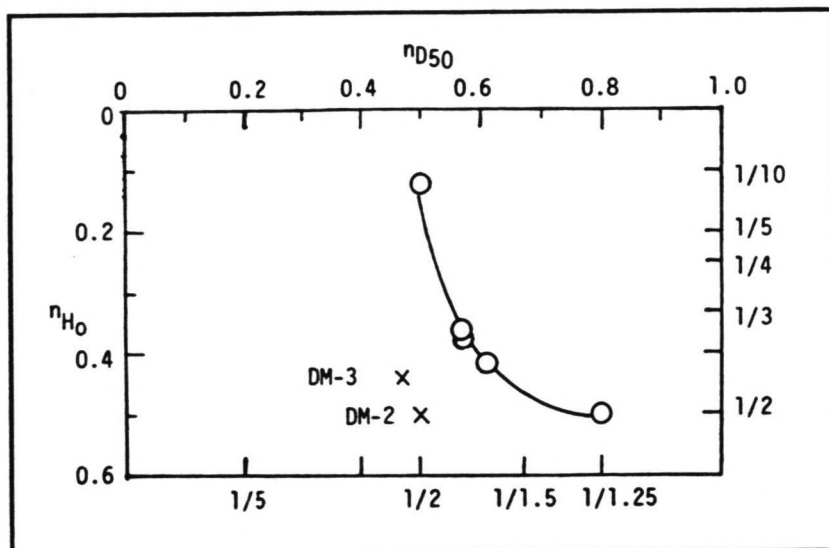


Figure 2.13 The relationship between the scale of the wave height (n_{H0}) and the scale of the grain diameter (n_{D50}), derived by Noda ('78).

Preservation of these parameters is impossible, because this requires:

$$n_D = (n_H)^{-0.5}$$

and

$$n_H = n_D$$

Neglecting the viscosity gives a linear scaling law, which does not include a time scale, because only equilibrium profiles are considered. The relations required are:

$$n_h = n_l = n_L = n_H = n_D$$

$$n_{\tan\beta} = 1$$

$$n_{\rho_s} = n_\rho$$

Experiments scaled down according to this law showed considerable difference between model and prototype.

Noda showed that the dimensionless fall velocity ($\pi w/gT$) is a function of H_0/L_0 , H_0/D , $D*\sqrt{(g*H_0)/\nu}$ and $(\rho_s-\rho)/\rho$. Therefore rather than preserving dimensionless viscosity and grain diameter the dimensionless fall velocity should be preserved. This gives an undistorted Froude model:

$$n_w^2 = n_T^2 = n_L = n_H = n_h = n_l$$

$$n_{\tan\beta} = 1$$

Experiments showed indeed a closer similarity for this scaling law.

Noda also studied the influence of the model sediment size and found a relation between the scale of the wave height (n_{H_0}) and the scale of the mean diameter ($n_{D_{50}}$). This relation is shown in figure 2.13.

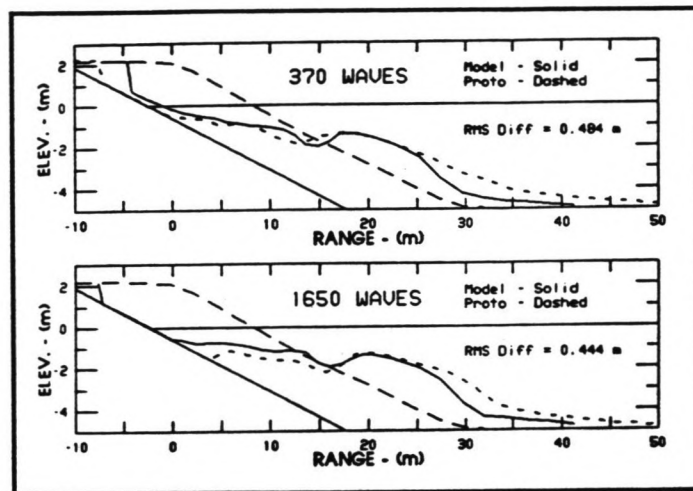


Figure 2.14 Comparison between model and prototype beach profiles for regular waves (Hughes & Fowler '90).

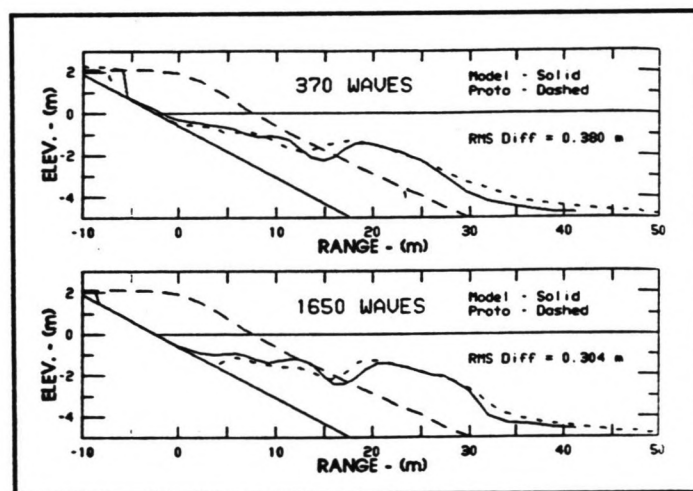


Figure 2.15 Comparison between model and prototype beach profiles with the wave height in the model increased by 10% (Hughes & Fowler '90).

To enhance the knowledge of the processes involved **Dean ('85)** also recommended the most direct approach of undistorted models with sediment particles scaled according to Froude, which preserves the fall velocity parameter, rather than the use of empirical model laws. The model should be sufficiently large that viscous and surface tension effects are negligible. Dean found a high degree of consistency between model and prototype for the incidence of storm bar formation.

The recommendations given by **Dean ('85)** were verified by **Kriebel, Dally & Dean ('86)** and **Hughes & Fowler ('90)**. Kriebel *et al* performed 4 types of laboratory experiments:

- * Comparison of equilibrium profiles with a linear initial slope
- * Comparison of equilibrium profiles with a concave initial slope, corresponding to $h = Ay^{(2/3)}$
- * Evaluation of the criterion for bar formation
- * Evaluation of storm bar behaviour under recovery conditions.

They compared their experiments with large scale data from experiments conducted by **Saville ('57)**. The experiments considering the equilibrium profiles showed good agreement with these prototype data, although for the accretive situation problems existed with wave-reflection from the beach and re-reflection from the paddle. The concave profiles seemed to give more realistic profiles as a result of more realistic wave breaking and shoaling.

Evaluation of the criterion for bar formation showed a higher value than suggested by **Dean ('73)**.

Dean found $(H/wT)_{cr} = 0.85$
while Kriebel *et al* found $(H/wT)_{cr} = 2 - 2.5$

Simulation of landward bar migration appeared to be very difficult due to the aforementioned reflection of waves in the tank.

Hughes & Fowler ('90) mentioned that the bottom shear stress in the model law suggested by Dean is not scaled correctly. This model law is therefore restricted to chiefly erosive processes in energetic, turbulence-dominated regions. Hughes & Fowler performed model tests of the large-scale experiments, conducted by **Dette & Uliczka ('87)**, **Uliczka & Dette ('87, '88)** with a model scale of 1:7½. The test results showed good agreement with the prototype, but they were better inside the (energetic) surf zone than outside this area. Even

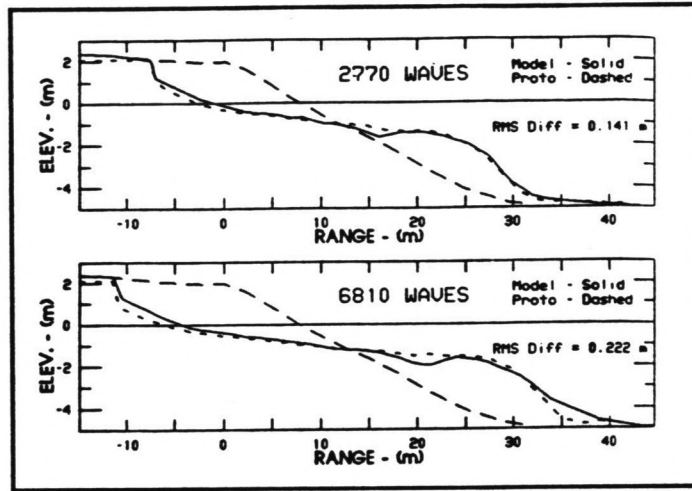


Figure 2.16 Comparison between model and prototype beach profiles for random waves (Hughes & Fowler '90).

better agreement was achieved by increasing the wave height in the model by 10% in order to fulfil a requirement derived by Xie ('81) (see figure 2.14 and 2.15). This requirement is as follows:

$$\left(\frac{u_{\max} - u_*}{w}\right)_p = \left(\frac{u_{\max} - u_*}{w}\right)_m$$

Where u_{\max} is the maximum orbital velocity, u_* is the critical threshold velocity of sediment motion and w is the fall velocity of the sediment particles. The subscripts p and m refer to prototype and model values respectively.

Tests showed that enhancement of the wave height is not needed for irregular waves. Scaling laws are usually derived for regular waves. In order to be able to apply these laws in reality the wave height in these scaling laws should be equal to the significant wave height in the case of random waves. Beach profiles scaled by this recommendation showed very good agreement, although the evolution time is about twice as long (see figure 2.16).

2.2.2.3 Different analytical scaling laws.

Different ways of deriving scaling laws were adapted by Hughes ('83), Kamphuis ('85), Hallermeier ('85), Wang, Toue & Dette ('90) and Powell ('88).

Hughes ('83) combined a dynamic similitude from forces involved in sediment transport with a beach profile similarity criterion, based on the dimensionless fall velocity. According to Hughes the important forces are the gravity and inertia forces, the latter being equal to a Reynolds stress times an area. From the requirement that all forces must have the same scale it follows that:

$$n_T = \frac{\lambda}{\mu}$$

Preservation of the dimensionless fall velocity gives:

$$n_T = \frac{\lambda}{\mu^{0.5}}$$

The model law, derived by Hughes is thus:

$$\lambda = \frac{\mu^{1.5}}{n_w}$$

$$n_T = \frac{\lambda}{\mu^{0.5}}$$

If the model is undistorted ($\lambda=\mu$) not only the fall velocity parameter but also the wave steepness and the surf similarity parameter ($\xi = \tan\beta/(H/L)$) are preserved.

Hughes verified his scaling law against the field data of the Hurricane Eloise. Tests with random waves did not give satisfactory results. Therefore model tests were performed with a monochromatic wave height giving the same energy density as the significant wave height in the case of random waves. The eroded profiles in the model resemble the prototype in terms of recession of dunes, eroded volume and beach face slope. These observations contradict the results which were reported by **Hughes & Fowler ('90)**.

Hughes' model law was evaluated by **Hallermeier ('85)** who mentioned that this law, which is only verified by one model test, contradicts the modelling relationship from **Vellinga ('82)**, which has an extensive empirical basis. Another objection against Hughes' scaling law is the analytical basis of dissipative forces acting on a nearly horizontal bed rather than the bulk dissipation of energy within the fluid, although this is what actually occurs in the breaker zone, especially in the case of dune erosion, which is investigated by Hughes.

Hallermeier ('85) evaluated and compared different scaling laws (**Noda '72**, **Lepetit & Leroy '77**, **Vellinga '82** and **Hughes '83**) and found that they all contradict each other. All these scaling laws are underspecified (two variables can be chosen freely) and therefore Hallermeier tried to find a unified modelling guidance. He argued that Dean's fall velocity parameter is an oversimplification as it does not include the beach slope. Instead, he suggested preservation of the parameter Ψ .

$$\Psi = \frac{v_h/u_*}{v_v} = \frac{l_h}{l_v * u_*}$$

Where u_* is the threshold velocity of sediment motion, v is the velocity and l is a typical length scale. The subscripts h and v refer to the horizontal and vertical direction respectively.

The model law developed by Hallermeier then becomes:

$$\lambda = n_T^2$$

$$n_T = \frac{\lambda}{\mu} * \frac{(\rho_m * g * D_m)^{0.25}}{D_p^{0.5}} * \left(\frac{\rho_m}{\rho_p}\right)^{0.5} * T_m^{0.25}$$

Hallermeier verified his law with data from the four experiments mentioned before and with own laboratory data. He found a fair degree of success and concluded that preservation of the parameter Ψ shows some congruence with the empirically based models, but only little agreement with model laws based on the preservation of the fall velocity parameter.

Some objections against this law are that the parameter Ψ , which must be preserved, is not dimensionless. The fall velocity is not included at all, and data on which Hallermeier based his "fair degree of success" are not very convincing.

Kamphuis ('85) discussed the scale effects resulting from different model laws based on preserving some of the following dimensionless parameters: The Reynolds number, the Shields parameter, the dimensionless density and geometric similitude. He found that the best results are achieved if the requirement for the Reynolds number is relaxed and all the others are satisfied (**Kamphuis ('75)**).

The scale effects resulting from the use of light-weight material are the piling up of beaches due to smaller particle accelerations in the model and the relative much higher weight of the particles in air. Kamphuis therefore stated that it is impossible to use light-weight material in a coastal movable-bed model, as was concluded by **Noda ('72)** and **Dalrymple & Thompson ('76)**

Another scale effect results if the same sediment size is used in the model. This is a result of the scale of the force to move the particle, which is equal to the scale of the diameter cubed. If the sediment size is the same in prototype and model, the force is also the same and therefore much exaggerated in the model.

Kamphuis himself stated that the disadvantage of this model is that it does not take into account material suspension, although very important. He suggested that it is perhaps better to preserve the dimensionless fall velocity according to Dean's recommendations.

A different approach to deriving scaling laws was adapted by Wang, Toue & Dette ('90). They considered the basic differential equation for sediment conservation:

$$\frac{\partial h}{\partial t} = \frac{\partial q}{\partial x}$$

where h is the depth of the profile, t is the time, x is a distance perpendicular to the shoreline and q is the volumetric sediment transport rate in x-direction, per unit width.

To maintain similitude between prototype and model it is required that:

$$\mu = \frac{\lambda}{(n_q * n_r)}$$

Another requirement they used is preservation of the surf similarity parameter ξ ($= \tan\beta/(H/L)$). For the case of suspended-load dominated transport, two model laws were developed:

Model law A

$$n_t = n_T = \frac{\lambda}{\mu^{0.5}}$$

$$\mu = (n_{\gamma'} * n_w * \lambda)^{1.5}$$

In this case the time scale is found from the assumption that the number of incoming waves is preserved. This is the same time scale as used by Hughes ('83).

Model law B

$$n_t = \frac{\mu}{n_u} = \mu^{0.5}$$

$$\mu = (n_w * n_{\gamma})^{0.4} * \lambda^{0.8}$$

In this case the morphological time scale is found from the preservation of the trajectory of a fallen particle. u is a horizontal velocity.

Comparison of different laboratory experiments showed a better agreement for model law *B*. More supporting evidence was found from the formulae for equilibrium beach profiles, derived from field data. **Vellinga ('82)** found:

$$A = 0.39 * w^{0.44}$$

While **Dean ('91)** showed:

$$A = 0.51 * w^{0.44}$$

The model laws derived by Wang *et al* gave:

$$A = \alpha * \left(\frac{\gamma' * w}{\sqrt{g}} \right)^n$$

Where $n = 0.67$ for model law *A*, and 0.4 for model law *B*. This shows that model law *B* is closer to the observations of Vellinga and Dean.

The last model law reviewed in this section is derived by **Powell ('88)**. He required preservation of permeability, relative magnitude of on- and offshore transport and threshold of motion. To preserve permeability **Yalin ('63)** found that the percolation slope J must be equal in model and prototype. The percolation slope is defined as follows:

$$J = \frac{k(Re) * v^2}{g * D_{10}}$$

The parameter k represents the permeability and is a function of the Reynolds number (Re), v is the velocity through the voids, g is the gravity acceleration and D_{10} is the 10 % undersize of the sediment.

Preservation of the percolation slope gives:

$$n_D = \frac{\mu * k_p}{k\left(\frac{Re_p}{\mu^{0.5} * n_D}\right)}$$

where:

$$\log k = 3.17 - 1.134 * \log(Re) + 0.155 * \log^2(Re)$$

The subscript p refers to prototype conditions. μ is the vertical scale and n_D is the scale of the sediment diameter.

To model the relative magnitude of on- offshore transport the dimensionless fall velocity should be preserved. This gives:

$$n_{\gamma} = \frac{\mu * n_{C_D}}{n_D}$$

where

$$n_{C_D} = \frac{C_{D,p}}{C_D\left(\frac{Re_p}{\mu^{0.5} * n_D}\right)}$$

γ is the specific density and C_D is the drag coefficient.

From **Komar and Miller ('73)** it was found that, to model the threshold of movement, the following equation should be satisfied:

$$n_{\gamma'} = \left(\frac{\mu}{n_D}\right)^{\frac{3}{4}}$$

By choosing the model scale, one of the equations should be relaxed in order to be able to solve the four equations. Usually permeability is considered to be less important Powell showed that in the particular case of $\mu = 17$ anthracite, with a specific density of 1.39, does satisfy the other equations rather well.

2.2.3 Scaling laws derived by preserving the criterion between erosive and accretive profiles.

Alternative scaling laws have been based on a comparison of the beach profile in the prototype with the beach profile in the model. To distinguish between different profile types a certain criterion for erosive or accretive beaches is derived. The two mostly used criteria are the fall velocity parameter (H/wT) introduced by **Dean ('73)** and the criterion of **Sunamura & Horikawa ('74)**:

$$\frac{H_0/L_0}{\tan\beta^{-0.27} * (D/L_0)^{0.67}} = C$$

Where H_0 is the deep water wave height, L_0 is the deep water wave length, D is the sediment diameter and $\tan\beta$ is the beach slope.

Kai, Rushu & Liang ('90) however found that these criteria depend on the scale of the model.

For Dean's criterion number $C = H/wT$ the scale of the criterion number C is equal to:

$$n_C = \frac{\mu}{n_w^{0.5}}$$

If the fall velocity in the model is equal to that in the prototype, the value of C in the model decreases if the vertical scale becomes larger.

For Sunamura & Horikawa's criterion with the same material in model and prototype the scale of the criterion number C becomes:

$$n_C = \left(\frac{n_H}{n_D}\right)^{0.67} * \left(\frac{\mu}{\lambda}\right)^{0.27} = \frac{n_H^{0.535}}{n_D^{0.67}}$$

This means that if the same sand size is used in the model and in the prototype ($n_D=1$) the criterion number in the model will become smaller if n_H becomes larger. If the same wave height is used in the model the model criterion number will increase if the scale of the sediment size becomes larger.

For these reasons Kai *et al* found a criterion which satisfied the scale relations. This criterion reads:

$$\frac{H}{L} = C * \left(\frac{w}{gT}\right)^{1.3} * \left(\frac{u_*}{w}\right)^{0.4} * (\tan\beta)^{-1.5}$$

Erosion occurs if C is greater than 0.83, while accretion takes place if C is less than 0.32.

2.2.4 Summary.

In section 2.2 many scaling laws are presented. These laws are either derived empirically, based on laboratory and/or full scale experimental data or analytically, based on various physical considerations. It is clear that there remains a lot of uncertainty about the scaling of the sediment in coastal movable-bed models.

Table 2.2 Scaling laws reviewed in section 2.2.

Source	Scaling relations	Distortion = 1
No different material allowed, no distortion allowed.		
Dalrymple & Thompson ('76)	$n_\gamma = 1$ $n_t = \sqrt{\mu} = \sqrt{\lambda}$ $n_D = \mu^{0.25}$	
Van Hijum ('74)	$n_\gamma = 1$ $n_t = \sqrt{\mu} = \sqrt{\lambda}$ $n_D = \mu$	
Kamphuis ('85)	$n_\gamma = 1$ $n_t = \sqrt{\mu} = \sqrt{\lambda}$ $n_D = \mu$	
Different material allowed, no distortion allowed.		
Noda ('78)	$n_t = \sqrt{\mu} = \sqrt{\lambda}$ $n_w = \sqrt{\mu}$	
Dean ('85)	$n_t = \sqrt{\mu} = \sqrt{\lambda}$ $n_w = \sqrt{\mu} \quad (D_m \geq 0.08 \text{ mm})$	
Hughes & Fowler ('90)	$n_t = \sqrt{\mu} = \sqrt{\lambda}$ $n_w = \sqrt{\mu}$	
Powell	$n_\gamma = (\mu * n_{CD})/n_D$ $n_\lambda = (\mu / n_D)^{0.75}$	
Different material allowed, distortion allowed.		
Vellinga ('82)	$n_t = \sqrt{\mu}$ $n_w = \mu^{2.29} / \lambda^{1.79}$	$n_t = \sqrt{\mu}$ $n_w = \sqrt{\mu}$
Wang, Toue & Dette ('90)	$n_t = \sqrt{\mu}$ $n_w = \mu^{2.5} / (n_\gamma * \lambda^2)$	$n_t = \sqrt{\mu}$ $n_w = \sqrt{\mu}/n_\gamma$
Hughes ('83)	$n_t = \lambda\sqrt{\mu}$ $n_w = \mu^{1.5} / \lambda$	$n_t = \sqrt{\mu}$ $n_w = \sqrt{\mu}$
Noda ('72)	$n_D * n_\gamma^{1.85} = \mu^{0.55}$ $\lambda = \mu^{1.32} * n_\lambda^{-0.386}$	$n_\gamma = \mu^{8.10}$ $n_D = \mu^{15.53}$
Hallermeier ('85)	$n_t = \sqrt{\mu}$ $n_\psi = 1$	

The two main features in the comparison of the scaling laws are the allowance of different material to be used in the model and the allowance of distorted models, i.e. models with a horizontal scale different from the vertical scale.

The model laws reviewed are summarized in table 2.2. For the model laws which allow distortion an extra column shows the results if the horizontal scale is equal to the vertical scale, resulting in an undistorted model.

3 Experiments.

In chapter 2 (literature survey), different scaling laws are presented. It is observed that many of them give different results for the scale of the sediment diameter. Further analysis of the different model laws was used for the design of the experiments conducted. The aim of the experiments was to investigate the behaviour of and the differences between sand and anthracite models of prototype sand and gravel beaches.

In this chapter the different scaling laws are compared. Using this comparison the experiments conducted for this project are designed. Next the experiments and measurements are described.

3.1 Comparison of the scaling laws.

Distinction between the scaling laws, reviewed in chapter two, can be made in terms of allowance of distorted models, i.e. models with a different horizontal and vertical scale.

Also a distinction is possible between models which allow different (usually light-weight) material to be used and other models which only allow sand as the model material (see table 2.2).

3.1.1 The fall velocity as a representation of the sediment.

Table 2.2 shows that for models which require the same material in the prototype and in the model, the scale of the grain diameter is given in order to find the model sediment size. For models which allow the use of a different material this is not possible. Rather than the scale of the grain diameter the scale of the fall velocity is given, since this is assumed to be an important parameter for sediment transport. Because the fall velocity is dependent on the sediment size and the density this is an easy way to represent the sediment used, excluding shape factor.

The relationship between the fall velocity and the sediment diameter and density can be derived in the following way:

The fall velocity is found from the balance of forces on a falling particle:

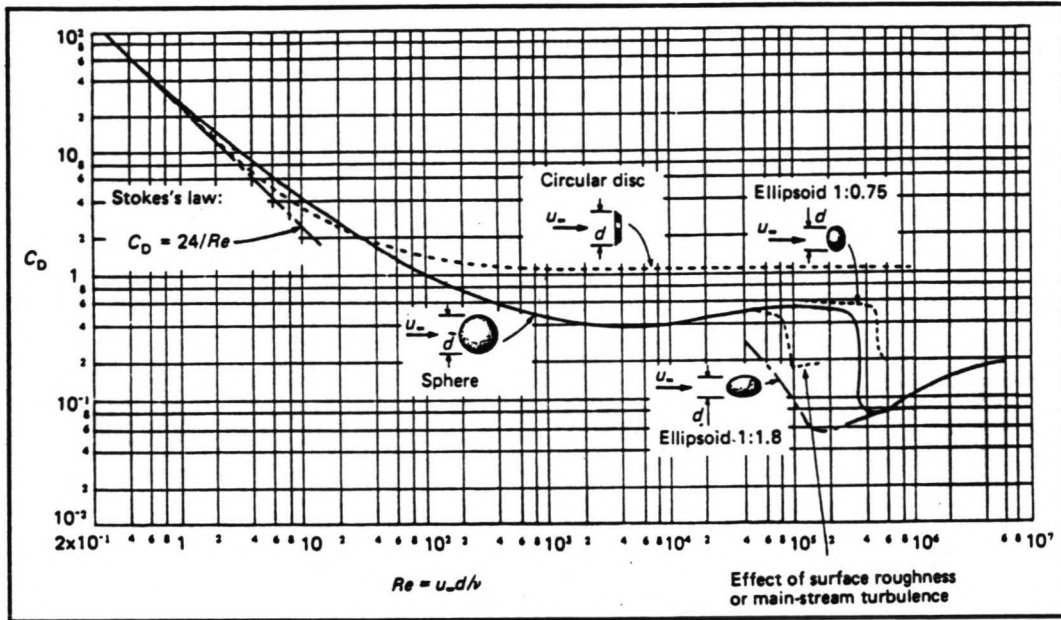


Figure 3.1 Relation between the Reynolds number and the drag-coefficient.

Submerged weight = drag force

$$\frac{\pi D^3}{6} (\rho_s - \rho) g = C_D \frac{1}{2} \rho w^2 \frac{\pi D^2}{4} \quad (3.1)$$

where D is the sediment grain diameter, ρ_s the density of the sediment, ρ the density of water, g the gravity acceleration, C_D the drag coefficient and w the fall velocity.

The drag coefficient depends on the Reynolds number wD/ν , as can be seen in figure 3.1. ν is the viscosity of water.

For small values of the Reynolds number ($Re < 40$) the drag coefficient is linearly dependent of the Reynolds number:

$$C_D = \frac{24}{Re} \quad (3.2)$$

Substitution in equation 3.1 gives:

$$w = 54.5 * 10^4 \gamma' D^2 \quad (3.3)$$

Where $\gamma' = (\rho_s - \rho)/\rho$

For large values of the Reynolds number ($40 < Re < 10^5$) the drag coefficient is independent on the Reynolds number. Substitution in equation 3.1 gives now:

$$w^2 = \frac{4 g D \gamma'}{3 C_D} \quad (3.4)$$

The drag coefficient depends on the shape factor. The shape factor is a parameter which expresses the degree of particle angularity and is defined as $D3/\sqrt{(D1*D2)}$, where $D3$ is the smallest diameter of the particle, $D1$ the largest and $D2$ the intermediate one. For spheres this shape factor is 1.0 which gives:

$$w = 5.06 \sqrt{\gamma' D} \quad (3.5)$$

Sand grains however are not perfect spheres and a typical value for the shape factor is 0.7. This gives:

$$w = 3.27 \sqrt{\gamma' D} \quad (3.6)$$

Using these relationships the scale of the sediment diameter can be found if the scale of the settling velocity is known.

If light-weight material is used, the shape factor can be different from that of sand. This is indeed to be expected as anthracite is usually angular, resulting in a smaller shape factor. This then may not give the exact value of the settling velocity but is more a representation of the sediment used in terms of density and grain diameter.

Note: The derivation of the fall velocity is very theoretical. Changes in viscosity due to temperature differences are not included. The sediment concentration is not taken into account either. If this concentration is large the fall velocity of the cloud will be smaller than the fall velocity of a single particle. Additionally the derivation of the fall velocity is done for particles in *still* water. The fall velocity under (breaking) waves can be very different.

It is interesting to note that for large Reynolds numbers the fall velocity is proportional to the square root of the relative density times the diameter:

$$w \propto \sqrt{\gamma' D} \quad (3.7)$$

The scale of the fall velocity must therefore be equal to the scale of the relative density times the scale of the diameter:

$$n_w = \sqrt{n_{\gamma'} n_D} \quad (3.8)$$

If the same material is used ($n_\gamma = 1$) this results in:

$$n_w = \sqrt{n_D} \quad (3.9)$$

For undistorted models, using the same material, most of the scaling laws require (see table 3.1):

$$n_w = \sqrt{\mu} \quad (3.10)$$

This includes:

$$n_D = \mu \quad (3.11)$$

The sediment size is scaled down according to the vertical scale.

3.1.2 Comparison of model sediment diameters for different scaling laws.

As the relationship between the sediment size and density and the fall velocity is known, the model sediment size can be derived, according to the different scaling laws.

For most model laws two variables can be chosen freely. The other variables are then found from the scaling laws.

In this case the sediment density is restricted by the available materials, which are sand and anthracite. The relative density of sand is:

$$\gamma' = \frac{2650 - 1000}{1000} = 1.65$$

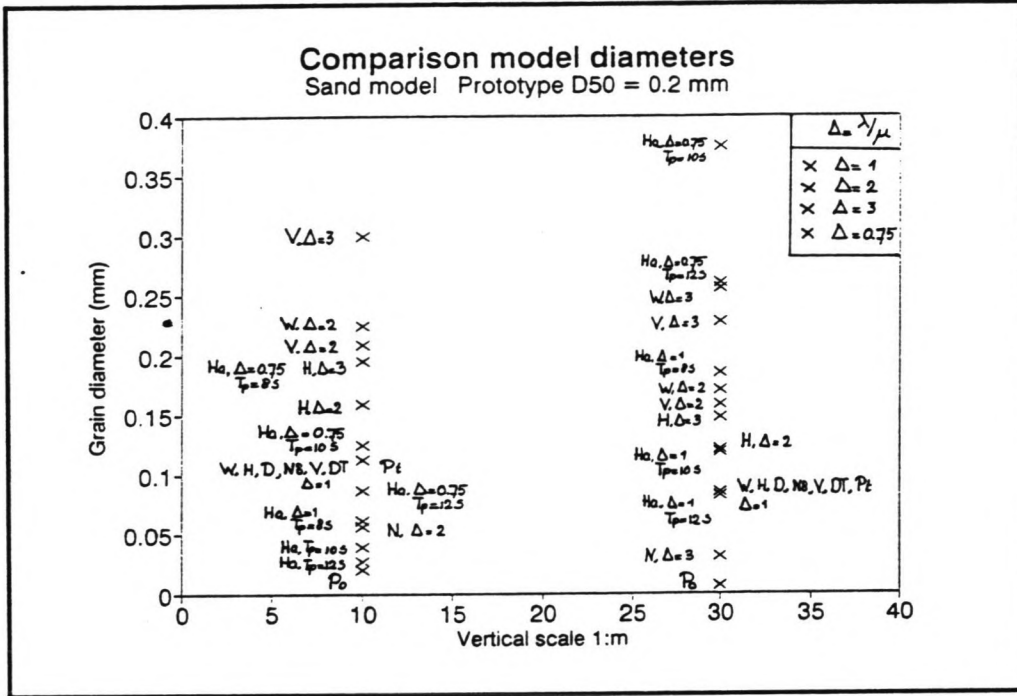


Figure 3.2 Required model sand diameter according to different scaling laws. Prototype sand with a mean diameter $D_{50} = 0.2$ mm.

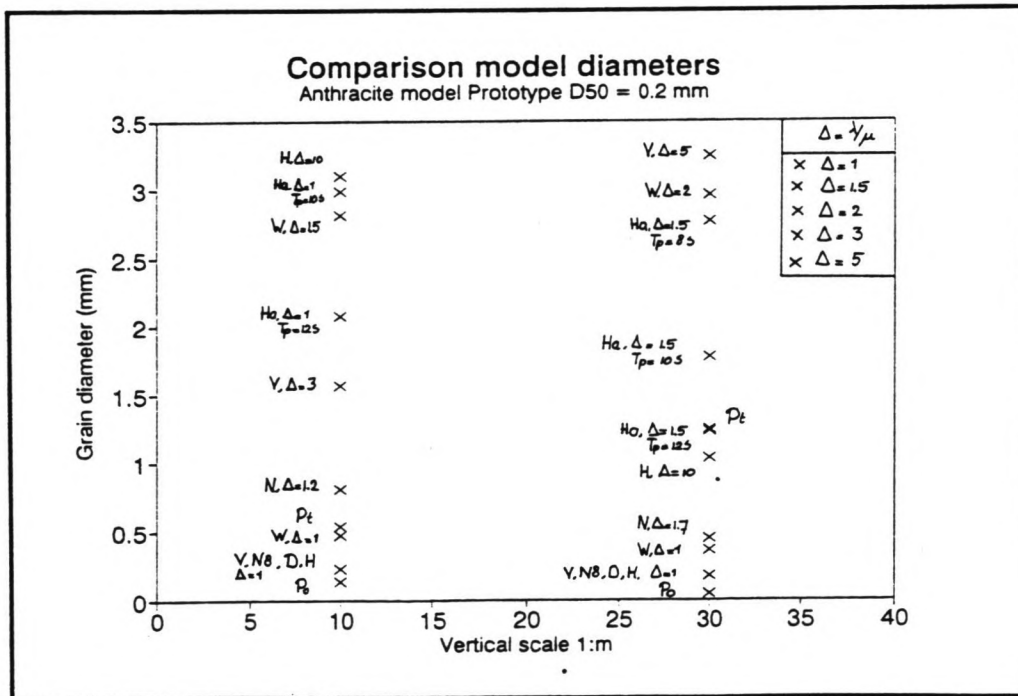


Figure 3.3 Required anthracite diameter according to different scaling laws. Prototype sand with a mean diameter $D_{50} = 0.2$ mm.

While for anthracite the relative density is equal to:

$$\gamma' = \frac{1390 - 1000}{1000} = 0.39$$

The scales of the relative densities (n_r) are therefore 1.0 and $1.65/0.39 = 4.23$ for sand and anthracite respectively.

The vertical scale is restricted by the physical limits of the equipment, like length and depth of the channel and the limits of the wavemaker. The wave paddle, used for the experiments described later, was designed for model scales around $1:30$. However larger model scales are possible. Practical values for the vertical scale are $\mu = 10$ and $\mu = 30$.

Using the aforementioned values for the scale of the relative density and the vertical scale, the model sediment size is calculated according to the different model laws.

The values for the grain diameters of the prototype beaches are chosen to be equal to $D = 0.2 \text{ mm}$, $D = 2.0 \text{ mm}$ and $D = 10.0 \text{ mm}$ to cover a wide range of material sizes from fine sand to gravel. The results are shown in figure 3.2 to 3.7.

3.2 Choice of the experiments.

In section 3.1.1 it was shown that for an undistorted sand model the grain diameter is scaled down according to the vertical scale. This means that in a small scale model the size of the sediment will be very small. Problems rise if the sediment size gets below a critical value, because the material becomes cohesive and the properties of the sediment change. This lower limit for the sediment size is about 0.08 mm . (Dean '85)

Because of the cohesive effects, often light-weight material is used in small-scale models. However, there are still doubts about the validity of the use of light-weight material in coastal movable-bed models.

To investigate the behaviour of light-weight material models, laboratory experiments should be compared with field data. This is however a very difficult and expensive task. A different way to get an idea about the behaviour of light-weight material models is to compare such a model with laboratory data of a sand model, representing the same prototype beach. The advantage of comparing two models of the same scale is that no scale-effects are

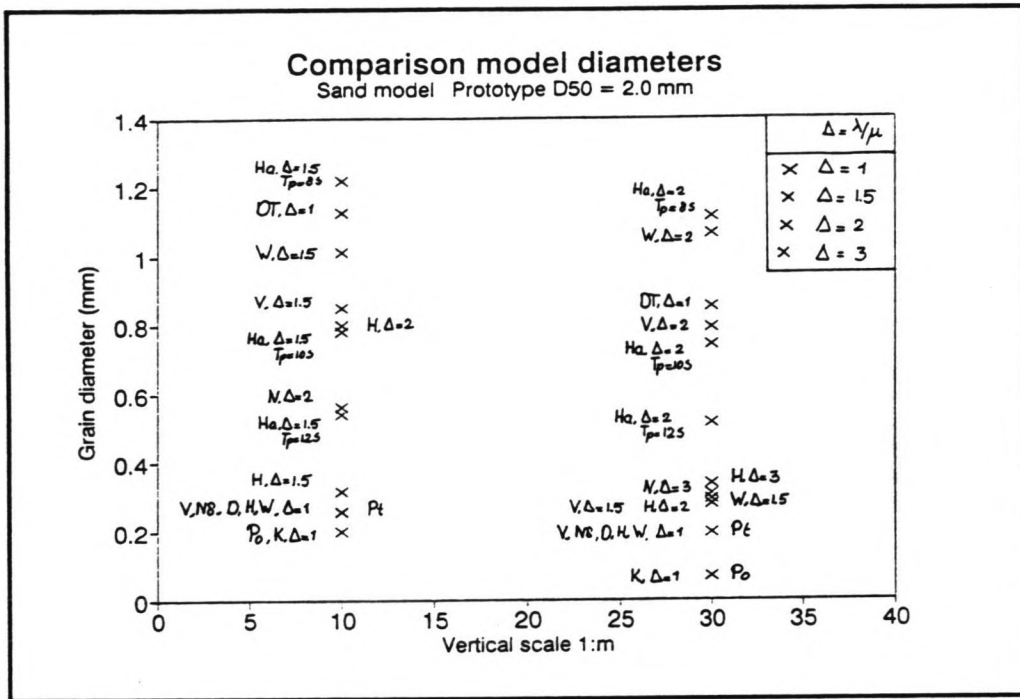


Figure 3.4 Required model sand diameter according to different scaling laws. Prototype sand with a mean diameter $D_{50} = 2.0$ mm.

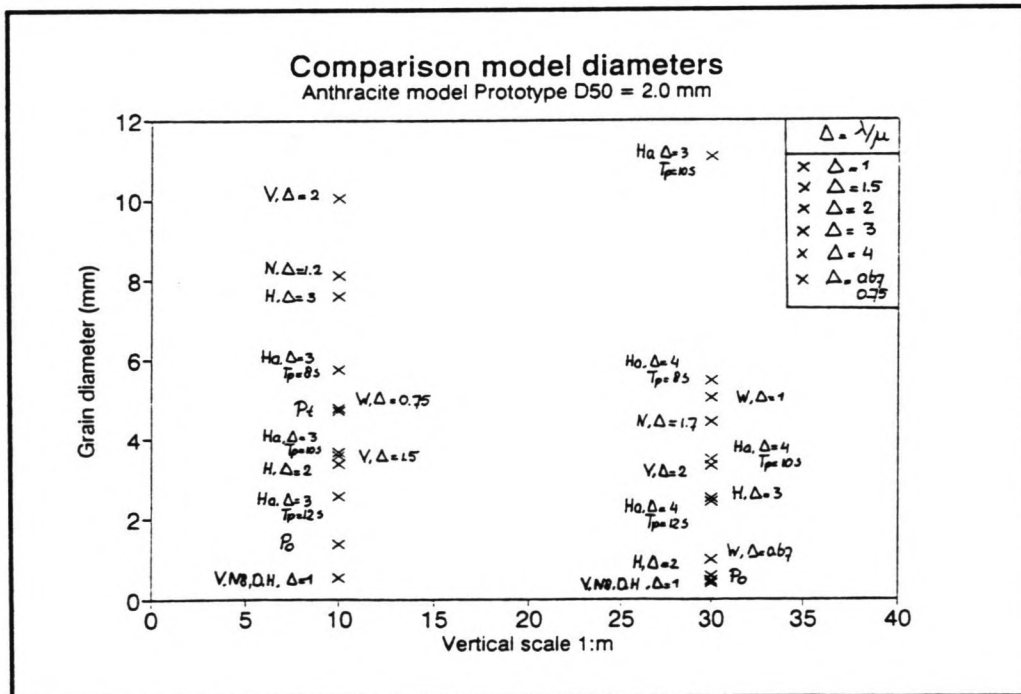


Figure 3.5 Required anthracite diameter according to different scaling laws. Prototype sand with a mean diameter $D_{50} = 2.0$ mm.

introduced. The differences between both models are purely related to the difference in material.

Comparison of light-weight material models with sand models is the aim of the experiments conducted in this project.

3.2.1 Undistorted model experiments.

* First set of experiments.

At first the difference between anthracite and sand models was investigated for the case of undistorted models.

The sediment size in the model was determined by the available material. The sand available in the laboratory had a mean diameter, D_{50} of 1.0 mm (see appendix A). It is reasonable to assume a $1:10$ model scale, which means that this sand represents a gravel beach with a mean diameter of 10.0 mm .

To model this prototype beach with anthracite, the grain diameter of the anthracite must be 4.23 mm . But the anthracite available had a mean diameter of 3.0 mm (see appendix A). In order to represent the same prototype beach a model scale of $1:14$ was chosen for the anthracite model. The difference in model scale was assumed to be small enough to avoid large scale-effects.

3.2.1.1 Wave conditions.

The evolution of the beach profile must be investigated for different wave conditions. For every model three wave heights and three wave periods were chosen, resulting in nine runs for the sand model and nine runs for the anthracite model.

The wave heights and wave periods, used in the experiments depended on the prototype conditions and the scale of the model and were restricted by the physical limits of the wavemaker.

The deep water prototype wave height can be very large. But larger waves will break when they propagate into shallow water and the maximum breaker height at the coast will be about 0.8 times the water depth. The wave paddle can generate random waves with a maximum significant wave height of 0.20 m . This means that for a $1:10$ model the maximum significant wave height will be 2.0 m in prototype. The significant wave height used in the experiments were chosen as 1.0 , 1.5 and 2.0 m for prototype conditions. This corresponds to

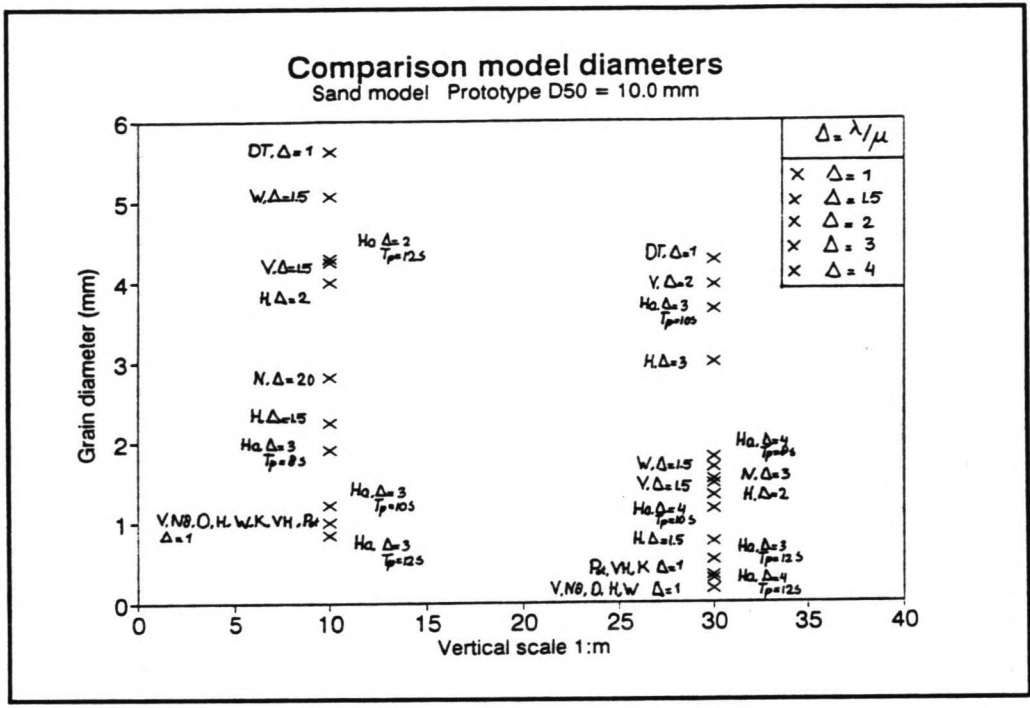


Figure 3.6 Required model sand diameter according to different scaling laws. Prototype gravel with a mean diameter of 10.0 mm.

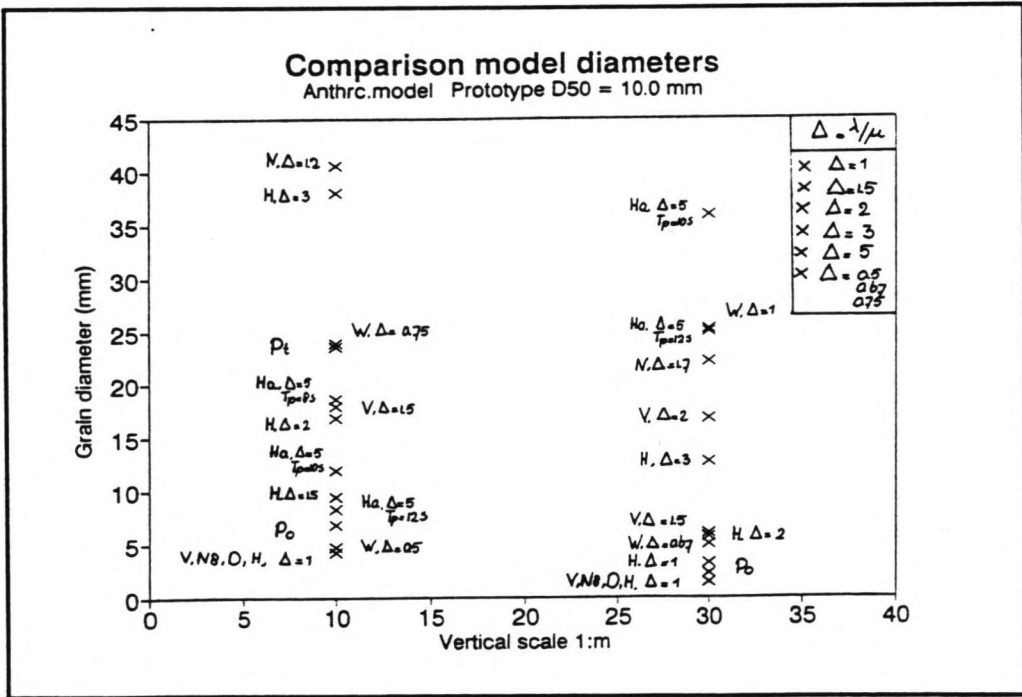


Figure 3.7 Required anthracite diameter according to different scaling laws. Prototype gravel with a mean diameter $D_{50} = 10.0$ mm.

0.10, 0.15 and 0.20 m in the model.

Wave periods vary usually between 5 and 15 seconds. For the experiments values of 7.0, 10.0 and 13.0 seconds were chosen for the zero-crossing period. During the experiments however it turned out that 13.0 seconds was beyond the limit of the wave paddle and in stead of 13.0 a value of 12.0 seconds was used as the largest zero-crossing period. The model values for the wave period are therefore: 2.21, 3.16 and 3.79 seconds. The experimental data are summarized in table 3.2.

Table 3.2 Experimental data for the first set of experiments.

Model scale	Model material	Sediment size (mm)		Wave height (m)		Wave period (s)	
		prototype	model	prototype	model	prototype	model
1:10	sand	10.0	1.0	1.0	0.10	7.0	2.21
1:10	sand	10.0	1.0	1.5	0.15	10.0	3.16
1:10	sand	10.0	1.0	2.0	0.20	12.0	3.79
1:14.1	anthracite	10.0	3.0	1.0	0.0709	7.0	1.86
1:14.1	anthracite	10.0	3.0	1.5	0.106	10.0	2.66
1:14.1	anthracite	10.0	3.0	2.0	0.142	12.0	3.20

3.2.1.2 The dimensionless fall velocity parameter.

The dimensionless fall velocity parameter (H/wT) is often used as a criterion for the distinction between on- and offshore transport. In chapter 2 it was shown that the critical value lies between 0.85 and 2.5 according to different researchers (see section 2.1.1.2). The parameter H/wT gives an indication of the type of profile, which can be expected to develop for certain wave conditions and sediment sizes. This is shown in figure 3.8 for a critical value of H/wT of 1.0. The dimensionless fall velocity was calculated for the wave conditions and sediment sizes used in the experiments. The results are shown in table 3.3.

Because the model is undistorted, the fall velocity is scaled down as the square root of the vertical scale. The time scale is also equal to the square root of the vertical scale.

Legend for figure 3.2 to 3.7.	
D	Dean ('85)
DT	Dalrymple & Thompson ('76)
H	Hughes ('83)
Ha	Hallermeier ('86)
K	Kamphuis ('85)
N	Noda ('72)
N8	Noda ('78)
Po	Powell ('88) From the criterion for onshore and offshore transport.
Pt	Powell ('88) From the criterion for the threshold of sediment motion.
V	Vellinga ('82)
VH	Van Hijum ('74)
W	Wang, Toue & Dette ('90)

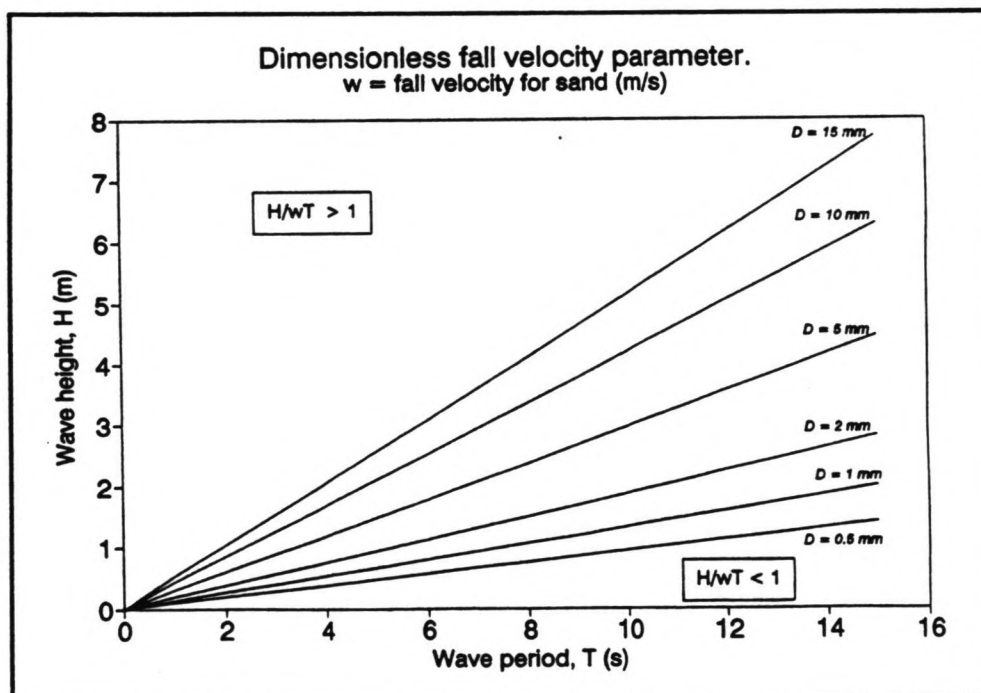


Figure 3.8 The dimensionless fall velocity parameter for different sediment sizes, depending on the wave conditions.

Hence it can be shown that the scale of the dimensionless fall velocity is equal to 1.0:

$$\Omega\left(\frac{H}{wT}\right) = \frac{\mu}{\sqrt{\mu} \sqrt{\mu}} = 1$$

Values of the dimensionless fall velocity parameter in the model are therefore the same as in the prototype.

Table 3.3 The dimensionless fall velocity parameter for the first set of experiments.

Values for H/wT		$D_{50} = 10.0 \text{ mm}$		
H(m)	T(s)			
	7.0	10.0	12.0	
1.0	0.340	0.238	0.198	
1.5	0.510	0.357	0.298	
2.0	0.680	0.476	0.397	

* Second set of experiments.

As can be seen in table 3.3, all the wave conditions used in the experiments give values of H/wT smaller than the critical value. It is expected that for these experiments the transport will be onshore, resulting in accretion at the beach.

To study the behaviour of beach profiles under erosive conditions the value of H/wT should be above the critical one. This can be realized by increasing the wave height, decreasing the wave period or choosing a smaller sediment size (see figure 3.8). For a 1:10 model scale, a larger wave height or a much smaller wave period is impossible as a result of the restrictions imposed by the wave paddle. Therefore a conceptual model scale of 1:30 was used in the second set of experiments. The maximum possible significant wave height is now 6.0 m. in prototype.

The smallest sediment size available in the laboratory had a mean diameter of 0.47 mm (see appendix A). For an undistorted model with a scale of $1:30$ this corresponds to a prototype beach material with a sediment size of 14.1 mm . For these experiments the prototype values of the wave period were chosen the same as in the first set of experiments ($\mu = 10$). This results in values for the wave period in the model of 1.28 , 1.83 and 2.19 seconds. In order to get erosive conditions the wave height must be very large as can be seen in figure 3.8. The experimental data for the second set of experiments are summarized in table 3.4. The value for the dimensionless fall velocity parameter is presented in table 3.5.

To model this prototype beach with anthracite, the mean diameter must have a value of 2.0 mm . The anthracite available had a mean diameter of 1.9 mm (see appendix A). However the amount of anthracite was too small to perform any experiments.

During the experiments it turned out that the waves corresponding to a prototype wave height of 6.0 meter were so steep that they were breaking just beyond the paddle, far offshore. This means that wave energy was dissipated offshore, which resulted in much smaller wave heights near the beach. It can be concluded that with the sizes of sediment available, erosive conditions could not be achieved.

Table 3.4 Experimental data for the second set of experiments.

Model scale	Model material	Sediment size (mm)		Wave height (m)		Wave period (s)	
		prototype	model	prototype	model	prototype	model
1:30	sand	14.1	0.47	3.0	0.10	7.0	1.28
1:30	sand	14.1	0.47	4.5	0.15	10.0	1.83
1:30	sand	14.1	0.47	6.0	0.20	12.0	2.19

Table 3.5 The dimensionless fall velocity parameter for the second set of experiments.

Values for H/wT		$D_{50} = 14.1 \text{ mm}$		
H(m)	T(s)			
	7.0	10.0	12.0	
3.0	0.859	0.601	0.501	
4.5	1.29	0.902	0.751	
6.0	1.72	1.20	1.00	

* Third set of experiments.

A different set of experiments was performed with the 0.47 mm sand. To compare the behaviour of sand models with a different scale, and investigate the scale-effects between them, the same prototype conditions as for the first set of experiments were used. In the first set of experiments the prototype value of the mean diameter, D_{50} , was 10.0 mm . The model scale for the third set of experiments is therefore:

$$\mu = \frac{D_p}{D_m} = \frac{10.0 \text{ mm}}{0.47 \text{ mm}} = 21.28$$

The conditions for the third set of experiments are summarized in table 3.6.

The dimensionless fall velocity parameter will be the same as for the first set of experiments (see table 3.3).

Table 3.6 Experimental data for the third set of experiments.

Model scale	Model material	Sediment size (mm)		Wave height (m)		Wave period (s)	
		prototype	model	prototype	model	prototype	model
1:21	sand	10.0	0.47	1.0	0.0470	7.00	1.52
1:21	sand	10.0	0.47	1.5	0.0705	10.0	2.17
1:21	sand	10.0	0.47	2.0	0.0940	12.0	2.60

3.2.2 Distorted model experiments.

Distorted models have a horizontal scale which is different from the vertical scale. This means that for a distortion of 2.0 ($\lambda = 2\mu$) the beach profile in the model will be twice as steep as in the prototype. However, it is often unclear how to scale down the waves in a distorted model.

* First method.

One way of deriving the model wavelength is by calculating the model wave period, using the time scale. From the model wave period the deep water wave length in the model can be calculated using the formula:

$$L_0 = \frac{g T^2}{2 \pi} \quad (3.12)$$

Where L_0 is the deep water wave length, g is the gravity acceleration and T is the wave period. This gives:

$$L_m = \frac{g T_m^2}{2 \pi} = \frac{g \left(\frac{T_p}{\sqrt{\mu}} \right)^2}{2 \pi} = \frac{g T_p^2}{2 \pi \mu} \quad (3.13)$$

The subscripts m and p refer to model and prototype respectively. This results in undistorted waves in the model.

* Second method.

Another way of deriving the model wave length is by calculating the prototype deep water wave length from:

$$L_0 = \frac{g T^2}{2 \pi} \quad (3.14)$$

Next the model wave length can be found by dividing the prototype wave length by the horizontal scale:

$$L_m = \frac{L_p}{\lambda} = \frac{g T_p^2}{2 \pi} = \frac{g T_p^2}{2 \pi \Delta \mu} \quad (3.15)$$

Where Δ is the model distortion ($\Delta = \lambda/\mu$).

3.2.2.1 Distorted models according to Vellinga's law.

Vellinga ('86) stated explicitly that for distorted models scaled down according to the relations he derived, the waves still had to be undistorted in order to scale shoaling, refraction and diffraction of the waves properly. This means that for a distorted model the same wave conditions as in an undistorted model can be used, because in both scaling laws the time scale is the same ($n_t = \sqrt{\mu}$).

For this reason the experiments conducted as undistorted models can be interpreted as distorted models, representing a different prototype beach.

Vellinga's model law reads:

$$\lambda = \frac{\mu^{1.28}}{n_w^{0.56}}$$

Assuming a distortion $\Delta = 2.0$ ($\lambda = 2\mu$) the scale of the fall velocity can be calculated. For the first set of experiments with a vertical scale of 1:10 this becomes: $n_w = 0.917$, for the second set of experiments with a vertical scale of 1:30 the scale of the fall velocity is $n_w = 1.59$ and for the third set of experiments, with a vertical scale of 1:21 the scale of the fall velocity is $n_w = 1.34$.

This means that the first and the second set of experiments are both models of a prototype beach with a mean diameter of $D_{50} = 0.84 \text{ mm}$ and the second set of experiments is a model of a prototype beach with a mean diameter of $D_{50} = 1.19 \text{ mm}$.

3.2.2.2 The dimensionless fall velocity parameter.

It can be shown easily that Vellinga's model law does not preserve the dimensionless fall velocity in distorted models. The scale of the wave height is equal to the vertical scale, the time scale is equal to the square root of the vertical scale and for a distortion $\Delta = 2.0$ the scale of the fall velocity is equal to $n_w = 0.29\sqrt{\mu}$. This gives:

$$n_{\left(\frac{H}{wT}\right)} = \frac{\mu}{0.29\sqrt{\mu}\sqrt{\mu}} = \frac{1}{0.29} = 3.45$$

Wave conditions which suggest erosive profiles in prototype ($H/wT > 1.0$) show still accretive conditions in the model. An example for the model with a vertical scale of 1:30 is presented in table 3.7. It is interesting to investigate what will actually happen in the model.

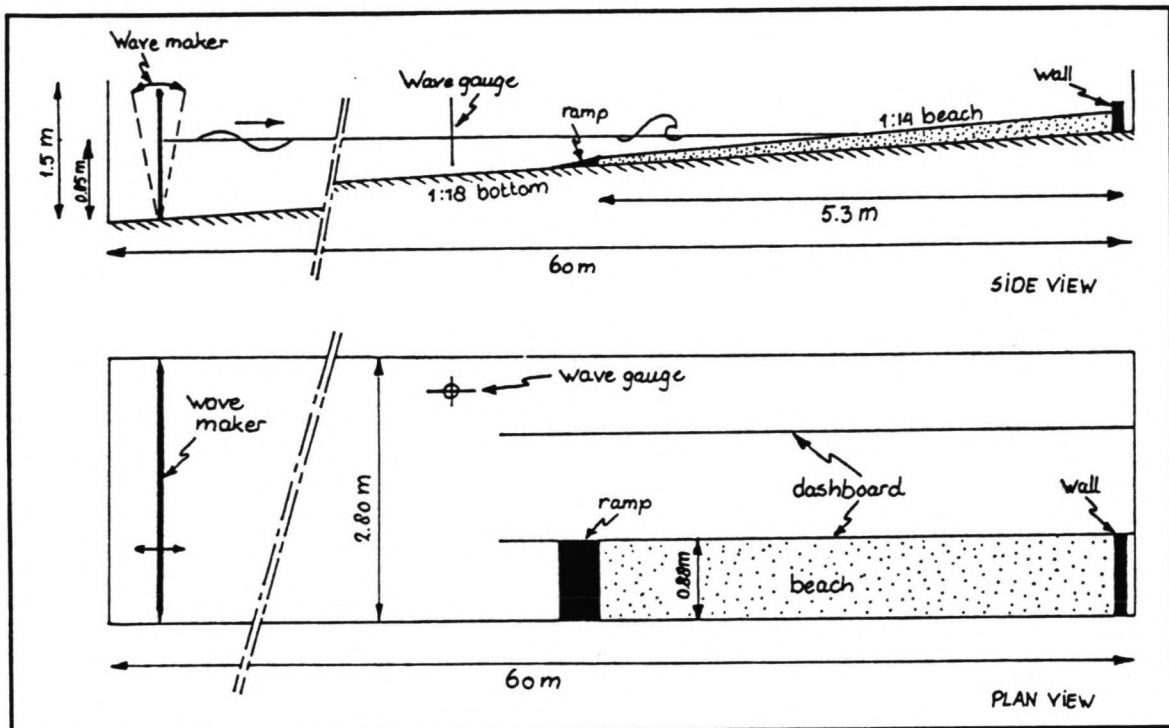


Figure 3.9 Wave tank, wave maker and model beach used in the experiments.

Table 3.7 Values for H/wT in a model with distortion 2.

Values for H/wT $D_{50} = 1.19$ mm (full scale) $\mu = 30$ $\Delta = 2$				
Wave height (m) (full scale)		Wave period (s) (full scale)		
		7.0	10.0	12.0
3.0	prototype	2.96	2.07	1.73
	model	0.859	0.601	0.501
4.5	prototype	4.43	3.11	2.59
	model	1.29	0.902	0.751
6.0	prototype	5.92	4.14	3.45
	model	1.72	1.20	1.00

3.3 Description of the experiments.

The model experiments for this project were performed in the large wave tank in the Hydraulics Laboratory of the Civil Engineering Department of Imperial College.

This wave tank is 60 m long, 1.5 m deep and 2.80 m wide. At the end the tank is divided into two channels. The one used in this project was 0.88 m wide (see figure 3.9).

3.3.1 Waves.

To perform the experiments random waves were generated in the wave tank. Random waves form a more realistic representation of reality than monochromatic waves, with a single wave height and wave period.

Wave data were collected from a wave gauge in the tank.

3.3.1.1 Wave generation.

The waves were generated by a random wave generator. The wave paddle was driven by a computer program, called "Paddkos". Input data for this program are:

- * A file containing the wave signals (in volts) to drive the paddle. The signals correspond to a spectrum with a certain significant wave height and zero-crossing period.
- * A numerical parameter, which has a value of 590.
- * The number of readings. This number represents the length of the signal sent to the paddle. The frequency of the signal is 25 Hz. For half an hour of waves the number of readings is thus: $25 * 30 * 60 = 45,000$.

The file containing the wave signals is generated by the program "Jefwaves". Input data for this file are:

- * The water depth. For the experiments performed this was about 0.85 m.
- * The length of the signal in seconds. For half an hour of waves the length of the signal is 1,800 seconds.
- * The number of frequency components in the spectrum. This number is 80.
- * The number of components above the 85% level, which is 30.

The program can generate a spectrum using observed data or it can calculate the spectrum from one of the following formulae: Pierson-Moskowitz, Jonswap or Goda. In this project the Jonswap spectrum was used, which was specifically derived for the North Sea. The formula reads:

$$S(f) = \alpha H_s^2 T_p^{-4} f^{-5} \exp[-1.25 (T_p f)^{-4}] * \gamma^{\exp[-(T_p f - 1)^2 / 2 \sigma^2]}$$

where:

$$\alpha = \frac{0.0624}{0.230 + 0.0336\gamma - 0.185(1.9 + \gamma)^{-1}}$$

and

$$\begin{aligned} \sigma &= \sigma_a && \text{if } f \leq f_p \\ \sigma &= \sigma_b && \text{if } f \geq f_p \end{aligned}$$

$S(f)$ is the spectral density, f is the frequency of the waves, T is the wave period ($T = 1/f$). The subscript p refers to the peak in the spectrum. γ is the peak enhancement factor which varies between 1 and 7 and has a mean value of 3.3. For $\gamma = 3.3$ the values of σ_a and σ_b are respectively 0.07 and 0.09. Input data for the Jonswap spectrum are:

- * The model value of the significant wave height.
- * The model value of the peak frequency. This is the frequency corresponding to the peak of the spectrum and is usually calculated as:

$$\omega_p = \frac{2\pi}{1.1 T_z}$$

Where ω_p is the peak frequency and T_z is the zero-crossing period.

- * The lower and upper frequency limits. These were taken at $1/3 \omega_p$ and $2.0 \omega_p$. Increasing the range of frequencies requires a longer time to generate the signal.
- * The peak enhancement factor. The mean value of 3.3 is used for the experiments.

The program "Jefwaves" further required:

- * The paddle voltage limit, which is 4.99 volts.
- * The scale factor, which is $2^{13}/20 = 409.6$.

The program gives the bandwidth parameter, the Longuet-Higgins parameter and the paddle voltage standard deviation and then generates the wave signals for the paddle.

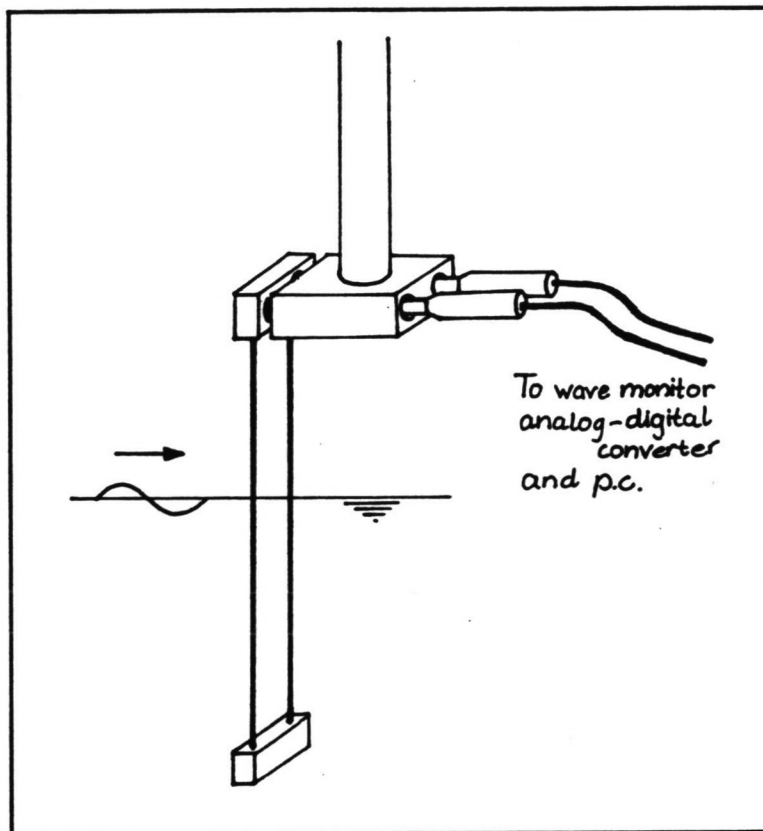


Figure 3.10 Wave gauge used to measure the variation in water level.

3.3.1.2 Wave data collection and analysis.

Wave data were collected in the tank at about 51 m from the wave paddle in a water depth of 0.35 m (see figure 3.10).

A resistance-type wave gauge was used to measure the variation of the water level, a lower resistance corresponding to a higher water level. Calibration of the wave gauge was required to find the wave heights.

To calibrate the wave gauge and collect the wave data the computer program "Collbabn" was used. Input data for this program are:

- * The number of wave gauges. In the experiments only one wave gauge was used.
- * The frequency of the signal, which is 25 Hertz.
- * The number of scans, which is equal to the length of the wave data record times the frequency of the signal (25 Hz). In reality usually 20 minute-records are used for collection of wave data. The same length was used in the first set of experiments although this corresponds to a longer period in reality. The number of scans is therefore 30,000. In the second and third set of experiments the duration of the wave signal was smaller. Therefore wave data were collected for only 10 minutes. The number of scans is now 15,000.

The calibration was performed by moving the wave gauge to different positions and record the value, measured by the computer using an analogue-digital converter. The calibration factor is given by the program and the wave data can be collected.

To analyze the wave data the computer program "Sght" was available, which gives the mean water level in the model, the number of zero crossings, the mean and the significant wave height and the zero-crossing period.

3.3.2 Beach profiles.

The model beach was built at the far end of the tank, about 53 to 58 m from the wave paddle. The beaches were made with a uniform initial slope.

The bottom of the channel in the beach region had a slope of $1:18$. From the literature review it was seen that the initial beach slope should be neither very steep nor very flat. Dependent on the amount of material available and the length of the beach an initial slope of about $1:14$ was used.

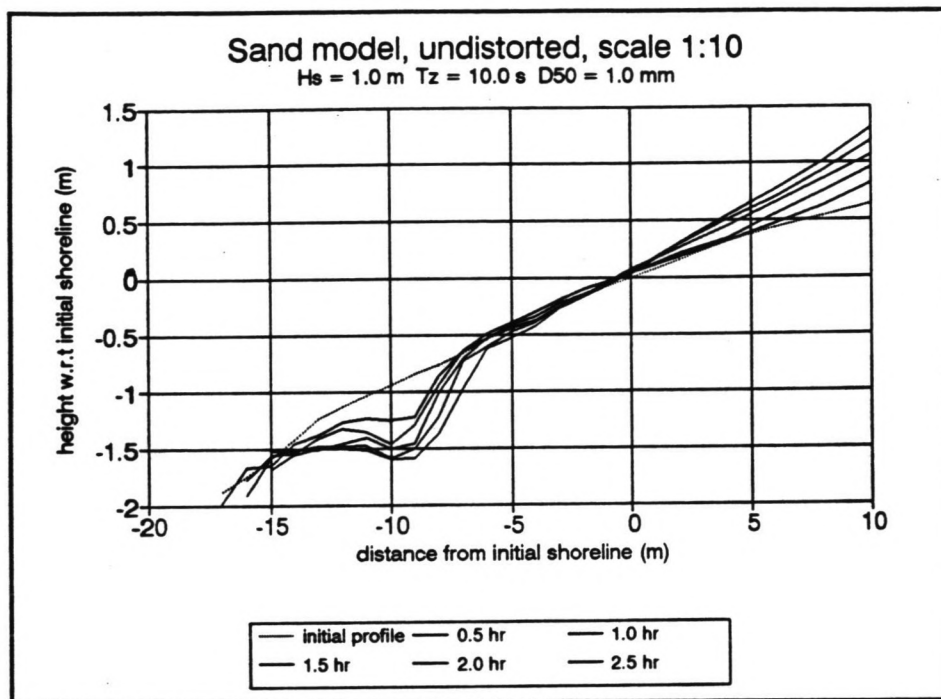


Figure 3.11 Beach profiles in the experiment with a beach length of 2.7 meter.

3.3.2.1 Length of the beach and amount of sediment.

The first experiments were performed with a beach length of 2.7 m. During these runs however it was clear that this beach was far too small.

At the top end of the beach a low wall was used to fix the beach in place. The wave run-up was reaching this wall, which influenced the beach profile. Rather than the creation of a berm at the top of the beach, the beach slope kept increasing due to the building-up of material against the wall.

In the surf zone sediment was picked up by the waves and moved onshore, digging out a step. Before the beach profile attained any form of equilibrium the bottom of the channel was reached, preventing further deepening of the profile. These two phenomena are shown in figure 3.11.

As a result it was decided to use much more sand (0.75 m^3 instead of 0.25 m^3) and make the beach almost twice as long. The new length was 5.2 m.

3.3.2.2 Duration of experiments.

From figure 3.11 it can be seen that even after 2.5 hours of waves an equilibrium profile was not attained yet. To decide how long each run had to last for, the time scale of the model was considered.

It was assumed that the duration of a storm is usually not longer than 12 hours. For a 1:10 model the time scale is equal to $n_r = \sqrt{10} = 3.16$. A storm of 12 hours is therefore modelled by 3.8 hours of waves. The first set of sand experiments had therefore a duration of 4 hours. The experiments with the anthracite models were only performed for 1.5 hours, because anthracite is much more mobile and most of the beach profile evolution took place in the first half hour.

The second and third set of experiments had a duration which was in prototype equal to the duration in the first set of experiments. This means that each run in the second set of experiments ($\mu = 30$) lasted 2.3 hours and each run in the third set of experiments ($\mu = 21$) lasted 2.7 hours.

3.3.2.3 Beach profile measurements.

The beach profile was measured by a normal ruler with a small horizontal plate at the end to prevent it from piercing into the beach (see figure 3.12). The water level was measured in the same way and was used as the reference level.

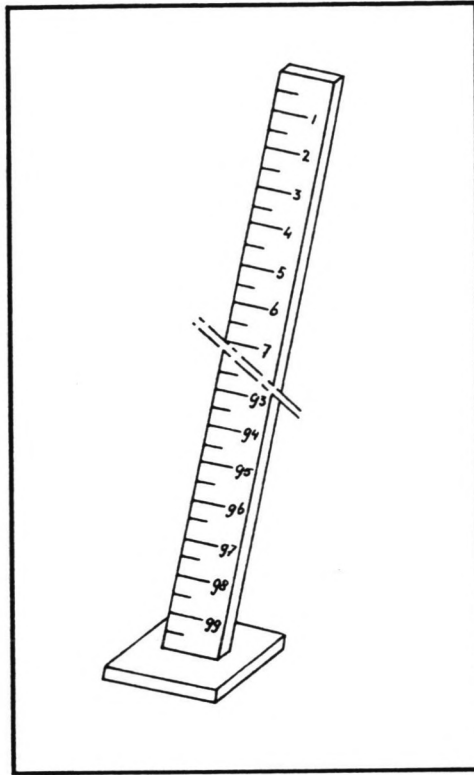


Figure 3.12 Ruler used to measure the depth of the profile.

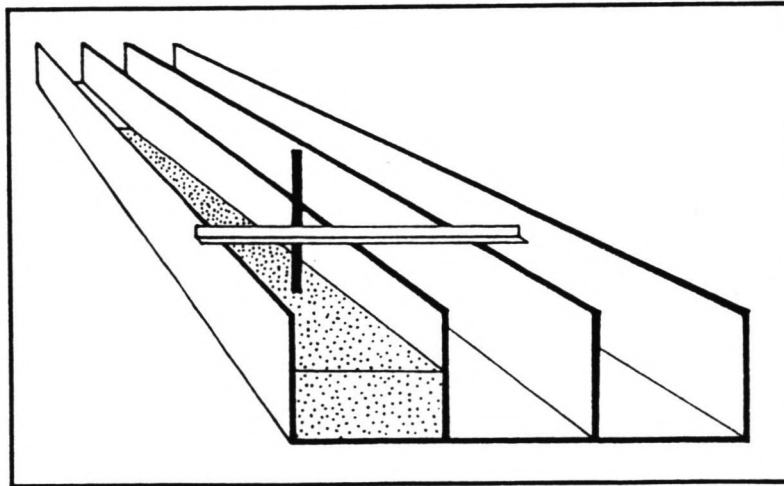


Figure 3.13 Method used to measure the depth of the profile.

The height of the profile was measured with respect to the height of the two dashboards of the channels. These dashboards were level and had the same height and could therefore be used as a datum. A beam was laid over these walls and the depth of the profile from the top of this beam was measured with the ruler (see figure 3.13).

The beach profile was measured along the middle of the channel to avoid side-effects caused by the walls as much as possible.

Measurements were taken every *200 mm* from the uprush limit to the shoreward end of the breaker zone. Because the profile was rather smooth in this region this was considered accurate enough. In the surf zone the profile was less smooth. Ripples were formed in this area and measurements were taken every *100 mm*. All the measurement data of the depth of the profile and their corresponding prototype values can be found in a separate volume: "The evolution of beach profiles under random waves, Measurement data". The graphs of the recorded beach profiles can be found in appendix C.

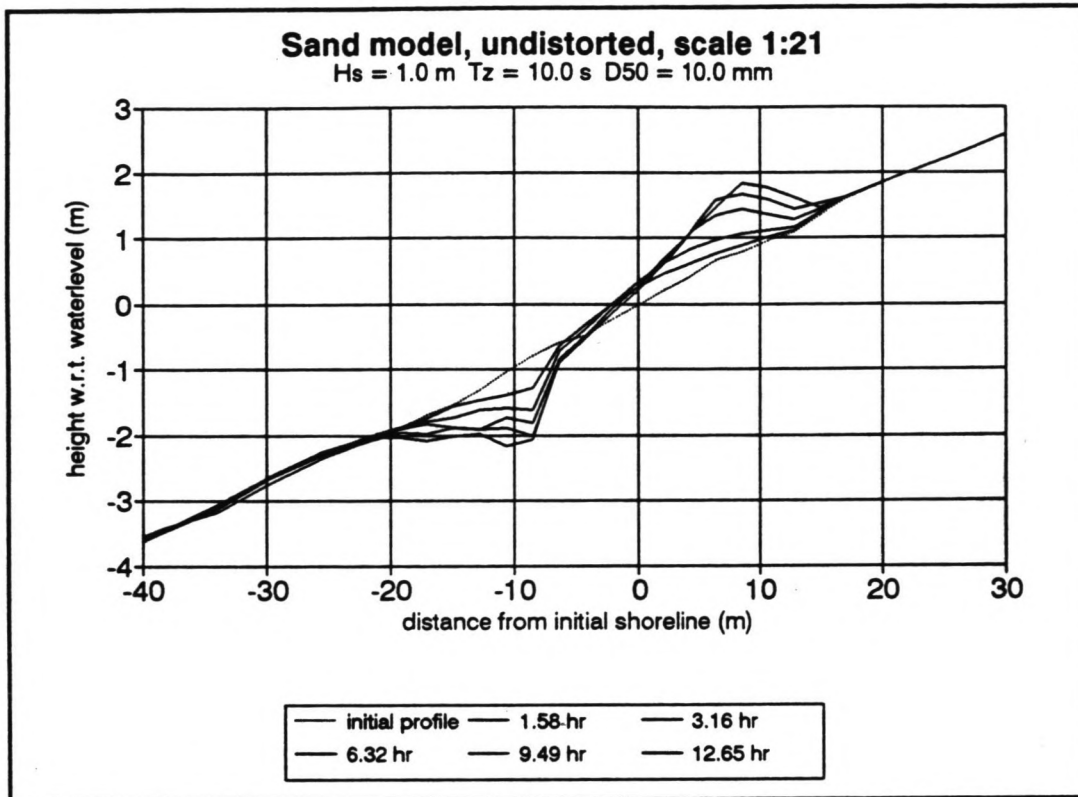


Figure 4.1 A typical example of the development of the "step" profile in the sand models.

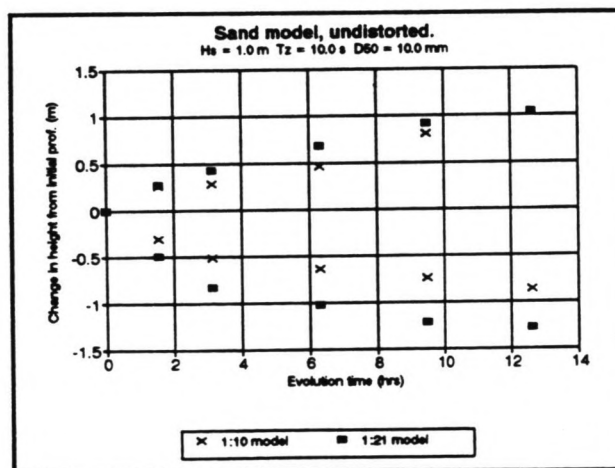


Figure 4.2 The change in depth of profile at the location of the berm and the step, as a function of evolution time.

4 Results.

4.1 General features.

In this chapter the results of the experiments, described in chapter 3, will be discussed. As mentioned before, only accretive conditions have been studied, due to restrictions, imposed by the physical limits of the experimental equipment and the sizes of sediment available. This means that all the profiles are "step"-type profiles, characterized by a berm at the beach, a step in the breaker zone and advancement of the shoreline. The graphs of all the beach profiles can be found in appendix C.

First these three general features and the major differences between sand and anthracite models are discussed. Next, a numerical analysis of the beach profiles is presented.

4.1.1 The berm.

The experiments showed the development of a berm at the beach. This berm is formed by sediment, picked up by the waves in the breaker zone, transported onshore and deposited at the foreshore. The foreshore is the region between the shoreward limit of the breaker zone and the point of maximum wave run-up. Figure 4.1 is a typical example of the development in time of such a berm.

It is clear that the beach profile did not yet attain a state of equilibrium after 4 hours in the model (corresponding to 12.65 hours in prototype), because the height of the berm is still increasing (see figure 4.2).

Because the material is transported by the waves, the length of the berm depends on the maximum run-up. Wave run-up increases if the wave height increases; a rule of thumb is that the height of maximum wave run-up is approximately equal to the significant wave height. However, longer wave periods also result in larger wave run-up. For these reasons some problems were observed in the experiments with the larger wave heights and periods. Because wave run-up reached the low wall at the top of the beach, the profile was influenced by this wall, as can be seen clearly in figure 4.3. Absence of this wall would have allowed larger wave run-up and therefore a longer berm. The berm crest would have been located further onshore. Data and graphs of the berm crest elevation can be found in appendix D1.

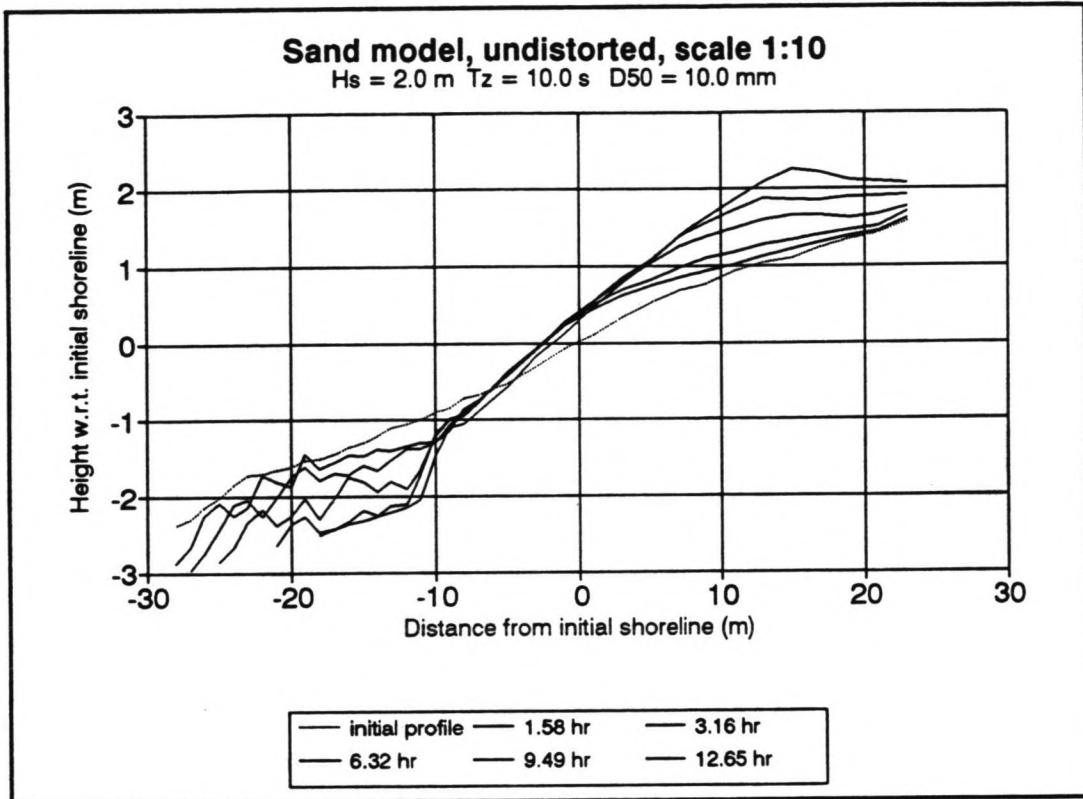


Figure 4.3 The influence of the wall at the top of the beach and the bottom of the tank on the beach profile in the 1:10 model.

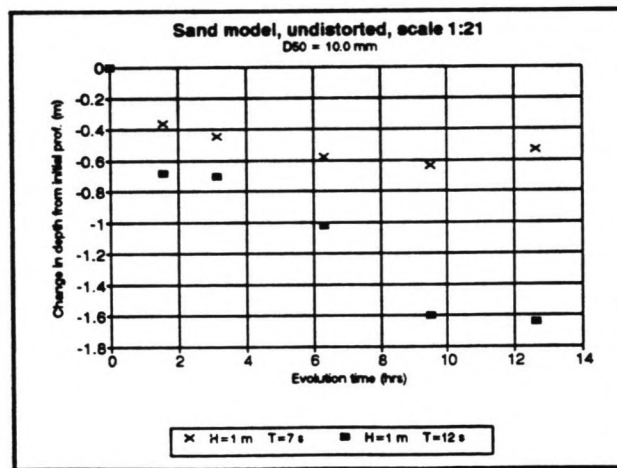


Figure 4.4 The change in depth of profile at the location of the step as a function of the evolution time.

4.1.2 The step.

The turbulence generated by the breaking waves caused the sediment to go into suspension. This sediment is then transported onshore, creating deepening of the profile in the breaker zone. Figure 4.1 shows a typical example of the formation of the step.

Although in some cases the development of the step seem to have achieved some state of equilibrium, in other cases the depth of the profile is still increasing as can be seen in figure 4.4.

Comparison of the different beach profiles (Appendix B) shows that the depth of the step increases for increasing wave heights and periods. This caused again some problems in the experiments with the larger waves, because the bottom of the tank was exposed before the end of the experiment, thus imposing an artificial limit on the beach profile evolution. This is shown in figure 4.3. Data and graphs of the deepening of the step can be found in appendix D1.

4.1.3 Shoreline advancement.

The accretive conditions and resulting deposition of sediment at the beach caused advancement of the shoreline and the creation of a wider beach above still water level. In general the shoreline advancement was achieved very rapidly and did not change much afterwards (see figure 4.5). However, in a few experiments the shoreline was observed to recede again after the earlier advancement. This was caused by the lack of sediment in the breaker zone to be transported onto the berm. Data and graphs of the advancement of the shoreline can be found in appendix E1.

4.1.4 Differences between sand and anthracite models.

In this section the major differences between the sand and anthracite models, observed in the experiments are discussed. The discussion concentrates on the general features, a detailed analysis of the models being presented later in this chapter.

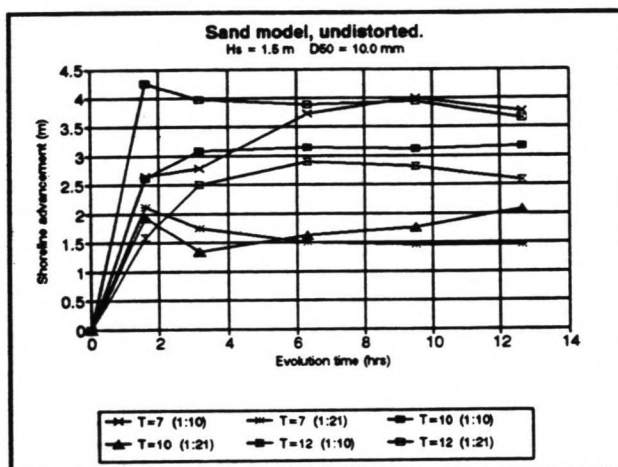


Figure 4.5 The shoreline advancement as a function of the evolution time.

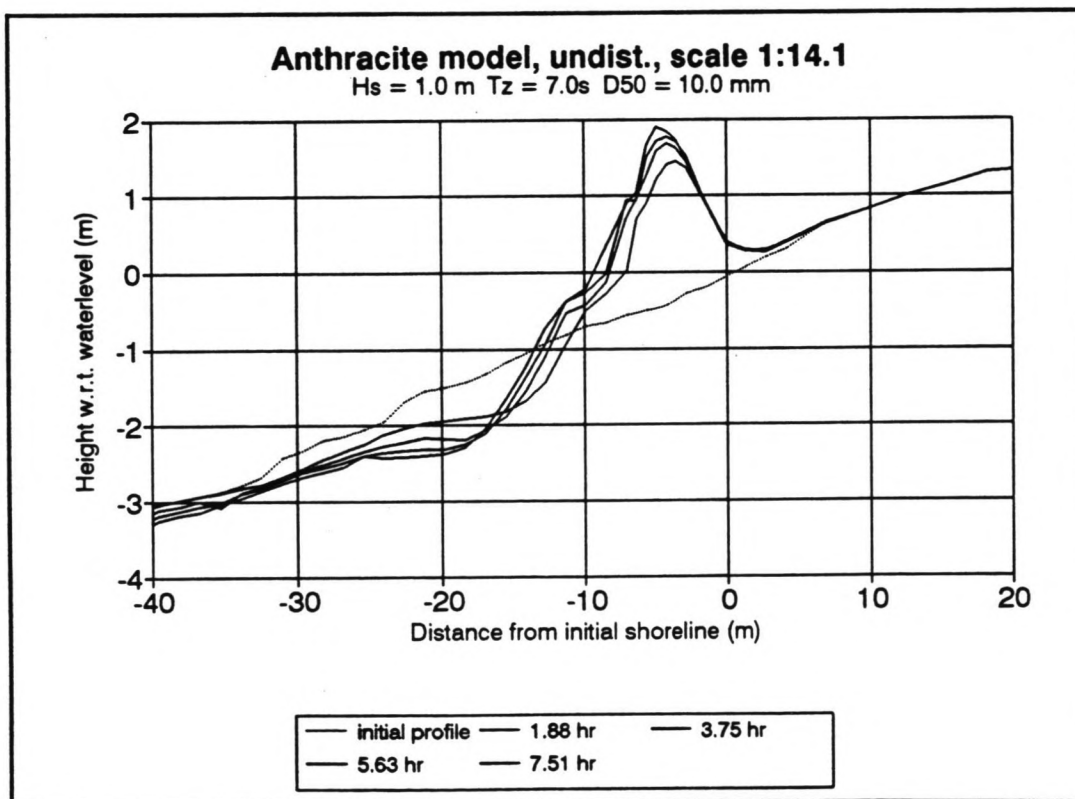


Figure 4.6 A typical example of the very steep beach profiles observed in the anthracite model.

* Sand models.

For the sand models which represented a prototype beach with a mean grain diameter of *10.0 mm*, the maximum elevation of the berm with respect to the initial profile varied between *0.3* and *1.3 m*, depending on the different wave conditions. This corresponded to values of *0.5* to *2.8 m* above still water level.

The maximum deepening of the step with respect to the initial profile varied between *0.3* and *1.6 m*. This meant a depth below still water level of *1.0* to *3.5 m*.

The berm crest was located between *6* and *22 m* from the initial shoreline, while the location of the deepest point of the step varied between *8* and *21 m* seaward of the initial shoreline.

These features resulted in typical "step" profiles, of which an example is shown in figure 4.1.

Beyond the breaker zone the formation of ripples was observed, with the larger and longer waves creating larger and longer ripples. Ripple lengths varied between *0.5* and *3.6 m*, while ripple heights had values of *0.1* to *0.6 m* approximately (full scale values).

* Anthracite models.

Although the anthracite models resulted in the same type of profile, with a berm at the beach and a step in the breaker zone, the differences with the sand model were very large. Unlike the sand models, which seemed to give a reasonable representation of the beach profiles in reality, the anthracite models showed the development of an unrealistic high and steep berm at the beach (see figure 4.6). The mechanism which created this large berm can be described as follows:

The anthracite was transported onshore by the waves. However, much less material was moved back seaward by the downrush. This is considered to be caused by three different factors:

- 1) The high permeability of the anthracite.

Values of the porosity of the sand and the anthracite, used in the models are measured. The results are shown in table 4.1. Although the porosity of the anthracite was not much larger, the anthracite used in the model had a larger permeability. This is a result of the larger particle size of the anthracite (*3.0 mm* compared to *1.0* and *0.47 mm* in the sand models) and consequently larger voids between the particles.

Table 4.1 Porosity of sand and anthracite.

Material	Porosity (%)
Sand BS 14/25	38.7
Sand BS 22/60	37.2
Anthracite Grade 3	45.6

The larger permeability enabled the water to percolate into the beach more easily than in the sand models, where the downrush was more parallel to the beach.

The vertical percolation resulted in an increase in deposition of sediment, compared to the more parallel downrush.

- 2) The relatively heavy weight of anthracite in air.

For anthracite models the scale of the specific gravity, $n_{\gamma'}$ is equal to:

$$n_{\gamma'} = \frac{\gamma'_p}{\gamma'_m} = \frac{1.65}{0.39} = 4.23$$

In order to have the same scale for the weight of the particles in water and in air the density of the model material should be equal to:

$$\frac{\rho_{sp}}{n_{\gamma'}} = \frac{2650}{4.23} = 626 \text{ kg/m}^3$$

However, the density of anthracite is 1390 kg/m^3 , which is 2.2 times as much. Because of the relatively heavy weight of anthracite in air most of the particles which are moved onshore, will stay there and will not be transported back seaward. This also resulted in an increase in deposition at the beach.

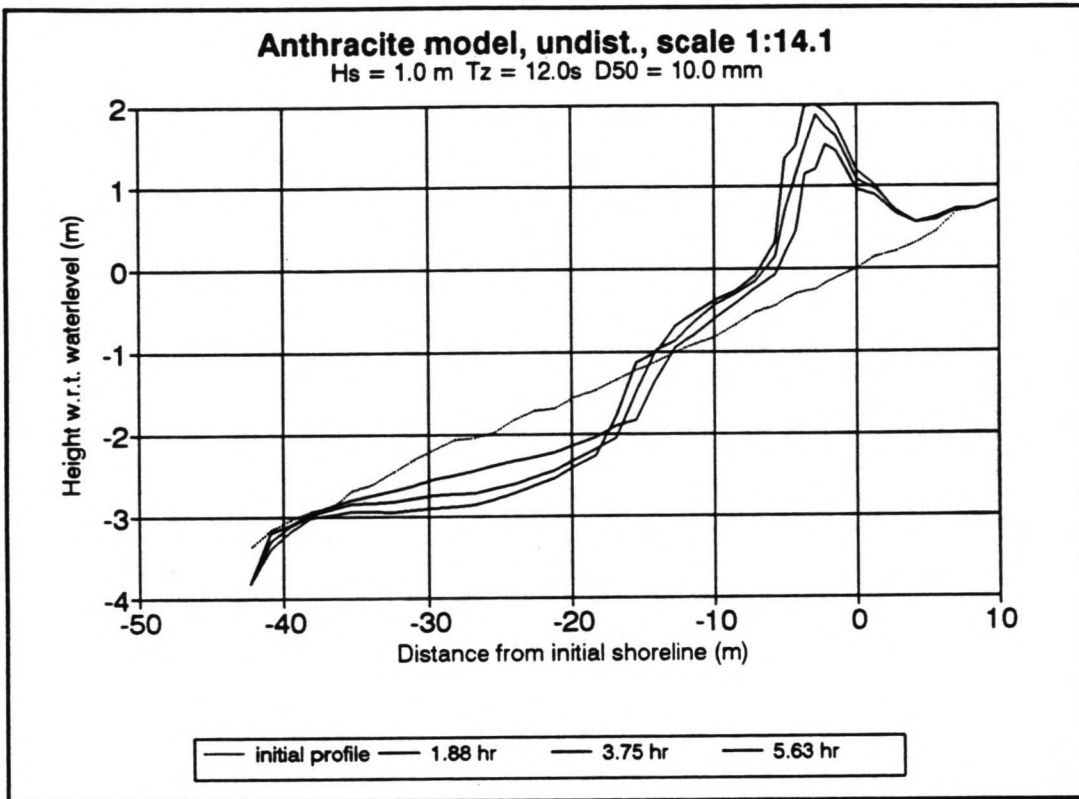


Figure 4.7 A typical example of the abrupt change in slope around the still water level, observed in the anthracite model.

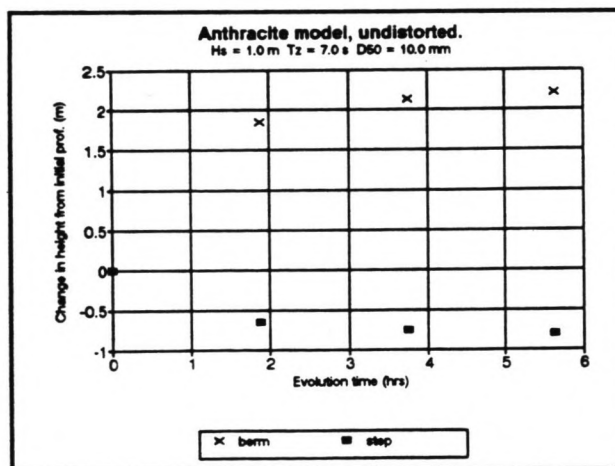


Figure 4.8 The change in depth of profile at the location of the berm and the step as a function of evolution time.

3) The different shape factor of anthracite.

This is probably the most important factor. The angle of repose of the sediment is influenced by the angularity of the particles, which is represented by the shape factor.

The angularity of anthracite is different from that of sand. Measurements of the angle of repose however, only indicated small differences between the angle of repose for sand and anthracite. For dry sand and dry anthracite the angle of repose was 28° and 32° respectively. The angle of repose for wet sediment can be up to 90° for both sand and anthracite.

Despite these small differences in angle of repose, the beach profiles were very different. Beach profiles in the anthracite model showed slopes of the berm-face of almost 90° . This was not observed in the sand models and does not happen in reality. Another phenomenon was the abrupt change in slope around the still water level in the anthracite model, which was not observed in the sand models (see figure 4.7).

Thus it is clear that the relation between the particle angularity, represented by the shape factor, the angle of repose and the beach profile remains uncertain and needs further study.

It was obvious in the experiments that anthracite is much more mobile than sand. Together with the three factors mentioned before, this resulted in a very quick development of a berm at the location of the initial shoreline. Within the first 10 minutes of the experiment (corresponding to half an hour in prototype) a very steep berm was formed, which prevented almost all wave run-up further onshore. This resulted in a further increase in berm height during the rest of the time. Most of the profile change took place in the first half hour of the experiments (Corresponding to almost 2 hours in prototype) as can be seen in figure 4.8.

Beyond the breaker zone no ripples at all were observed in the anthracite model. This may indicate a different kind of transport mechanism in which the whole surface-layer of the beach profile is moving, rather than the individual motion of saltating particles. However no proof of this theory can be given as it was impossible to observe the transport mechanism from above and the window in the side of the tank was located at a different position.

4.2 Analysis of beach profiles.

In this section the analysis of the beach profiles is presented. First the method of empirical eigenfunctions was used to analyze the data. Since this method was not very helpful in analyzing the beach profiles in this project, most of the analysis of the data is made in terms of beach slope.

4.2.1 The method of empirical eigenfunctions.

One way of analyzing beach profile data numerically is by using the method of empirical eigenfunctions. This method is described in **Winant, Inman & Nordstrom ('75)** and **Weishar & Wood ('83)** and is shortly summarized here. Next this method is applied to the beach profile data of the experiments and finally a brief discussion is given on the usefulness of this method.

4.2.1.1 Statistical method.

The beach profiles analyzed are described in terms of h_x , where h is the depth of the profile for a point at a distance x from the shoreline, measured at time t . These data are used to generate sets of empirical eigenfunctions, which best fit the data in the least squares sense. In order to generate these functions, two correlation matrices are formed, a spatial correlation matrix A and a temporal correlation matrix B . The elements of these matrices are defined as follows:

$$a_{ij} = \frac{1}{n_x n_t} \sum_{t=1}^{n_t} (h_{it} * h_{jt})$$

$$b_{ij} = \frac{1}{n_x n_t} \sum_{x=1}^{n_x} (h_{xi} * h_{xj})$$

where n_x is the number of points along the profile and n_t is the number of profiles recorded.

Like any matrix these matrices possess a set of eigenvalues (λ_n) and corresponding eigenvectors (e_n) which satisfy the equation:

$$A e_n = \lambda_n e_n$$

Because of the definition of the matrices A and B the sum of all the eigenvalues is equal to the mean square value of the data and each eigenvalue can be interpreted as being representative of a certain percentage of this mean square value.

In addition it can be shown that if λ_1 is the largest eigenvalue and e_{1x} the corresponding eigenvector, the function $e_{1x}(\lambda_1)^{0.5}$ is the best fit to the correlation matrix in the sense that:

$$\sum_{i,j} (a_{ij} - \lambda_1 e_{1i} e_{1j})^2 = \text{minimum}$$

Therefore the function $e_{1x}(\lambda_1)^{0.5}$ can be interpreted as the mean beach function. The other eigenvalues then represent the variance of the data from this mean beach function.

4.2.1.2 Analysis of the data from the experiments.

The method of empirical eigenfunctions was used to analyze the beach profiles of the first set of sand experiments and the following illustrates a typical result. For the experiment with a significant wave height of 1.0 m and a zero-crossing period of 7.0 seconds, 41 points along the profile had been measured ($n_x = 41$) and the experiment consisted of 9 profiles ($n_t = 9$).

In order to use the method of empirical eigenfunctions, a computer program was written to generate the correlation matrices and to determine their eigenvalues and corresponding eigenvectors (see appendix G).

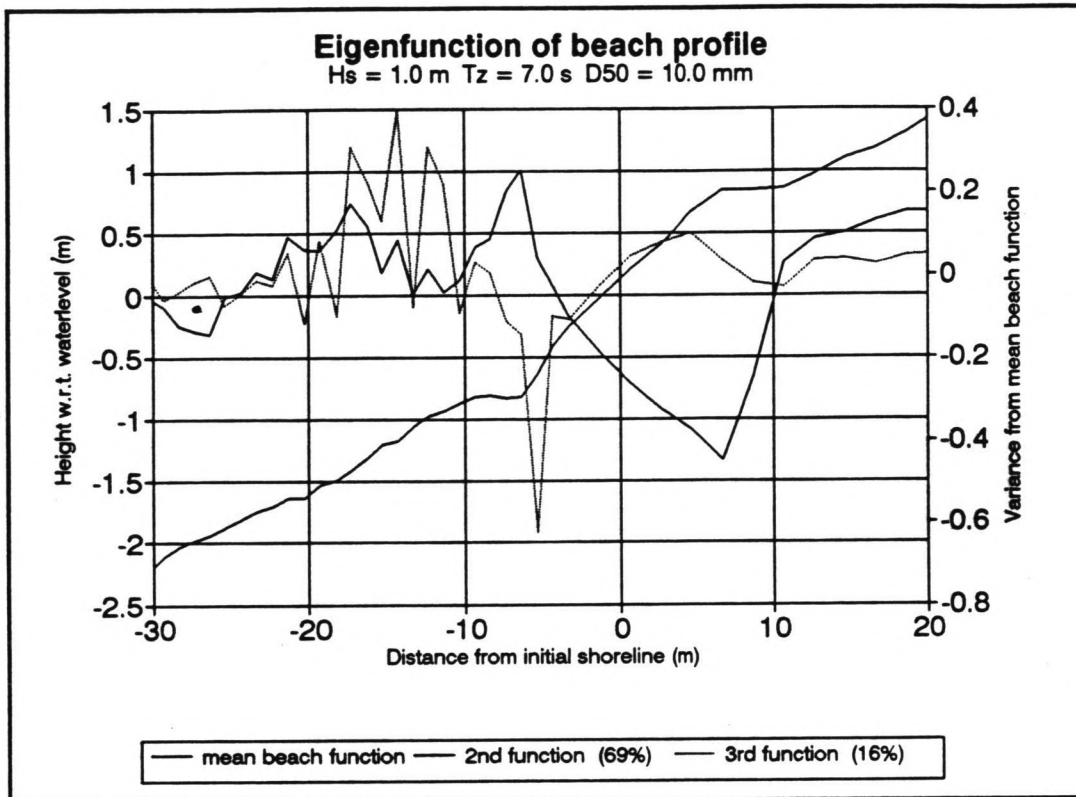


Figure 4.9 Results of the eigenfunction analysis.

Results of the statistical analysis are presented in table 4.2. For the 5 largest eigenvalues the percentages of the mean square value of the data are given, together with the percentage of the variance from the mean beach function.

Figure 4.9 shows the mean beach function $e_{1,x}(\lambda_1)^{0.5}$ and the eigenfunctions corresponding to the second and third eigenvalues, representing the variance from the mean beach function.

The mean beach function shows the berm and the step in the profile and the second eigenfunctions, which accounts for 69.11% of the variance, shows that the largest fluctuations in the beach profile indeed take place at the location of the berm and the step.

Table 4.2 Results of the statistical analysis.

	Percentage of the mean square value of the data.	Percentage of the variance from the mean beach function.
Mean beach function	99.75	
Eigenvalue 2	0.17	69.11
Eigenvalue 3	0.039	15.85
Eigenvalue 4	0.013	5.32
Eigenvalue 5	0.0076	3.08

4.2.1.3 Discussion.

Although the method of empirical eigenfunctions works well, it is not very helpful in the analysis of beach profiles in this project. The reasons are:

- 1) The mean beach function represents the mean of the initial profile and the 8 profiles measured in one experiment under certain wave conditions. This has no physical meaning as the initial profile is just a uniform slope in order to have a starting point in the experiments.
- 2) The second eigenfunction does present where the largest variations in the profile take place. However, this can also be seen very easily from the recorded beach profiles.

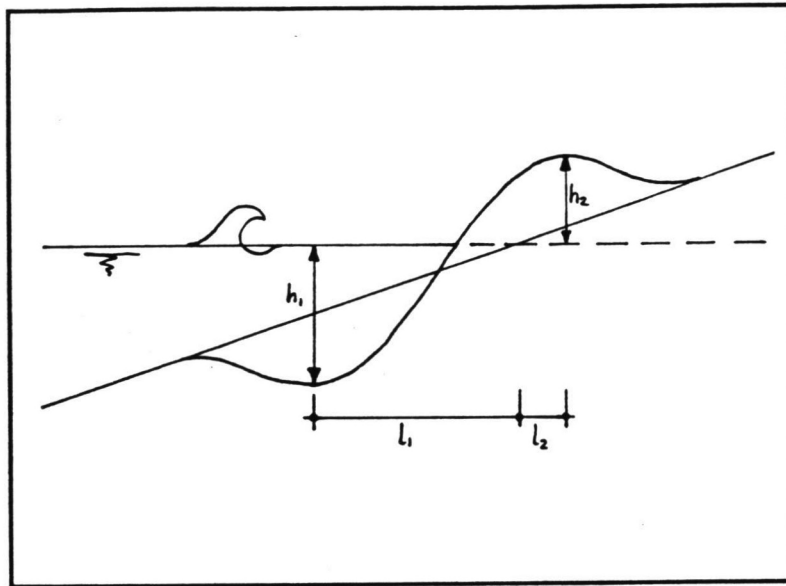


Figure 4.10 Definition sketch of the mean beach slope $\tan\beta$.

The method of empirical eigenfunctions is therefore not very helpful in the analysis of these beach profiles and is not used furthermore in this project.

The method would be very helpful however in the analysis of field data, where the mean beach function represents the mean profile for a certain location over a period of one or more years, with largely varying wave conditions. The other eigenfunctions would then indicate the seasonal or even shorter-term variations from this profile.

4.2.2 The beach slope as a representation of the beach profile.

In section 4.2.1 it was shown that the method of empirical eigenfunctions is not very helpful in the analysis of the beach profiles in this project. Therefore a different method of analyzing the profiles had to be found.

One possibility would be to compare the measured profiles with the " $h = Ay^n$ " model. However it is clear that this model assumes a monotonically decreasing beach slope. This means that if this method is used, it is impossible to study the behaviour of the characteristic berm and step of the profiles. For this reason the mean beach slope was used as a representation of the profile.

4.2.2.1 First evaluation of the beach slopes.

The mean beach slope, used as a representation of the beach profile, is defined as the slope between the highest point of the berm and the lowest point of the step, in order to include these two characteristic features into the analysis of the beach profiles. Values of the mean beach slope are calculated in terms of $\tan\beta$, where

$$\tan\beta = \frac{(h_1 + h_2)}{(y_1 + y_2)}$$

A definition sketch is shown in figure 4.10.

The mean beach slope between the berm crest and the trough of the step was calculated for different times in the evolution of the profile. These values can be found in appendix F1. The values of the mean beach slope after 12.65 hours of profile evolution in the sand model and 5.63 hours in the anthracite model (prototype values) are summarized in table 4.3.

Table 4.3 Values of the mean beach slope after the last measured profile.

	sand model 1:10	sand model 1:21	anthr. model 1:14	sand model 1:30
H/wT	tan β	tan β	tan β	tan β
0.198	0.138	0.159	0.202	
0.238	0.181	0.209	0.219	
0.298	0.127	0.179	0.235	
0.340	0.146	0.184	0.264	
0.357	0.154	0.148	0.219	
0.397	0.139	0.141		
0.476	0.165	0.139	0.243	
0.501				0.187
0.510	0.149	0.153	0.228	
0.601				0.138
0.680	0.148	0.111	0.195	
0.751				0.117
0.859				0.150
0.902				0.110

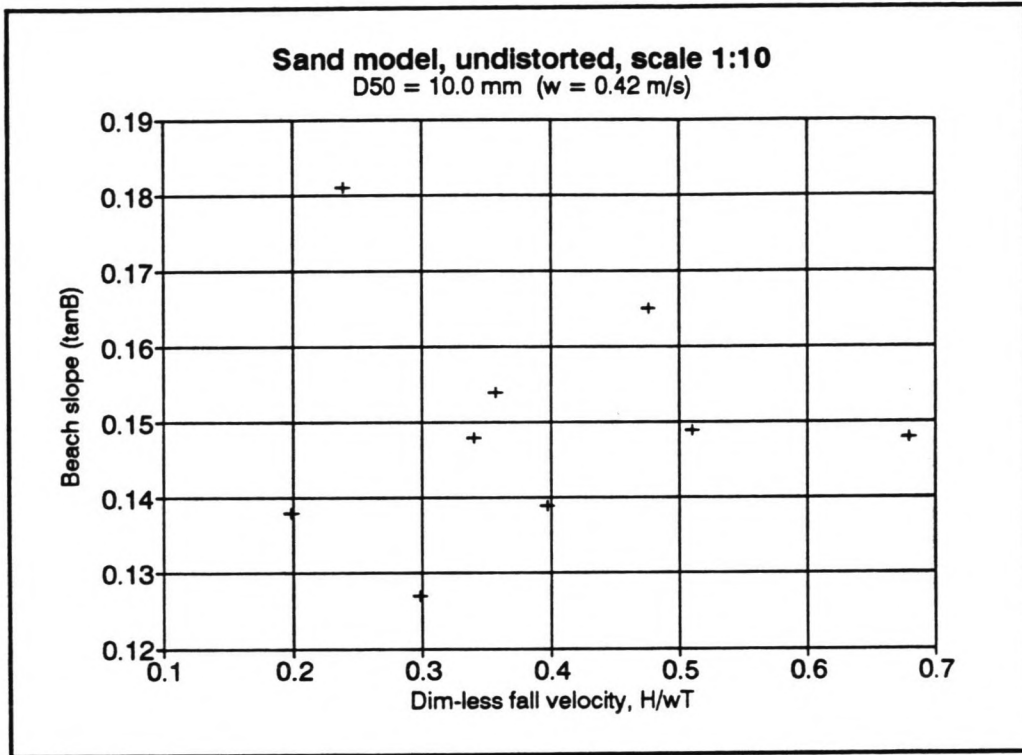


Figure 4.11 The mean beach slope as function of H/wT for the 1:10 sand model.

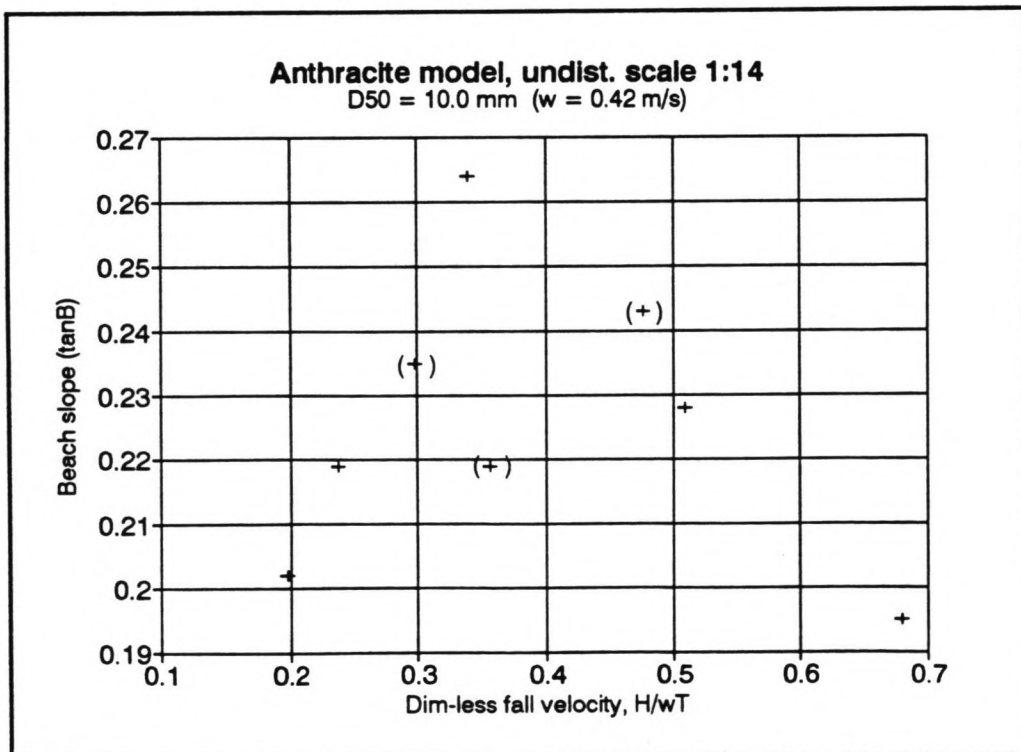


Figure 4.12 The mean beach slope as function of H/wT for the 1:14 anthracite model.

* The 1:10 sand model.

The mean beach slope in the 1:10 model varies between $\tan\beta = 0.127$ and $\tan\beta = 0.181$ as can be seen in figure 4.11, where $\tan\beta$ is plotted against the dimensionless fall velocity parameter H/wT . This figure shows that there is no clear relationship between these two parameters. This is caused by many different factors. The most important two are the reaching of the wall at the top of the beach and the exposure of the bottom of the tank at the location of the step, for the larger waves. These two phenomena obviously influence the beach profile and consequently the mean beach slope.

It is difficult to determine the extent to which the wall and the bottom have influenced the mean beach slope. Without the wall at the top of the beach, the berm crest would have been located further onshore, resulting in a flatter slope. However, the exposure of the bottom in the breaker zone may have created a lack of sediment to be transported onshore, which would have caused a lower berm crest than in reality. Thus in reality the berm crest may have been higher, resulting in a steeper mean beach slope.

The exposure of the bottom also restricted the deepening of the step. Without this restriction the mean beach slope would have been steeper. However the deepest point of the step may have been located further offshore causing a flatter mean beach slope.

The profiles which are affected by these features are the ones with:

$$H_s = 1.5 \text{ m } T_z = 12.0 \text{ s } (H/wT = 0.298).$$

$$H_s = 2.0 \text{ m } T_z = 10.0 \text{ s } (H/wT = 0.476).$$

$$H_s = 2.0 \text{ m } T_z = 12.0 \text{ s } (H/wT = 0.397).$$

But even if these three points are excluded, the relationship between $\tan\beta$ and H/wT is not clear. (The graphs of the profiles can be found in appendix C.)

Other reasons which may have affected the mean beach slope are the difference between the wave heights and periods used as input data for the wave maker and the actual wave heights and periods in the model, the uncertainties in the calculation of the fall velocity and the uncertainties in the definition of the berm crest and the deepest point of the step. These factors are discussed later.

* The 1:14 anthracite model.

The values of the mean beach slope for the anthracite model show clearly that the beach profiles in this model are much steeper than the profiles in the sand models. Values of $\tan\beta$ vary between 0.195 and 0.264. Like in the sand model with a 1:10 scale there is no clear relationship between the beach slope and H/wT (see figure 4.12).

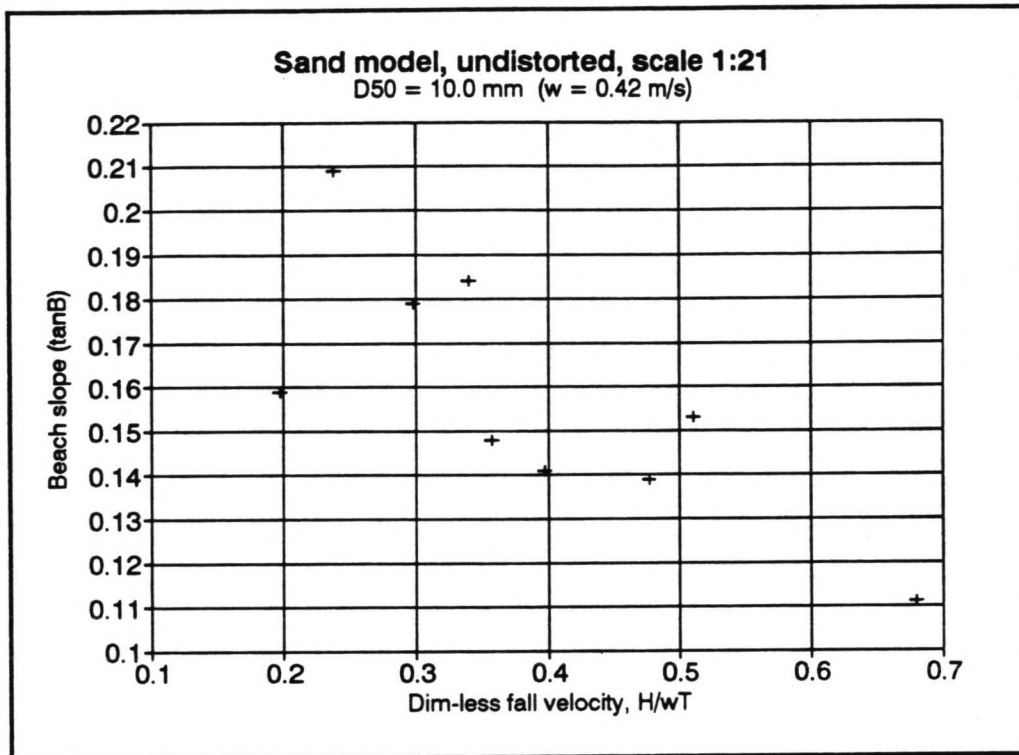


Figure 4.13 The mean beach slope as a function of H/wT for the 1:21 sand model.

Again problems were caused by the exposure of the bottom. In the case of $H_s = 1.5$ m and $T_z = 12$ s ($H/wT = 0.298$) the bottom was exposed after 1.5 hours of experiments, corresponding to an evolution time of 5.63 hours in prototype.

For the experiments with:

$$H_s = 1.5 \text{ m } T_z = 10 \text{ s } (H/wT = 0.357)$$

$$H_s = 2.0 \text{ m } T_z = 10 \text{ s } (H/wT = 0.476)$$

values of the beach slope are plotted for an evolution time of 3.75 hours rather than 5.63 hours, because exposure of the bottom was already observed at this time (1 hour of experiment). The beach slope for $H_s = 2.0$ m and $T_z = 12.0$ s ($H/wT = 0.397$) is even not shown at all, because the bottom of the tank was exposed after the first run of half an hour (1.88 hours in prototype). The graphs of the profiles can be found in appendix C.

It is again very difficult to say how the beach slopes would have changed if there had been no artificial limit on the profile development, caused by the bottom of the tank. The same considerations as for the 1:10 sand model are valid for the anthracite model.

However even in the experiments where the bottom was not exposed it was very difficult to define a deepest point of the profile (see for example the profile for $H_s = 1.5$ m and $T_z = 7.0$ s). This made it very difficult to define a mean beach slope.

Because of all these uncertainties in the beach profiles of the anthracite model it is impossible to derive a relationship between the mean beach slope and H/wT .

* The 1:21 sand model.

The values of the mean beach slope for the 1:21 sand model vary between $\tan\beta = 0.111$ and $\tan\beta = 0.209$ and are shown in figure 4.13. The data points are still rather widely scattered, although there is a trend of a decrease in the mean beach slope for increasing H/wT . This can be explained as follows:

An increase of H/wT means steeper waves and more erosive conditions. The larger H/wT , the less sediment will be transported onshore, resulting in a lower berm and consequently a flatter mean beach slope.

The wall and the bottom of the tank did not have any influence on the profiles in this set of experiments and from this point of view the data for the 1:21 model are more reliable than those for the 1:10 model.

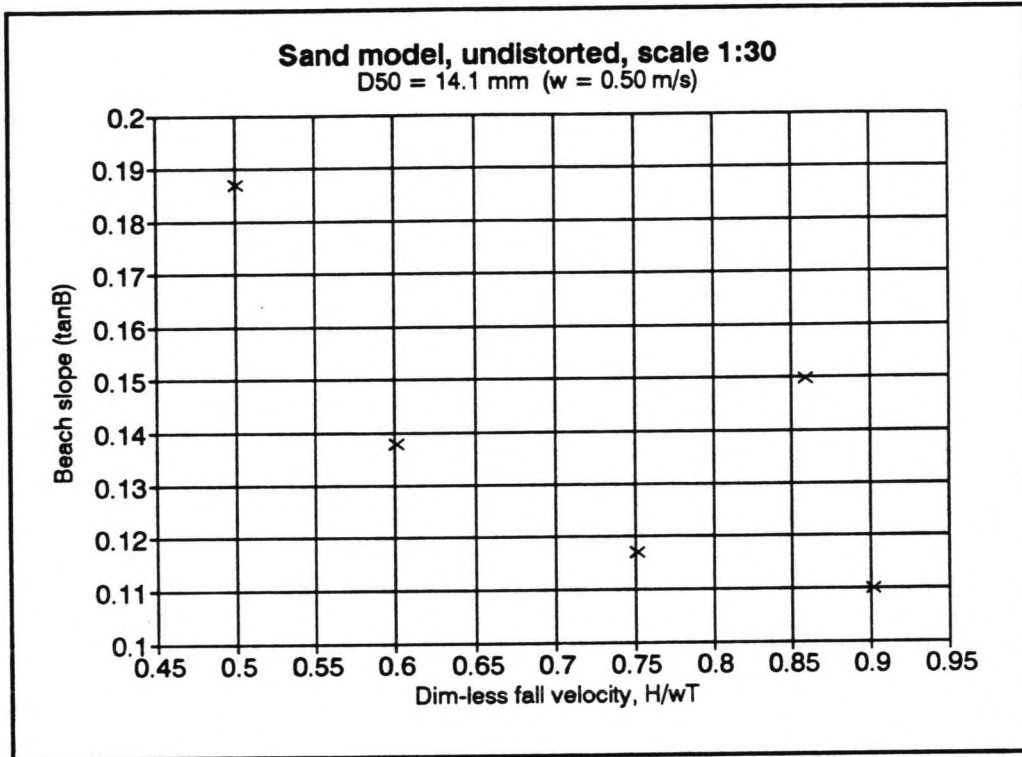


Figure 4.14 The mean beach slope as a function of H/wT for the 1:30 sand model.

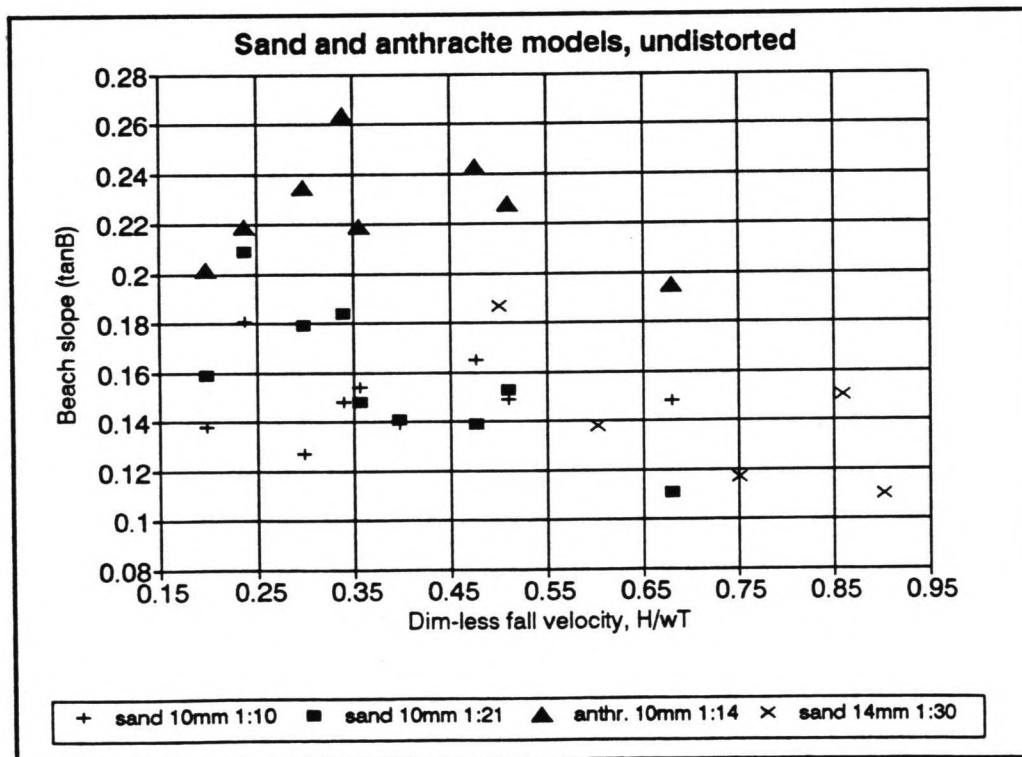


Figure 4.15 Comparison of the mean beach slope as a function of H/wT for the 4 different models.

* The 1:30 sand model.

The prototype conditions for the 1:30 model were different from the other three models. Wave heights varied between 3.0 and 6.0 m and the mean grain diameter of the sediment had a value of 14.1 mm rather than 10.0 mm. This resulted in larger values of H/wT as was presented before in table 3.5. (Note: The experiments with $H_s = 6.0$ m and $T_z = 10.0$ and 12.0 s have not been performed.) The two experiments with the largest values of H/wT showed no development of a berm. The wave conditions for these experiments were:

$$\begin{aligned} H_s &= 4.5 \text{ m} \quad T_z = 7 \text{ s} \quad (H/wT = 1.29) \\ H_s &= 6.0 \text{ m} \quad T_z = 7 \text{ s} \quad (H/wT = 1.72) \end{aligned}$$

For this reason the mean beach slope was only calculated for the 5 remaining experiments. Values of the mean beach slope vary between $\tan\beta = 0.117$ and $\tan\beta = 0.187$ and are shown in figure 4.14. They are again widely scattered, but like in the 1:21 model there is a trend of decreasing mean beach slope for increasing H/wT . However one has to be careful to draw conclusions from only 5 data points.

In this model some problems which may have influenced the relation between the mean beach slope and H/wT were related to the wave conditions. The steeper waves were breaking far offshore, resulting in different wave conditions at the beach from those used as input data for the wave maker. This problem is also discussed later.

* Summary.

The values of the mean beach slope, used as a representation of the beach profiles in the different models are shown together in figure 4.15. This figure shows that there is no clear relationship between the mean beach slope ($\tan\beta$) and the dimensionless fall velocity parameter (H/wT), although over-all there is a slight trend of a decreasing mean beach slope for increasing H/wT .

The data points of the 1:10 model do not show this trend which is mainly caused by the influence of the wall at the top of the beach and the bottom of the tank in this model.

Next the figure shows clearly that the anthracite model gives much steeper slopes than all the sand models. For this model also the bottom of the tank largely influenced the beach profiles.

4.2.2.2 Errors in measurement and calculation of H/wT and the mean beach slope.

The relation between the mean beach slope ($\tan\beta$) and the dimensionless fall velocity parameter (H/wT) has been affected by errors in the calculation or measurement of these two parameters.

Errors in H/wT result from differences in H/T between values of this parameter used as input data for the wave maker and recorded values of H/T from the wave gauge. Another factor influencing the value of H/wT is the calculation of the fall velocity, w .

Errors in the mean beach slope arise from errors in the measurements of the depth of the profile and from uncertainties in the definition of the berm crest and the deepest point of the step.

The magnitude of these errors and the influence on the relation between $\tan\beta$ and H/wT have been investigated and are discussed in this section.

* Errors in H/wT .

For the investigation of the errors in H/wT due to the differences in wave conditions between input data and recorded values, H/T is considered as a single parameter. Combination of the value of H_s from one run with the value of T_s of another run in the same experiment, would result in unrealistic values for the magnitude of the error in H/T .

Measured values of H_s and T_s can be found in appendix B. Although wave data were collected for every run, resulting in 8 wave data records per experiment, only 2 of them are presented in the appendix. The reason for this is that the input signal was exactly the same for each run and in general the measurements showed indeed little variation in values of H_s and T_s .

In appendix H the prototype values of H/T , derived from the collected wave data in the models are presented together with the values used as input data for the wave maker. An extra column shows the difference between these values in terms of the percentage error. It is clear that there are some differences between the input data and the recorded values. One reason for this is that the values for the input data are for deep-water conditions, while the wave gauge is situated in much more shallow water.

The largest differences occur for the steep waves in the 1:30 model. This was to be expected, because the steeper waves in this model were breaking far offshore, causing energy dissipation and a corresponding decrease in wave height. Recorded values of H/T are indeed substantially smaller than the input data (25 - 28 %).

* Errors in the calculation of w .

Errors in the calculation of the fall velocity arise mainly from the uncertainties in shape factor of the sediment. As shown in section 3.1.1 the fall velocity is a function of the drag coefficient, which depends on the shape of the sediment particles.

In the calculation of the fall velocity for sand a typical value of the shape factor of 0.7 was used. However, if the shape factor varied between for example 0.6 and 0.8 the fall velocities would have been different as can be seen in table 4.4.

table 4.4 *Fall velocities for different values of the shape factor.*

Fall velocity, w (m/s)			
D_{50} (mm)	Shape factor (-)		
	0.6	0.7	0.8
10.0	0.370	0.420	0.487
14.1	0.439	0.499	0.578

In the anthracite models the difference between the calculated and the actual fall velocity will be even larger. This is a result of the angular shape of the anthracite particles.

A larger angularity is characterized by a smaller shape factor, which would result in a smaller fall velocity. This means that the values of the mean beach slope calculated in the anthracite model would correspond to larger values of H/wT and the data points would have been shifted towards the right-hand-side of the graph in figure 4.15. This separates the data points even further from the data points of the sand models.

This shows that the shape factor is an important factor in the parameter H/wT , because of the influence on the fall velocity w . However the exact relation between particle angularity, represented by the shape factor, and the fall velocity is still unclear and merits further study.

* Errors in H/wT .

The variation in H/wT resulting from the variation in H/T and in w is presented in table 4.5. In order not to have unrealistic large variations in H/wT , it is assumed that the maximum value of H/T does not occur together with the minimum value of w and vice versa.

The values are presented in relation to the values of H/wT which were used before in the analysis of the mean beach slope.

Table 4.5 Variation in values of H/wT .

Variation in H/wT			
Values of H/wT used before.	sand model 1:10	sand model 1:21	sand model 1:30
0.198	0.175 - 0.225	0.171 - 0.219	
0.238	0.205 - 0.240	0.217 - 0.270	
0.298	0.278 - 0.338	0.282 - 0.338	
0.340	0.322 - 0.386	0.293 - 0.346	
0.357	0.344 - 0.405	0.341 - 0.405	
0.397	0.399 - 0.451	0.372 - 0.451	
0.476	0.504 - 0.541	0.447 - 0.541	
0.501			0.458 - 0.546
0.510	0.494 - 0.579	0.440 - 0.524	
0.601			0.519 - 0.633
0.680	0.686 - 0.772	0.664 - 0.772	
0.751			0.720 - 0.854
0.859			0.730 - 0.742
0.902			0.802 - 1.03
1.29			1.08 - 1.11
1.72			1.41 - 1.48

* Errors in the depth of the profile.

Measurements of the depth of the profile were made with a normal ruler. This was a very simple but still very accurate method. For example at locations above the maximum wave run-up, where the height of the beach profile did not change, the measured height was

indeed exactly the same every time. Measurement errors are therefore of the order of plus or minus 1.0 mm . This corresponds to values of 0.01 to 0.03 m in prototype, depending on the model scale.

The location of the measurement points along the profile was established from signs on the side-wall of the tank. This was also reasonable accurate. Some problems in measuring the height at the exact location were observed for the very steep slopes, caused by the small horizontal plate at the end of the ruler. Errors in the location of the measurement points are therefore of the order of plus or minus 10 mm . This corresponds to 0.10 to 0.30 m in prototype, depending on the scale of the model. All the measurement data of the depth of the profile and their corresponding prototype values can be found in a separate volume: "The evolution of beach profiles under random waves, Measurement data".

Errors in measurements of the depth of the profile or the location of the measurement points therefore caused only minor errors in the values for the mean beach slope. Much larger errors in the mean beach slope were introduced by the influence of the bottom and the low wall at the top of the beach, as was mentioned before. Another factor influencing the value of the mean beach slope is the irregularity in the profile beyond the breaker zone, due to the formation of ripples. This is especially important in the $1:10$ model. These irregularities made it difficult to define the deepest point of the step.

In the first evaluation of the mean slope, only actually measured points of the profile were used to calculate the mean beach slope. In order to get more reliable values for the mean beach slope, the profiles were evaluated again and the mean beach slope was calculated using more realistic values for the berm crest and deepest point of the step. The analysis is presented in the next section.

4.2.2.3 Revised evaluation of the mean beach slope.

In this section the beach profiles are re-analyzed in terms of the mean beach slope. This time more realistic values were used for the height of the berm and the depth of the step. Especially for the $1:10$ model estimated values were used for the berm crest elevation and the deepening of the step, which would have occurred in absence of the wall and the bottom of the tank.

Revised values for the mean beach slope are presented in table 4.6.

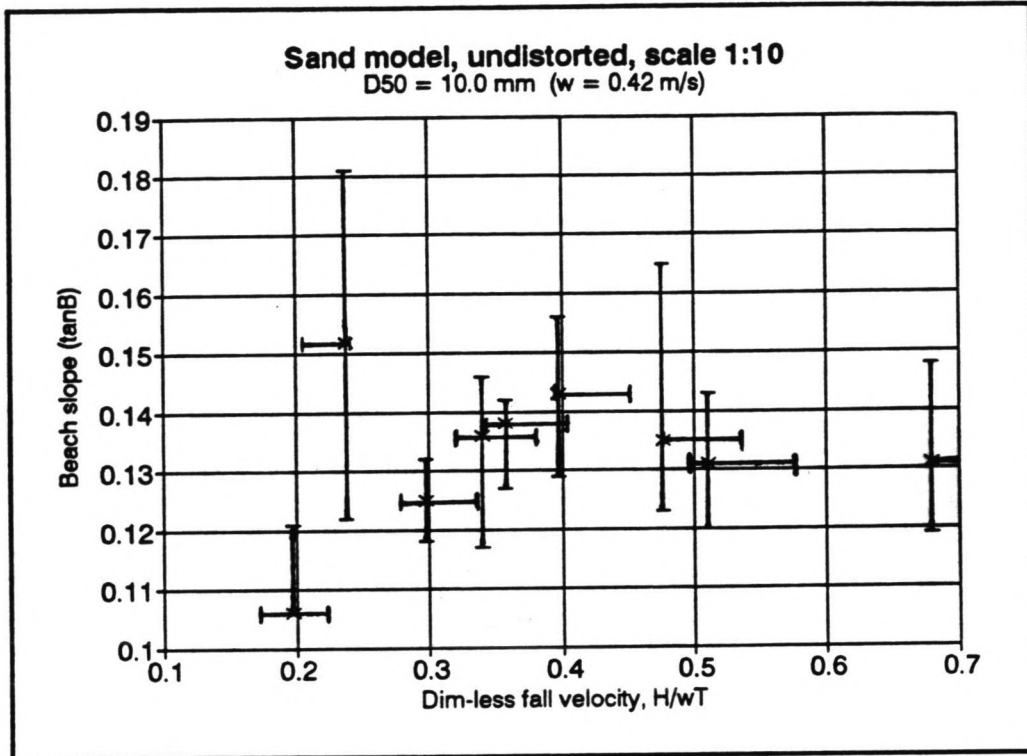


Figure 4.16 Revised analysis of the mean beach slope as a function of H/wT for the 1:10 sand model.

Table 4.6 Revised values for the mean beach slope.

H/wT	sand model 1:10	sand model 1:21	sand model 1:30
	tan β	tan β	tan β
0.198	0.106	0.154	
0.238	0.152	0.197	
0.298	0.125	0.157	
0.340	0.136	0.171	
0.357	0.138	0.134	
0.397	0.143	0.149	
0.476	0.135	0.132	
0.501			0.155
0.510	0.131	0.153	
0.601			0.164
0.680	0.131	0.116	
0.751			0.139
0.859			0.141
0.902			0.116

* The 1:10 sand model.

Figure 4.16 shows the values of the mean beach slope for the 1:10 model. In general the new values are slightly smaller than those calculated previously. For comparison: The average value of the mean beach slopes in the first analysis was:

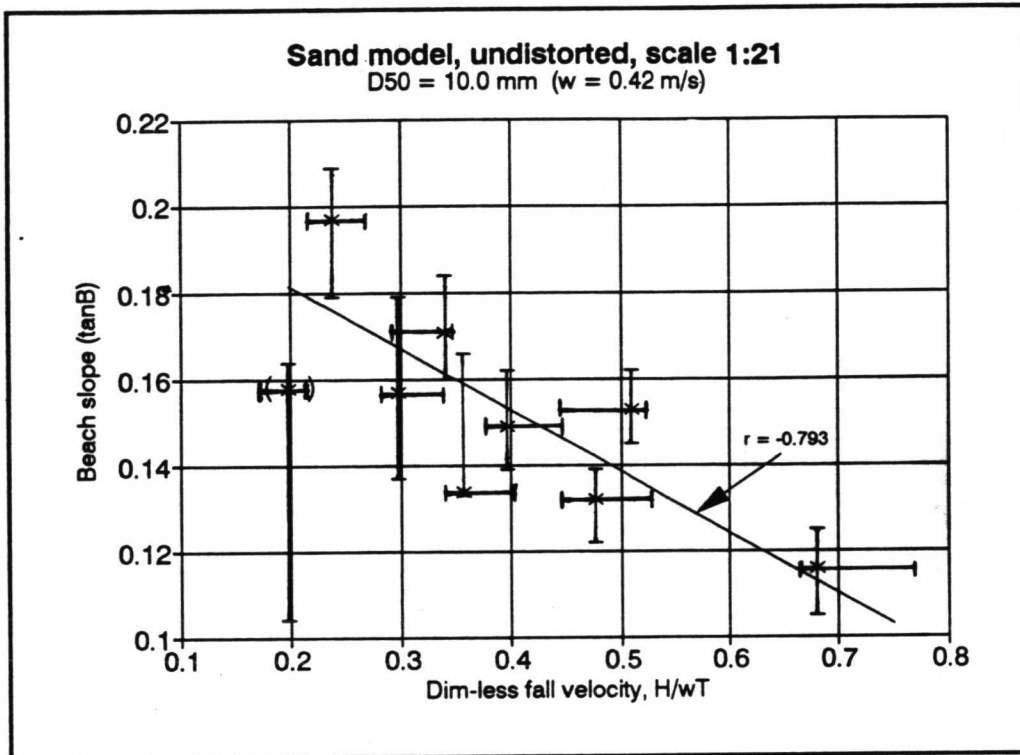


Figure 4.17 Linear regression analysis of the mean beach slope as a function of H/wT for the 1:21 sand model.

$$\overline{\tan\beta} = 0.150$$

while the average value for the new slopes was:

$$\overline{\tan\beta} = 0.133$$

The difference between these two values is about 12%

It is obvious that there are still many uncertainties in the values of the mean beach slope and a clear relationship between $\tan\beta$ and H/wT cannot be derived for the 1:10 model.

* The 1:21 sand model.

For the 1:21 sand model, values of the mean beach slope are presented in figure 4.17. There is a clear trend of decreasing slope for increasing H/wT . The value of $\tan\beta$ for $H/wT = 0.198$ however is an exception. This is a result of the absence of a berm at the beach in this profile, where $H_s = 1.0$ m and $T_z = 12.0$ s (see appendix C). The absence of the berm can be explained as follows:

The parameter H/wT can be interpreted as the ratio of a parameter representing a driving velocity to move the sediment particles (H/T) and a parameter representing a resisting velocity, which forces the particle back to its rest-position (w). However, in order to achieve sediment motion the driving velocity must exceed a certain threshold velocity. If the ratio of H/T to w becomes too small, the velocity to move the particle will be smaller than the threshold velocity and no sediment transport will occur.

To give an indication of the magnitude of the threshold velocity, The Shields-parameter is considered, which is defined as:

$$\theta_c = \frac{\tau_c}{(\rho_s - \rho) g D_{50}}$$

where τ_c is the critical value of the bed shear stress, at which sediment just begins to move, ρ_s is the density of the sediment, ρ is the density of water and D_{50} is the mean diameter of the sediment. The threshold velocity is defined as:

$$u_* = \sqrt{\left(\frac{\tau_c}{\rho}\right)}$$

Substitution into the Shields-parameter gives:

$$\theta_c = \frac{u_*^2}{\gamma' g D_{50}}$$

where $\gamma' = (\rho_s - \rho)/\rho$.

Shields recommended a critical value for θ_c of about 0.03 in uni-directional flow. This gives a value of the threshold velocity of $u_* = 0.0697 \text{ m/s}$.

The value of H/T in this experiment is equal to 0.0833 m/s. This is indeed close to the threshold velocity, which explains why there is hardly any sediment transport and consequently no development of a berm at the beach. For this reason the data point for $H/wT = 0.198$ is excluded from the analysis.

Note: The Shields-parameter is derived for sediment transport in uni-directional flow and is not absolutely valid in this case of oscillatory motion under waves. However it gives a rough indication of the value of the threshold velocity of sediment motion.

A linear regression analysis was applied to the remaining data points in order to study the relation between $\tan\beta$ and H/wT . The result of this linear regression is a relationship between these two parameters and a regression coefficient, which represents the extent to which the mean beach slope is determined by H/wT .

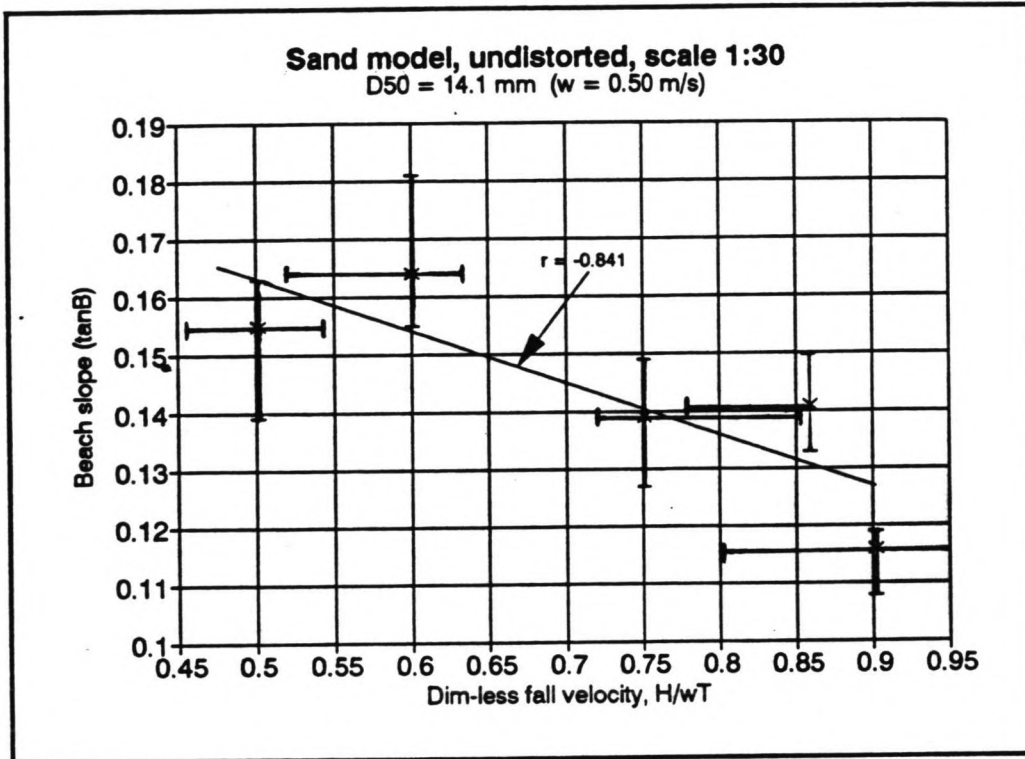


Figure 4.18 Linear regression analysis of the mean beach slope for the 1:30 sand model.

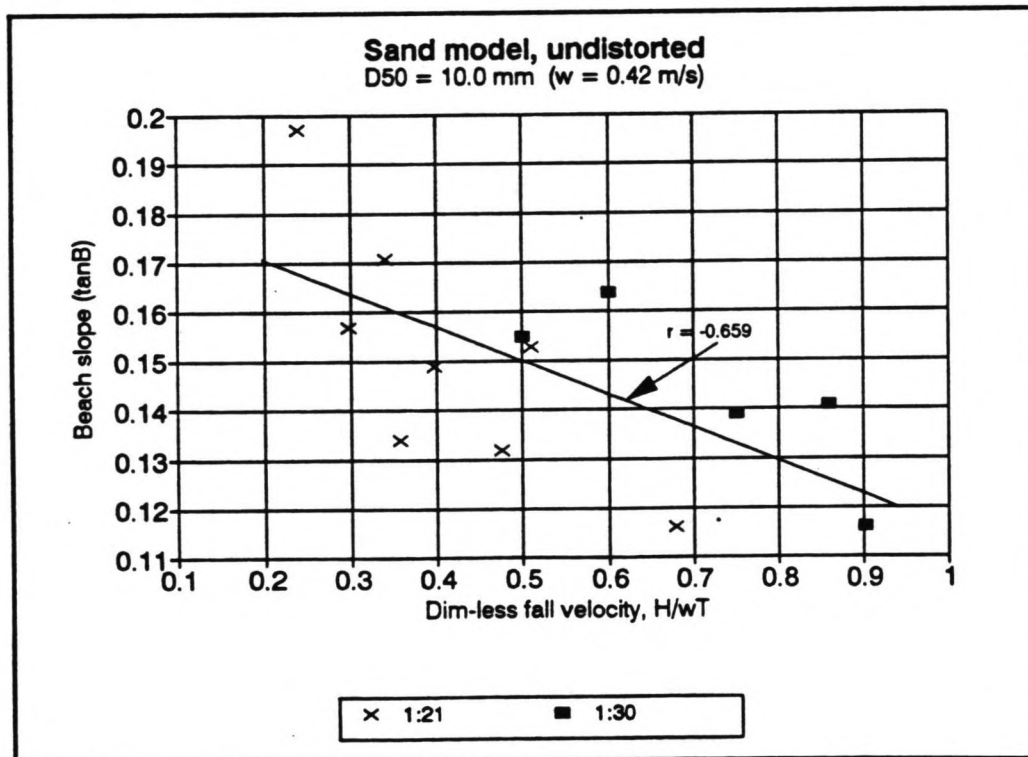


Figure 4.19 Linear regression analysis of the mean beach slope as a function of H/wT for data of the 1:21 and the 1:30 sand models.

The relationship for this model reads:

$$\tan\beta = -0.143 * \left(\frac{H}{wT} \right) + 0.210$$

The regression coefficient for this relation is: $r = -0.793$.

Because of the threshold velocity of sediment motion this relation is only valid for values of H/wT greater than 0.2. Obviously there is also an upper limit of H/wT for this relationship, imposed by the critical value of H/wT between accretive and erosive conditions. Although it remains unclear what the exact value of this upper limit is, it is at least 0.9, because this was the value of H/wT in the 1:30 model for which still accretive conditions were observed.

* The 1:30 sand model.

The mean beach slope for the 5 data points in the 1:30 model also shows a clear trend of decreasing mean beach slope for increasing H/wT (see figure 4.18). The points are less scattered than in the earlier analysis.

A linear regression for this model resulted in:

$$\tan\beta = -0.0904 * \left(\frac{H}{wT} \right) + 0.208$$

The regression coefficient, r was -0.841 which means that 84.1% of the value of the mean beach slope is determined by the value of H/wT . However, as mentioned before, it is dangerous to draw definitive conclusions from only 5 data points.

* Comparison of the mean beach slope for the 1:21 and the 1:30 sand models.

Because the analysis of the beach profiles in both the 1:21 and the 1:30 model showed a decrease in $\tan\beta$ for increasing values of H/wT , they are plotted together in figure 4.19. The figure shows that the data points for the 1:30 model all lie above the ones for the 1:21 model, but the trend is still the same.

A linear regression applied to these 13 data points gave the following equation for the mean beach slope as a function of H/wT :

$$\tan\beta = -0.0687 * \left(\frac{H}{wT} \right) + 0.185$$

The regression coefficient is smaller than in the separate analyses of the two models and has a value of $r = -0.659$. This shows that the relation between $\tan\beta$ and H/wT for the two models together is not so good. One reason for the difference in the data can result from scale-effects between the two models, which are very difficult to quantify.

4.2.2.4 Summary.

In section 4.2.2. the analysis of the beach profiles is presented in terms of the mean beach slope, which was defined as the average slope between the highest point of the berm and the lowest point of the step.

Although relationships were derived between $\tan\beta$ and H/wT for the 1:21 and the 1:30 sand models, the 1:10 sand model and the anthracite model did not show a relation between these two parameters.

For the 1:10 model this is mainly caused by the influence of the wall and the bottom of the tank. The exposure of the bottom of the tank also largely influenced the profiles in the anthracite model. However even more important in this model was the uncertainty in the fall velocity due to uncertainties in the shape factor of the lighter anthracite. The different shape factor is considered to be the most important reason for the very steep slopes observed in the anthracite model.

4.2.3 Analysis in terms of three characteristic points of the beach profile.

It was noted in section 4.2.2 that the mean beach slope is in general too variable to use as a representation of the beach profile. From a practical point of view the mean beach slope is not a very helpful parameter either, because it does not clearly describe the shape of the new beach profile which will develop after a certain period of wave attack.

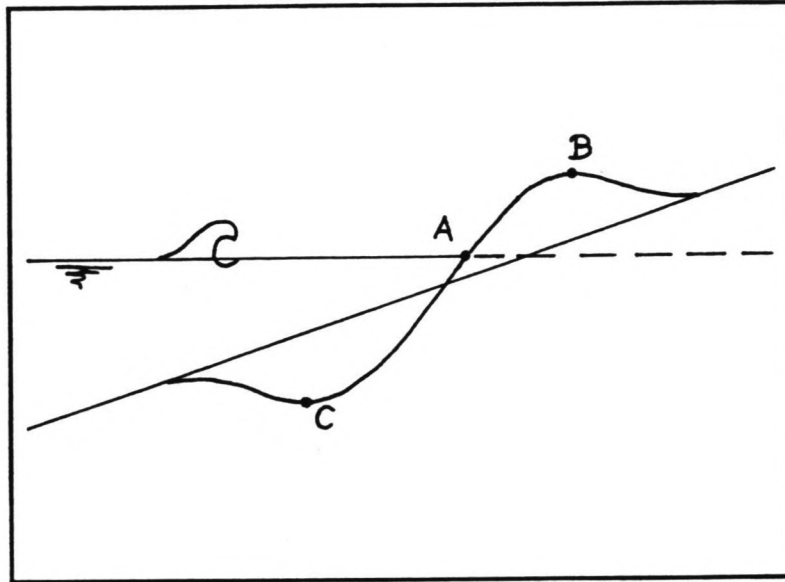


Figure 4.20 Definition sketch of the three characteristic points of the beach profile.

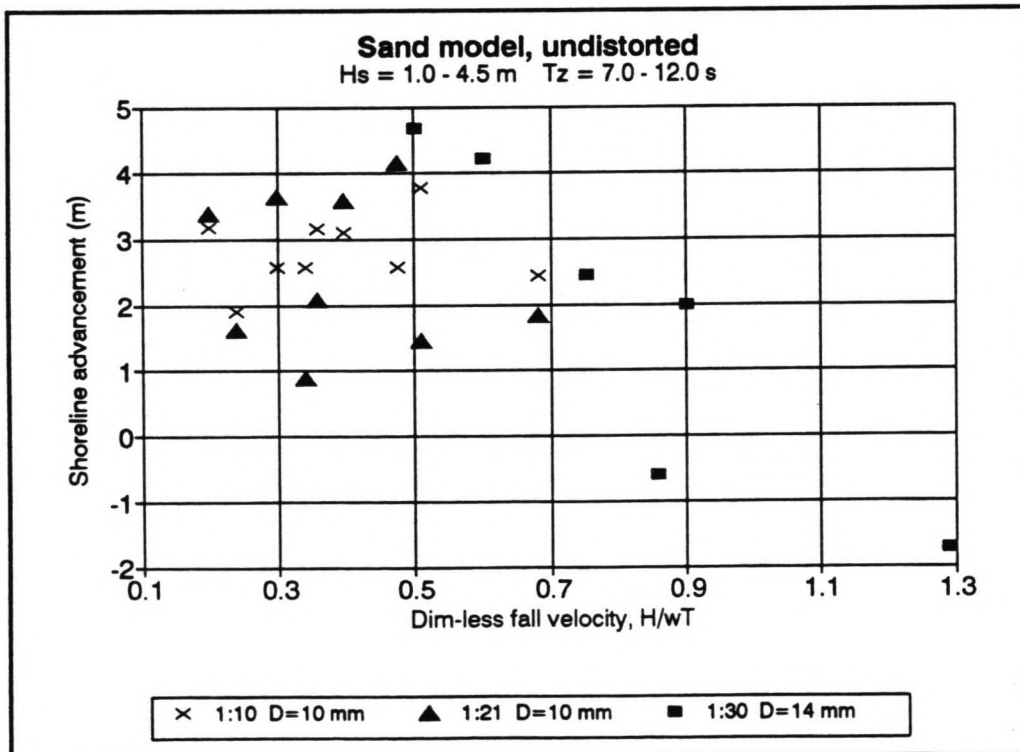


Figure 4.21 The change of the shoreline position as a function of H/wT for the three sand models.

In order to be able to predict the new beach profile, if the sediment characteristics and wave conditions are known, one needs to know the behaviour of the three characteristic points of the beach profile (see figure 4.20):

- The position of the new shoreline (A).
- The location and the height of the berm crest (B).
- The location and the depth of the deepest point of the step (C).

If these three points are known with respect to the initial profile, one can sketch the new profile, assuming that at the top of the beach and at the seaward limit of active motion this profile approaches asymptotically the initial profile. This results from the fact that there is no change in profile above the level of maximum wave run-up nor beyond the limit of active motion. The limit of active motion is determined by the magnitude of the orbital velocity at the bed and the threshold velocity of the sediment and therefore by the wave conditions, the water depth and the sediment characteristics.

For the three sand models the three characteristic points of the beach profile are calculated and tabulated in appendix D2 and E2.

Note: The berm crest elevation, the deepening of the step and the position of the new shoreline were calculated before, but like in the case of the mean beach slope a second calculation was made, using more realistic values for the berm crest height and the depth of the step.

* The shoreline position.

The values for the position of the shoreline after 12.65 hours of profile evolution are presented in figure 4.21 as a function of H/wT . The value for the experiment in the 1:30 model with $H_s = 6.0$ m and $T_s = 7.0$ s is not plotted, because this experiment was only performed for 1.4 hours, corresponding to an evolution time of 6.32 rather than 12.65 hours.

For the 1:10 and the 1:21 models there is no relation at all between the advancement of the shoreline and the parameter H/wT , apart from the fact that they all show accretion of the beach at the shoreline. The data for the 1:30 model show a recession of the shoreline for the larger values of H/wT . If the movement of the shoreline is taken as a criterion between erosive and accretive profiles, the critical value for H/wT derived from these experiments would be about 1.0, the same value as recommended by the Shore Protection Manual ('84).

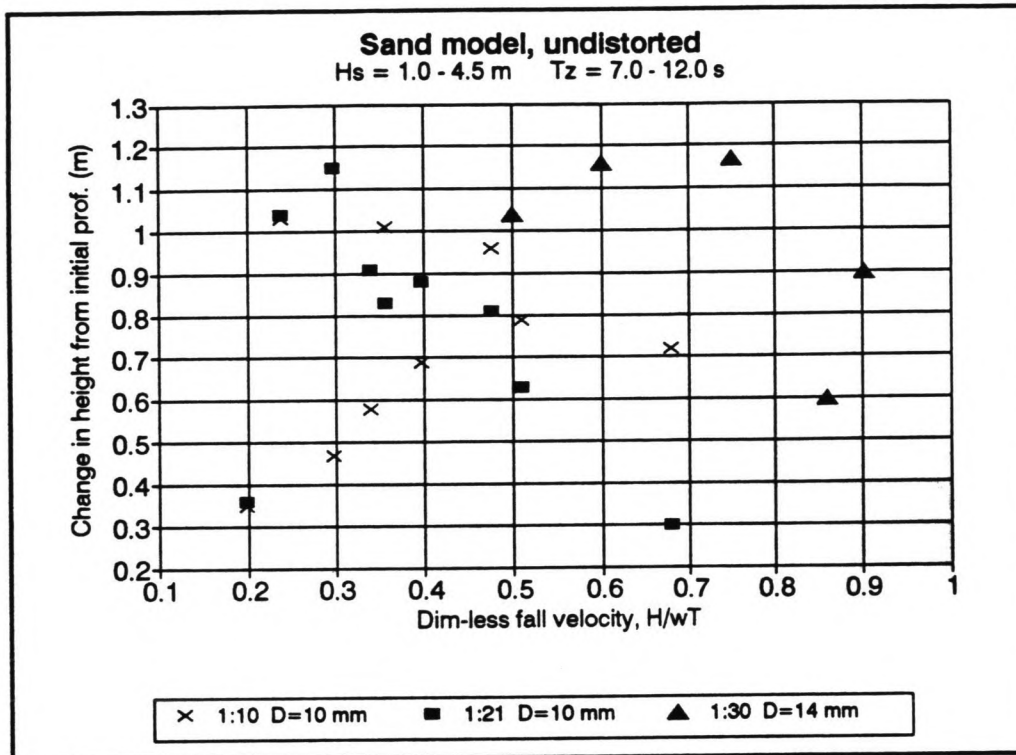


Figure 4.22 The elevation of the berm crest from the initial profiles as a function of H/wT for the three sand models.

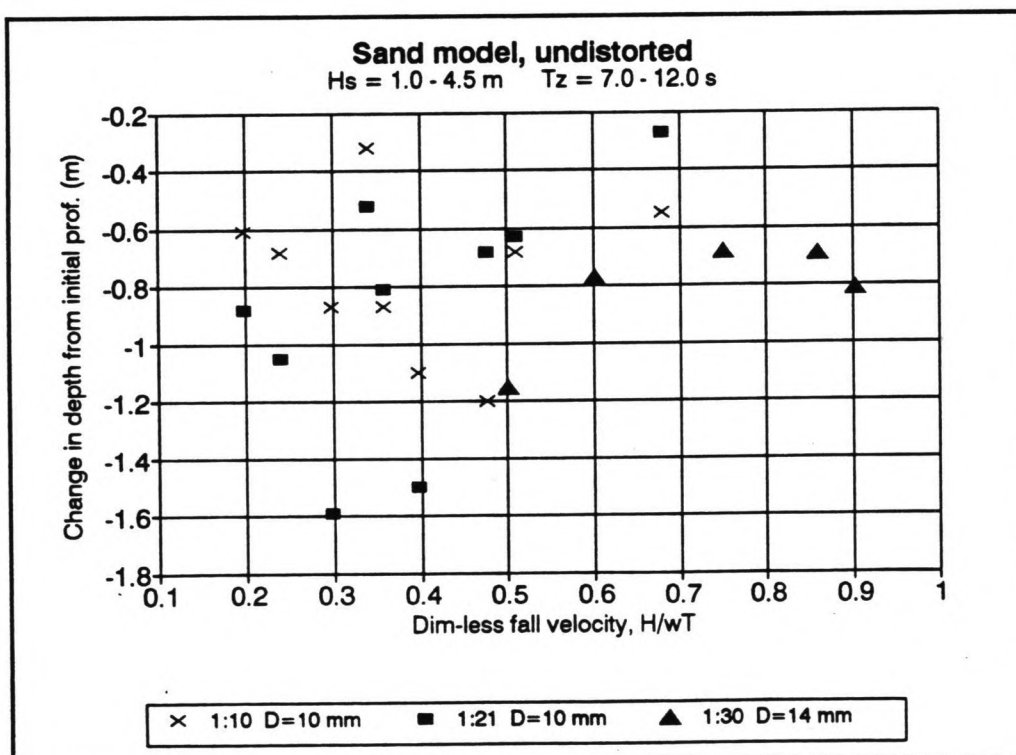


Figure 4.23 The deepening of the step from the initial profile as a function of H/wT for the three sand models.

* The elevation of the berm crest.

Values for the elevation of the berm crest with respect to the initial profile are presented in figure 4.22 again as function of H/wT . The data points are widely scattered. If for the same reasons as in section 2.2.2.3 the berm crest elevation for $H/wT = 0.198$ is excluded, the data points for the 1:21 model show a clear trend of decrease in berm height for increasing H/wT . However this trend is not observed in the data of the other two models and over-all there is not such a trend either. Thus it is clear that a relationship between berm crest elevation and H/wT cannot be derived.

* The deepening of the step.

Values of the deepening of the step are even more scattered than those for the elevation of the berm (see figure 4.23). This is partly a result of the difficulties in defining the deepest point of the step and of the problems related to the exposure of the bottom. But even for the 1:21 and the 1:30 models, which were not influenced by the bottom, there is no relation at all.

4.3 Summary.

In chapter 4 the results of the experiments, performed in this project were presented. All the experiments were performed under accretive conditions resulting in typical "step" profiles. The characteristic features of this "step" profile are the development of a berm at the beach, the deepening of a step in the breaker zone and advancement of the shoreline. Three methods of analyzing the beach profiles were presented.

The method of empirical eigenfunctions was not very helpful in the analysis of the beach profiles in this project, but would be useful for the analysis of field data.

The mean beach slope represented the beach profiles reasonable well for the 1:21 and 1:30 sand models, but did not show a good relation for the 1:10 sand model and the anthracite model.

From a practical point of view it is desirable to be able to predict the new beach profile in terms of the three characteristic features. However it was impossible to find a relation between the wave conditions and sediment characteristics, represented by H/wT , and the parameters of the three characteristic points.

The analysis of the beach profiles in the anthracite model showed large differences with the sand models. These differences were mainly caused by the angularity of the anthracite, which results in a different shape factor and consequently a different fall velocity.

5 Conclusions and recommendations.

Conclusions.

- * The literature survey showed that it is still not known exactly what the criterion is to distinguish between erosive and accretive beach profiles. The one which is most widely used is the dimensionless fall velocity parameter, H/wT . However the critical value, which determines whether the net sediment transport is onshore or offshore, remains uncertain.
- * The literature review also showed that it remains unclear what the best way is to scale the grain diameter of the sediment in a physical model. Many scaling laws give contradictory results. There are especially doubts about the validity of the use of light-weight material in the model.
- * A model scale of $1:10$ in the large wave tank of the Hydraulics Laboratory of Imperial College was too large for the amount of sediment available and the wave conditions applied. The model beach must be about 1.0 m longer and the amount of sediment needs to be at least twice as much in order not to have any influence on the beach profile from the bottom of the tank or the wall at the top of the beach.
- * Measurements of the depth of the profile can be performed accurate enough using a normal ruler. Because of the many uncertainties in the factors influencing the beach profile, like shape factor and fall velocity of the sediment, and the difference between the measured depth and the actual global profile due to the formation of ripples, there is no need for a more sophisticated measuring device.
- * The method of empirical eigenfunctions is not very useful for the analysis of beach profiles in laboratory experiments. This results from the fact that the mean beach function in this analysis does not have a physical meaning, as it is the mean profile of the artificially created initial profile and the consecutive profiles, which develop under certain wave conditions.
The method is very helpful however in the analysis of field data.

- * The critical value for H/wT which is the criterion for the development of either accretive or erosive beach profiles, is at least greater than 0.9, because in the experiment with a value of $H/wT = 0.90$ the resulting beach profile still showed the development of a berm, indicating accretive conditions. Above this value the development of a berm was not observed, but the beach profiles did not show significant erosion either.
 Analysis of the position of the shoreline indicated a critical value of the parameter H/wT of about 1.0. Around this value the process changed from shoreline advancement to shoreline recession.
- * There is no relation between the dimensionless fall velocity parameter, H/wT and the elevation of the berm crest or the deepening of the step from the initial profile.
 Neither is there a relation between H/wT and the advancement of the shoreline under accretive conditions.
- * The mean beach slope, defined as the average slope between the highest point of the berm and the lowest point of the step, decreases for increasing values of H/wT . The reason is that if the value of H/wT becomes larger, the net onshore sediment transport rate decreases, resulting in a lower berm and consequently a milder mean beach slope.
- * The shape factor is an important factor in the parameter H/wT , as it influences the fall velocity of the sediment. Especially for different materials, like anthracite, the value of this shape factor is unknown. This results in uncertainties about the conditions which determine the evolution of the beach profile.
- * Beach profiles in the sand models had not yet reached equilibrium after 4.0 hours of profile evolution, which correspond to 12.65 hours in prototype.
 Anthracite is much more mobile than sand, resulting in a more rapidly change in beach profile for anthracite models. Consequently the beach profile evolution attains a state of equilibrium more rapidly.
- * Anthracite models do not give a realistic representation of the beach profile in reality. Especially above the still water level the differences are very large: Unrealistic high berms and steep slopes developed. This is mainly caused by the angularity of the anthracite particles, represented by a smaller shape factor than for sand. This different shape factor results in extremely large angles of repose and a very different beach profile.

Recommendations.

- * Further study is required to establish the criterion to distinguish between onshore and offshore sediment transport. At the moment the parameter H/wT is the most widely used criterion, although the critical value remains uncertain.
- * Many scaling laws are based on the preservation of the fall velocity of the sediment. It must be investigated if the fall velocity is the correct parameter to represent the sediment. If the particles are transported as bed-load or by saltation rather than as suspended-load, the fall velocity is not important and a different representation of the sediment in terms of density, grain diameter and other characteristics has to be derived.
- * In order to be able to use light-weight material in coastal movable-bed models, more knowledge is required about the beach profile evolution and the sediment transport mechanism in light-weight material models . Model data should preferably be compared with field data.
More research is particularly needed on the shape factor of all the different model materials (including sand) and its influence on the fall velocity, angle of repose and beach profile.
- * Finally, further study is required on the validity of distorted models. Distorted models are sometimes used if the scale of the model requires such a small sediment diameter that the sediment becomes cohesive and cannot be used in the model.

REFERENCES

Allen, J.R. (1985) Field evaluation of beach profile response to wave steepness as predicted by the Dean model. *Coastal Engineering*, vol. 9, pp. 71-81.

Boon, J.D. & Green, M.O. (1988) Caribbean beach-face slopes and beach equilibrium profiles. *Proceedings of the 21st International Conference on Coastal Engineering, ASCE*, pp. 1618-1630.

Bruun, P. (1954) Coast erosion and the development of beach profiles. Technical Memorandum, no. 44, Beach Erosion Board.

Collins, J.I. & Chestnut, C.B. (1975) Tests on equilibrium profiles of model beaches and the effects of grain shape and size distribution. In: Proceedings ASCE Symposium Modelling Techniques. San Francisco, CA, pp.907-926.

Dalrymple, R.A. & Thompson, W.W. (1976) Study of equilibrium profiles. *Proceedings of the 15th International Conference on Coastal Engineering, ASCE*, pp. 1277-1296.

Dean, R.G. (1973) Heuristic models of sand transport in the surf zone. *Proceedings of the Conference on Engineering Dynamics in the Surf Zone, Institution of Civil Engineers, Australia, Sydney*, pp. 208-214.

Dean, R.G. (1985) Physical modelling of littoral processes. In: Physical modelling in coastal engineering. R.A. Dalrymple, Ed., A.A. Balkema, Rotterdam, The Netherlands, pp. 119-139.

Dean, R.G. (1991) Equilibrium beach profiles: Characteristics and application. *Journal of Coastal Research*, vol.7, no. 1, pp. 53-83.

Dette, H.H. & Uliczka, K. (1987) Prototype investigation on time-dependent dune recession and beach erosion. *Proceedings of Coastal Sediments '87, ASCE*, pp. 119-139.

Gourlay, M.R. (1980) Profiles, processes and permeability. *Proceedings of the 17th International Conference on Coastal Engineering, ASCE*, pp. 1320-1339.

Hallermeier, R.J. (1985) A unified modelling guidance based on a sedimentation parameter for beach changes. *Coastal Engineering*, vol. 9, pp. 37-70.

- Hattori & Kawamata (1980)** On/offshore transport and beach profile change. *Proceedings of the 17th International Conference on Coastal Engineering, ASCE*, pp. 1175-1194.
- Hughes, S.A. (1983)** Movable bed modelling law for coastal dune erosion. *Journal of Waterway, Port, Coastal and Ocean Engineering, ASCE*, vol. 109, no. 2, pp. 164-179.
- Hughes, S.A. & Fowler, E.F. (1990)** Validation of movable-bed modelling guidance. *Proceedings of the 22nd International Conference on Coastal Engineering, ASCE*, pp. 2457-2470.
- Iwagaki & Noda (1962)** Laboratory study of scale-effects in two-dimensional beach processes. *Proceedings of the 8th Coastal Engineering Conference, ASCE*, pp. 194-210.
- Johnson, J.W. (1949)** Scale-effects in hydraulic models involving wave motion. *Transactions of American Geophysical Union*, vol. 30, no. 4, August '49.
- Kai, Y., Rushu, R. & Liang, W. (1990)** Beach profile change under varying wave climates. *Proceedings of the 22nd International Conference on Coastal Engineering, ASCE*, pp. 1535-1543.
- Kamphuis, J.W. (1975)** The coastal mobile bed model. C.E. Research Report, no. 75, department of Civil Engineering, Queen's University, August.
- Kamphuis, J.W. (1985)** On understanding scale effects in coastal mobile bed models. In: Physical modelling in coastal engineering ed. R.A. Dalrymple, pp. 141-162.
- Komar, P.D. & Miller, M.C. (1973)** The threshold of sediment movement under oscillatory waves. *Journal of Sedimentary Petrology*, vol. 43, no. 4, pp. 1101-1110.
- Kriebel, D.L., Dally, & Dean, R.G. (1986)** Undistorted Froude model for surf zone sediment transport. *Proceedings of the 20th International Conference on Coastal Engineering, ASCE*, pp. 1296-1310.
- Lepetit, J.P. & Leroy, J. (1977)** Etalonnage sédimentologique du modèle réduit d'ensemble. Rap. 14 (Avant-Port Ouest de Dunkerque), Dépt. Lab. Nat. D'Hydr., Electricité de France, Chatou, 73 pp.
- Mimura, N., Otsuka, Y. & Watanabe, A. (1986)** Laboratory study on two-dimensional beach transformation due to irregular waves. *Proceedings of the 20th International Conference on Coastal Engineering, ASCE*, pp. 1393-1406.
- Moore, B.D. (1982)** Beach profile evolution in response to changes in water level and wave height. Master Thesis, Department of Civil Engineering, University of Delaware.

Nairn (1990) Prediction of cross-shore sediment transport and beach profiles evolution. PhD Thesis, Department of Civil Engineering, Imperial College of Science, Technology and Medicine, London.

Nayak (1970) Equilibrium profiles of model beaches. *Proceedings of the 12th International Conference on Coastal Engineering, ASCE*, pp. 1321-1329.

Nishi, R., Sato, M. & Nakamura, K. (1990) Laboratory study on beach processes due to random waves. *Proceedings of the 22nd International Conference on Coastal Engineering, ASCE*, pp. 2117-2130.

Noda, E.K. (1972) Equilibrium beach profile scale-model relationship. *Journal of Waterways, Harbours and Coastal Engineering Division, ASCE*, pp. 511-528.

Noda, H. (1978) Scale relations for equilibrium beach profiles. *Proceedings of the 16th International Conference on Coastal Engineering, ASCE*, pp. 1531-1541.

Powell, K.A. (1988) The dynamic response of shingle beaches to random waves. *Proceedings of the 21st International Conference on Coastal Engineering, ASCE*, pp. 1763-1773.

Saville, T. (1957) Scale effects in two-dimensional beach studies. *Transactions of the 7th General meeting of the International Association of Hydraulic Research, vol.1, pp. A3-1 to A3-10.*

Suh, K. & Dalrymple R.A. (1988) Expression for shoreline advancement of initially plane beach. *Journal of Waterway, Port, Coastal and Ocean Engineering, ASCE, vol. 114, no. 6, pp. 770-777.*

Sunamura, T. & Horikawa, K. (1974) Two-dimensional beach transformation due to waves. *Proceedings of the 14th International Conference on Coastal Engineering, ASCE*, pp. 920-938.

Sunamura, T. (1984) Quantitative predictions of beach-face slope. *Geol. Soc. Am. Bull., vol.95, pp. 242-245.*

Uliczka, K. & Dette, H.H. (1987) Prototype investigation on time-dependent dune recession and beach erosion. *Proceedings of Coastal Sediments '87, ASCE*, pp. 1430-1444.

Uliczka, K. & Dette, H.H. (1988) About the influence of erosion volume on cross-shore sediment movement at prototype scale. *Proceedings of the 21st International Conference on Coastal Engineering, ASCE*, pp. 1721-1735.

Van de Graaff, J. (1977) Dune erosion during a storm surge. *Coastal Engineering*, vol. 1, pp. 99-134.

Van Hijum, E. (1974) Equilibrium profiles of coarse material under wave attack. *Proceedings of the 14th International Conference on Coastal Engineering, ASCE*, pp. 939-958.

Vellinga, P. (1978) Movable bed model test on dune erosion. *Proceedings of the 16th International Conference on Coastal Engineering, ASCE*, pp. 2020-2039.

Vellinga, P. (1982) Beach and dune erosion during storm surges. *Coastal Engineering*, vol. 6, pp. 361-387.

Vellinga, P. (1984) A tentative description of a universal erosion profile for sandy and rock beaches. *Coastal Engineering*, vol. 8, pp. 177-188.

Wang, H., Toue, T. & Dette, H.H. (1990) Movable-bed modelling criteria for beach profile response. *Proceedings of the 22nd International Conference on Coastal Engineering, ASCE* pp. 2566-2579.

Waters, C.H. (1939) Equilibrium studies of sea beaches. Master Thesis, University of California at Berkeley.

Weishar, L.L. & Wood, W.L. (1983) An evaluation of offshore and beach changes on a tideless coast. *Journal of Sedimentary Petrology*, vol. 53, No. 3, pp. 847-858.

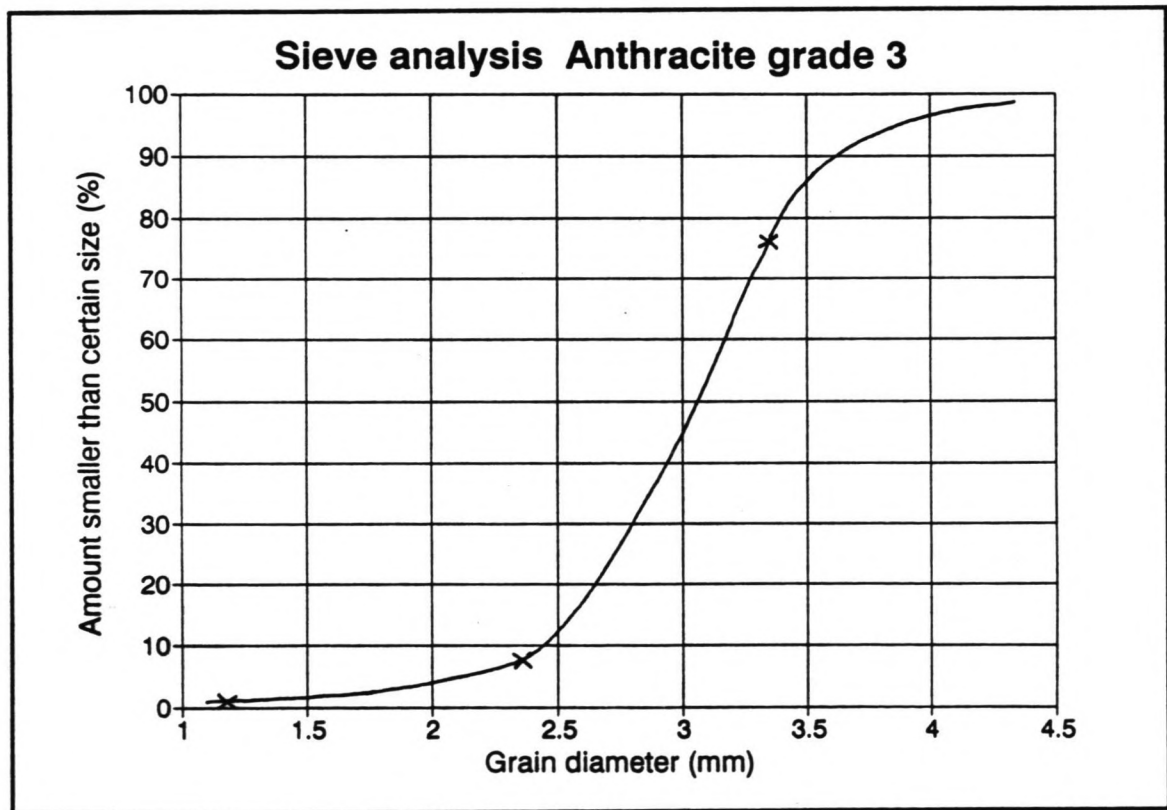
Winant, C.D., Inman, D.L. & Nordstrom, C.E. (1975) Description of seasonal beach changes using empirical eigenfunctions. *Journal of Geophysical Research*, vol. 80, No. 15, pp. 1979-1986.

Xie, S.-L. (1981) Scouring patterns in front of vertical breakwaters and their influences on the stability of the foundations of the breakwaters. Department of Civil Engineering, Delft University of Technology, Delft, The Netherlands.

Yalin, M.S. (1963) A model shingle beach with permeability and drag forces reproduced. *Tenth Congress of the International Association for Hydraulic Research*.

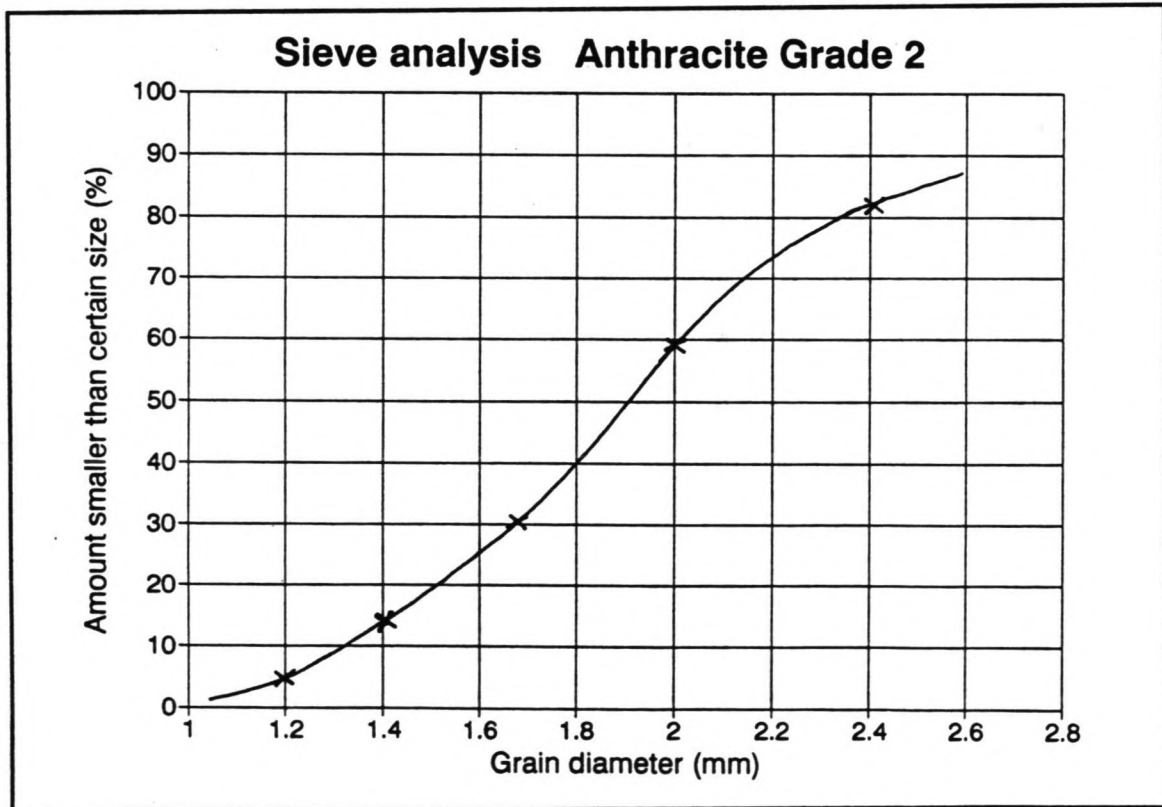
Appendix A Sieve analysis.

Sieve analysis of the <i>Grade 3</i> anthracite.			
D (mm)	Weight (g)	Weight (%)	Cumulative distribution (%)
1.18 - 2.36	52.45	7.48	7.48
2.36 - 3.35	482.01	68.73	76.21
> 3.35	166.84	23.79	100.00
Total:	701.30		



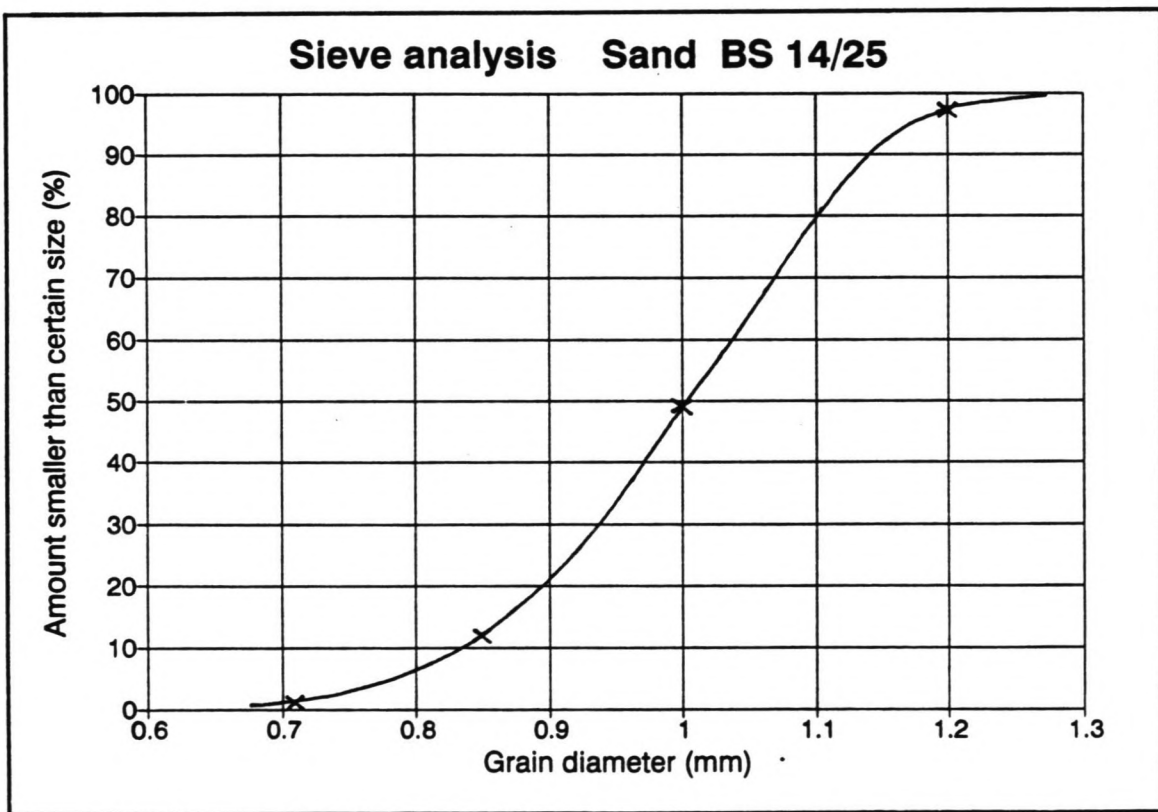
The mean diameter, D_{50} , of the *Grade 3* anthracite is 3.0 mm.

Sieve analysis of the <i>Grade 2</i> anthracite.			
D (mm)	Weight (g)	Weight (%)	Cumulative distribution (%)
< 1.20	23.10	4.76	4.76
1.20 - 1.405	46.58	9.60	14.36
1.405 - 1.68	77.22	15.91	30.27
1.68 - 2.00	140.00	28.85	59.12
2.00 - 2.411	110.54	22.78	81.90
> 2.411	87.83	18.10	100.00
Total:	485.27		



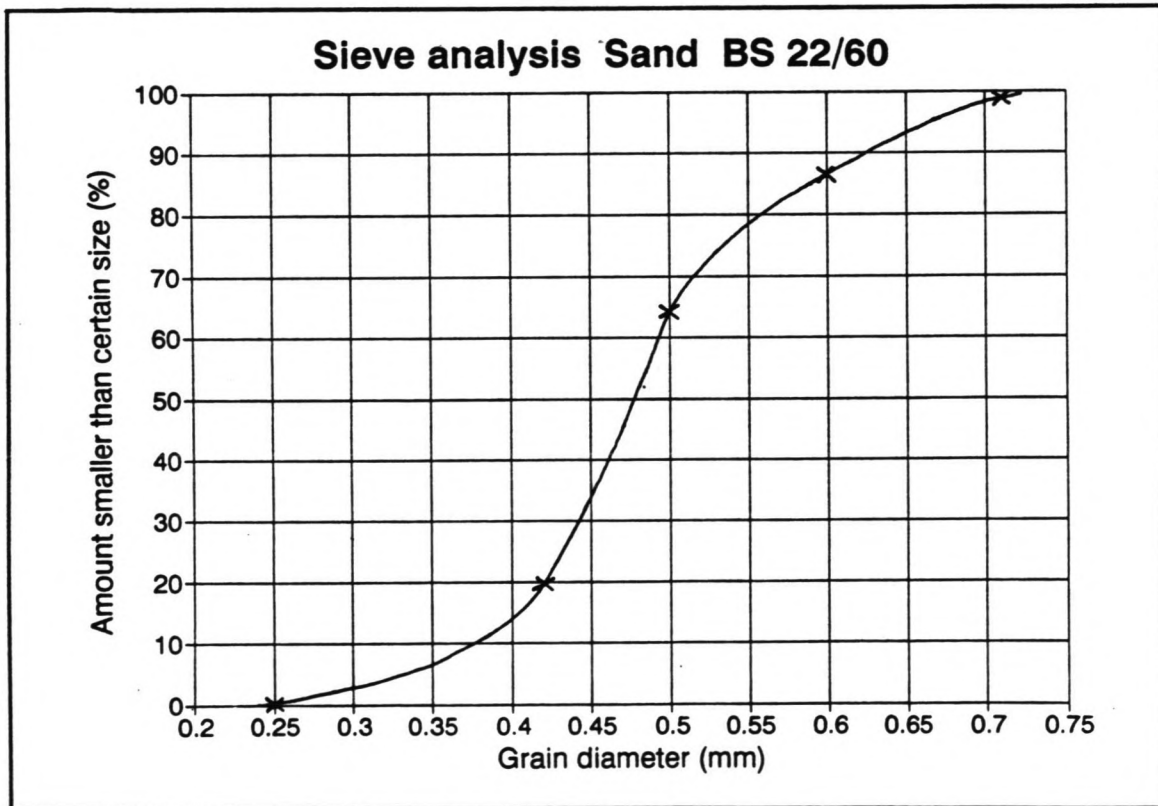
The mean diameter, D_{50} , of the *Grade 2* anthracite is 1.9 mm.

Sieve analysis of the BS 14/25 sand.			
D (mm)	Weight (g)	Weight (%)	Cumulative distribution (%)
< 0.710	22.25	1.11	1.11
0.710 - 0.850	217.13	10.81	11.92
0.850 - 1.00	747.70	37.23	49.15
1.00 - 1.20	963.20	47.97	97.12
> 1.20	57.71	2.87	99.99
Total:	2007.99		



The mean diameter, D_{50} , of the BS 14/25 sand is 1.0 mm.

Sieve analysis of the BS 22/60 sand.			
D (mm)	Weight (g)	Weight (%)	Cumulative distribution (%)
< 0.250	3.72	0.289	0.289
0.250 - 0.420	252.16	19.61	19.90
0.420 - 0.500	570.45	44.37	64.27
0.500 - 0.600	284.50	22.13	86.40
0.600 - 0.710	159.63	12.42	98.81
> 0.710	15.26	1.19	100.00
Total:	1285.72		



The mean diameter, D_{50} , of the BS 22/60 sand is 0.47 mm.

Appendix B Wave data.

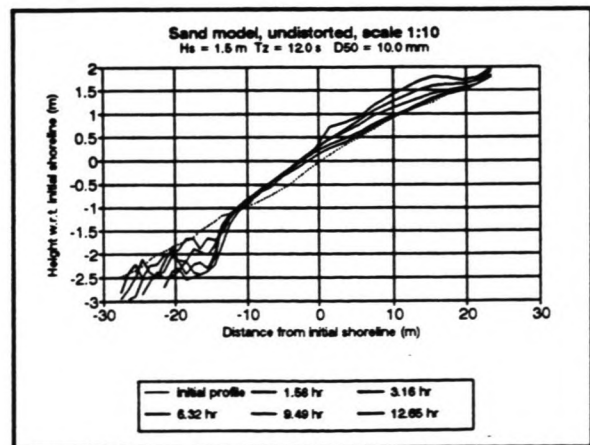
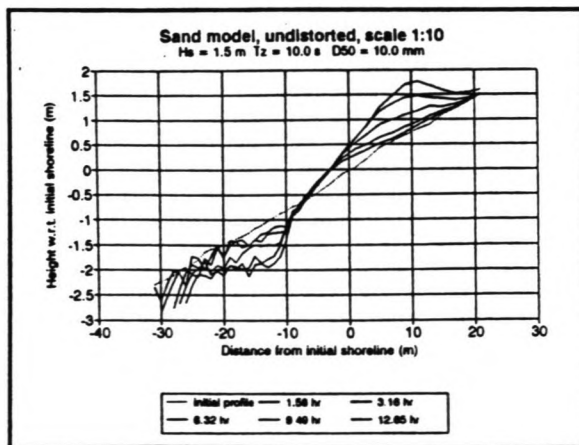
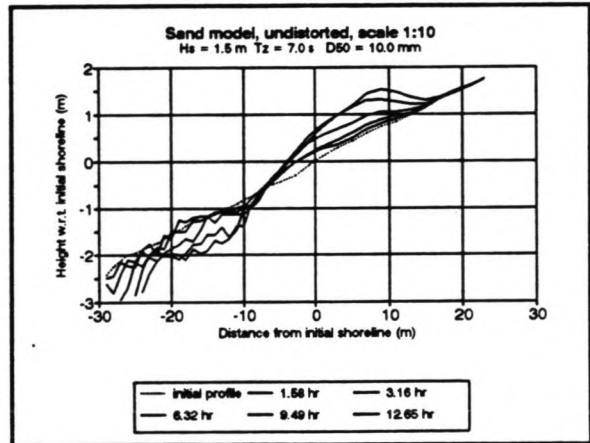
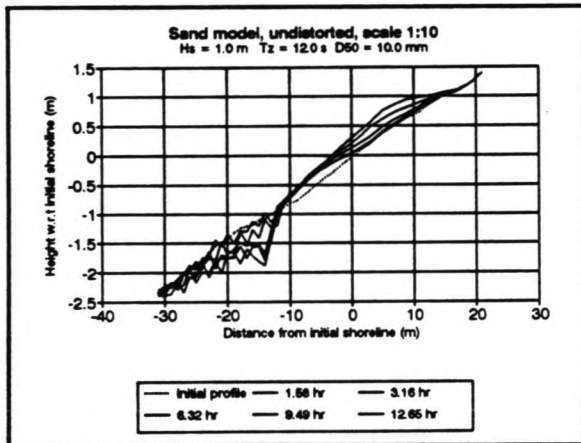
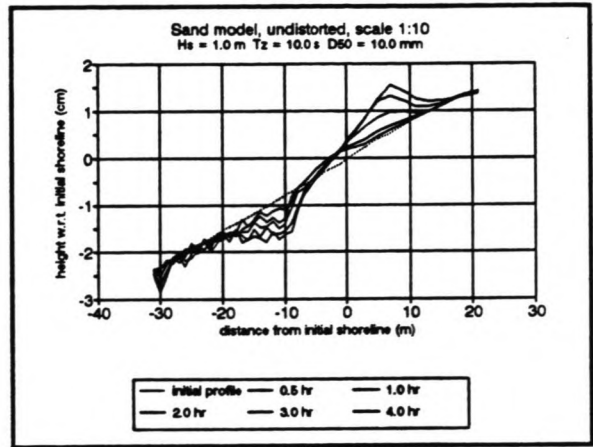
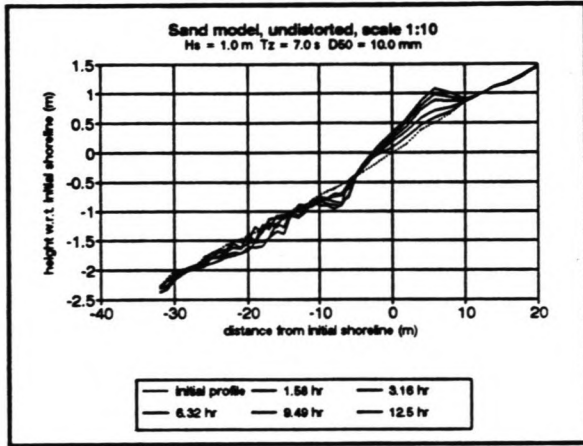
Sand model scale 1:30								
File (.COL)	Input data	zero (volts)	calibration factor (cm/V *10 ⁻²)	MWL (volts)	No. of zero crossings	H _{mean} (cm)	T _z (s)	H ₁ (cm)
M300070A	H ₁ = 3.0 m T _z = 7.0 s	2146	2.194	2138	470	5.228	1.277	8.170
M300070H	H ₁ = 3.0 m T _z = 7.0 s	2146	2.194	2018	485	4.577	1.237	7.414
M300100A	H ₁ = 3.0 m T _z = 10.0 s	2146	2.194	2018	359	5.400	1.671	8.494
M300100F	H ₁ = 3.0 m T _z = 10.0 s	2146	2.194	2026	364	5.310	1.648	8.461
M30012NA	H ₁ = 3.0 m T _z = 12.0 s	2146	2.194	2027	324	4.968	1.851	8.098
M30012ND	H ₁ = 3.0 m T _z = 12.0 s	2047	2.409	2016	329	5.359	1.825	8.828
M45007A	H ₁ = 4.5 m T _z = 7.0 s	2047	2.409	2014	465	7.544	1.292	12.08
M45007F	H ₁ = 4.5 m T _z = 7.0 s	2047	2.409	2013	461	7.159	1.300	11.42
M45010A	H ₁ = 4.5 m T _z = 10.0 s	2047	2.409	2011	361	8.871	1.662	13.97
M45010G	H ₁ = 4.5 m T _z = 10.0 s	2048	2.415	2030	358	9.034	1.679	14.21
M45012A	H ₁ = 4.5 m T _z = 12.0 s	1898	2.442	1879	322	8.667	1.868	14.19
M45012G	H ₁ = 4.5 m T _z = 12.0 s	1898	2.442	1876	316	8.244	1.889	13.34
M60007A	H ₁ = 6.0 m T _z = 7.0 s	1898	2.442	1879	448	9.707	1.340	15.26
M60007D	H ₁ = 6.0 m T _z = 7.0 s	1898	2.442	1881	445	9.696	1.348	15.26

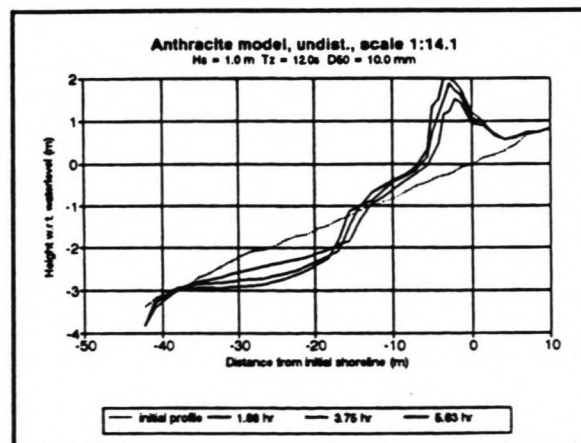
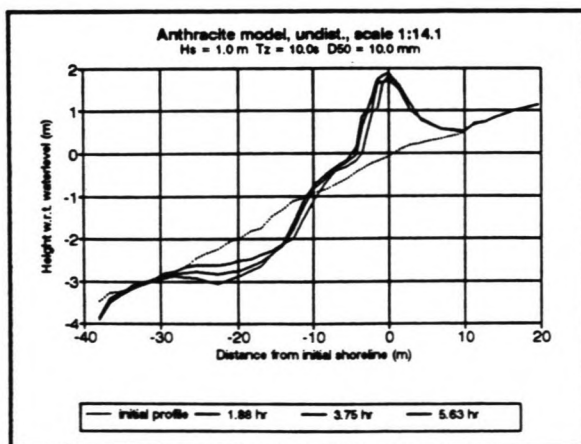
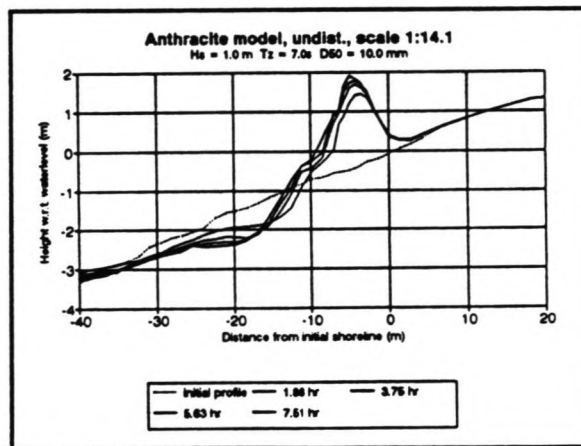
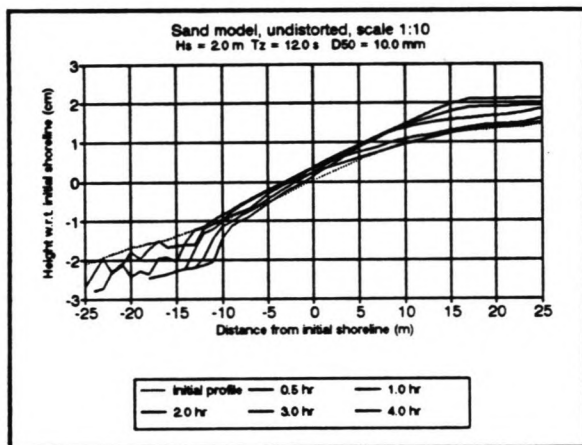
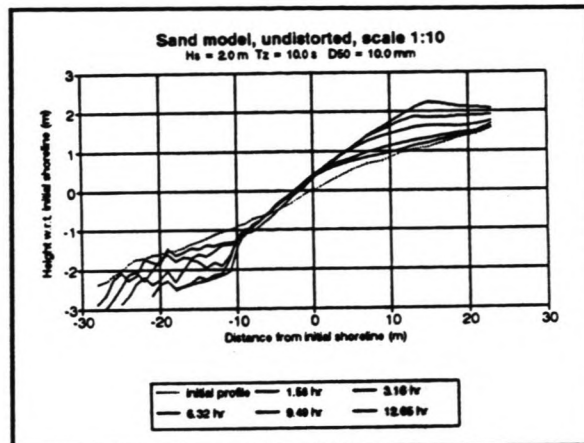
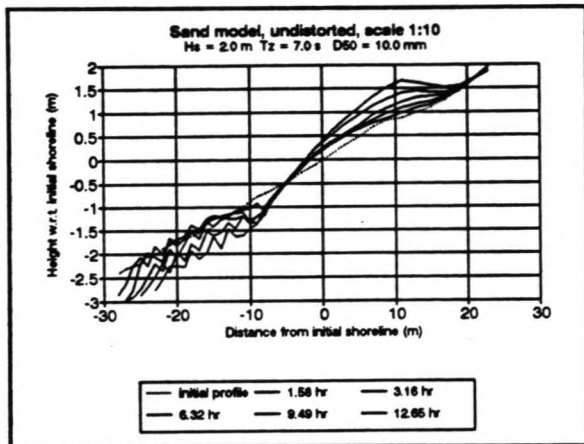
Sand model scale 1:10								
File (.COL)	Input data	zero (volts)	calibration factor (cm/V *10 ⁻²)	MWL (volts)	No. of zero crossings	H _{mean} (cm)	T _z (s)	H _z (cm)
M100070A	H _z = 1.0 m T _z = 7.0 s	2009	1.950	1999	625	5.75	1.92	9.20
M100070D	H _z = 1.0 m T _z = 7.0 s	2015	1.966	2009	630	5.812	1.904	9.443
M100100B	H _z = 1.0 m T _z = 10.0 s	2251	1.609	2012	496	4.037	2.422	6.836
M100100F	H _z = 1.0 m T _z = 10.0 s	2251	1.609	2008	485	4.119	2.469	6.945
M100120A	H _z = 1.0 m T _z = 12.0 s	2021	1.933	2010	409	4.624	2.938	7.844
M100120E	H _z = 1.0 m T _z = 12.0 s	2021	1.933	2007	418	4.471	2.870	7.710
M150070A	H _z = 1.5 m T _z = 7.0 s	2081	1.953	2076	629	8.939	1.907	14.51
M150070G	H _z = 1.5 m T _z = 7.0 s	2081	1.953	2070	612	9.196	1.960	14.66
M150100A	H _z = 1.5 m T _z = 10.0 s	2021	1.933	2004	472	7.831	2.541	13.16
M150100F	H _z = 1.5 m T _z = 10.0 s	2028	1.945	2006	475	7.928	2.524	13.35
M150120A	H _z = 1.5 m T _z = 12.0 s	1530	3.977	1363	398	7.639	3.011	12.87
M150120E	H _z = 1.5 m T _z = 12.0 s	1530	3.977	2009	397	14.46	3.023	24.14
M200070A	H _z = 2.0 m T _z = 7.0 s	2033	2.088	2011	621	12.50	1.931	20.10
M200070B	H _z = 2.0 m T _z = 7.0 s	2013	2.111	2013	617	12.73	1.946	20.57
M200100A	H _z = 2.0 m T _z = 10.0 s	2013	2.111	2008	480	11.40	2.503	19.44
M200100E	H _z = 2.0 m T _z = 10.0 s	2005	2.126	2003	467	11.82	2.569	19.85
M200120A	H _z = 2.0 m T _z = 12.0 s	1947	2.135	1924	419	10.24	2.859	17.37
M200120F	H _z = 2.0 m T _z = 12.0 s	1947	2.135	1919	434	9.913	2.768	17.01

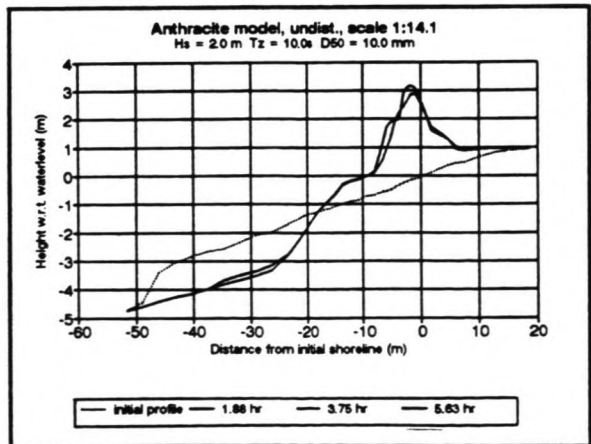
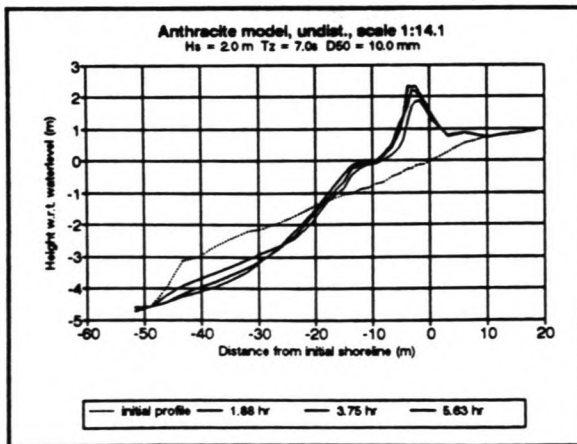
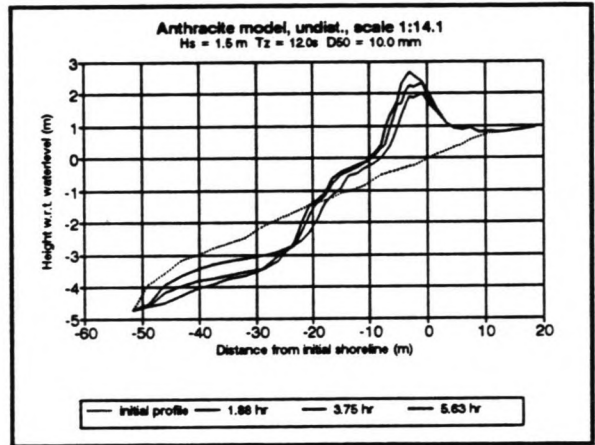
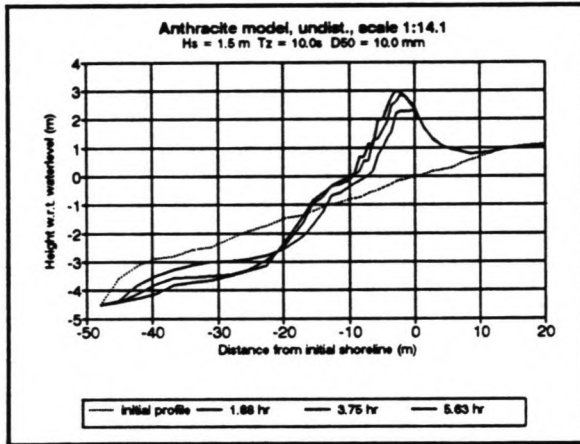
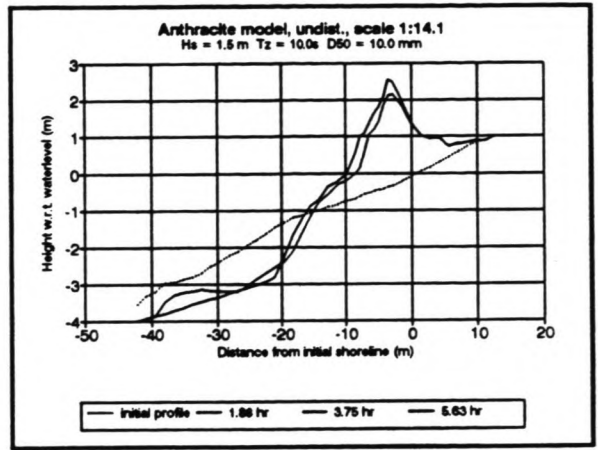
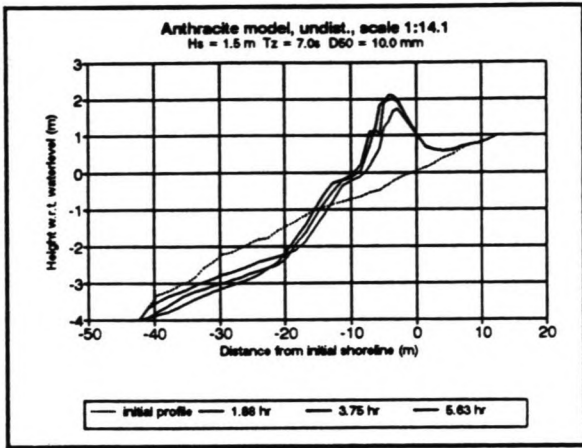
Anthracite model scale 1:14								
File (.COL)	Input data	zero (volts)	calibration factor (cm/V *10 ⁻²)	MWL (volts)	No. of zero crossings	H _{mean} (cm)	T _z (s)	H _z (cm)
M709486A	H _z = 1.0 m T _z = 7.0 s	1912	2.155	1902	678	4.421	1.771	7.004
M709186C	H _z = 1.0 m T _z = 7.0 s	1925	2.116	1628	676	4.351	1.775	6.889
M709266A	H _z = 1.0 m T _z = 10.0 s	1925	2.116	1909	563	3.784	2.133	6.180
M709266C	H _z = 1.0 m T _z = 10.0 s	1925	2.116	1909	548	3.856	2.189	6.213
M709320A	H _z = 1.0 m T _z = 12.0 s	1925	2.116	1909	508	3.363	2.361	5.734
M709320C	H _z = 1.0 m T _z = 12.0 s	1925	2.116	1908	520	3.392	2.306	5.848
M106086A	H _z = 1.5 m T _z = 7.0 s	1925	2.116	1907	681	6.431	1.764	10.25
M106186B	H _z = 1.5 m T _z = 7.0 s	1925	2.116	1907	683	6.450	1.758	10.33
M106266A	H _z = 1.5 m T _z = 10.0 s	1925	2.116	1909	546	5.747	2.196	9.376
M106266M	H _z = 1.5 m T _z = 10.0 s	2197	2.133	2178	557	5.991	2.154	9.814
M106320A	H _z = 1.5 m T _z = 12.0 s	2194	2.110	2178	480	5.761	2.496	9.757
M106320C	H _z = 1.5 m T _z = 12.0 s	2194	2.110	2173	478	5.802	2.510	9.788
M142186A	H _z = 2.0 m T _z = 7.0 s	2194	2.110	2174	710	8.425	1.689	13.29
M142186B	H _z = 2.0 m T _z = 7.0 s	2208	2.113	2189	718	8.523	1.671	13.44
M142266B	H _z = 2.0 m T _z = 10.0 s	2208	2.113	2181	558	7.596	2.152	12.42
M142320A	H _z = 2.0 m T _z = 12.0 s	2208	2.113	2181	493	7.158	2.430	12.21
M142320B	H _z = 2.0 m T _z = 12.0 s	2208	2.113	2180	489	7.295	2.453	12.50

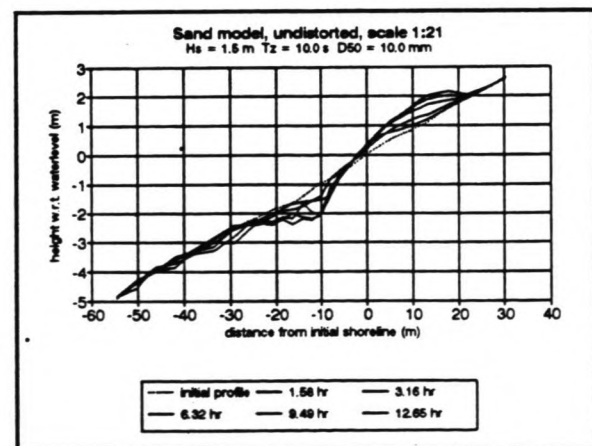
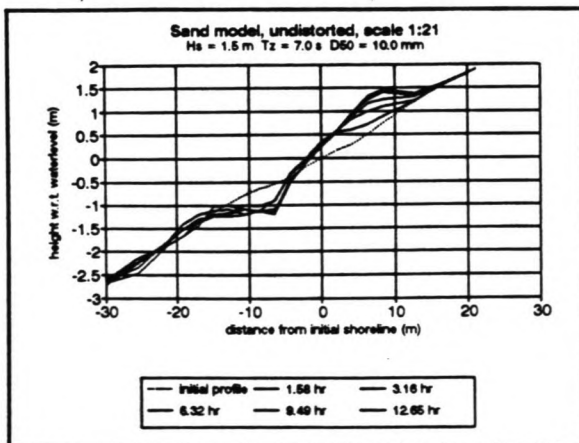
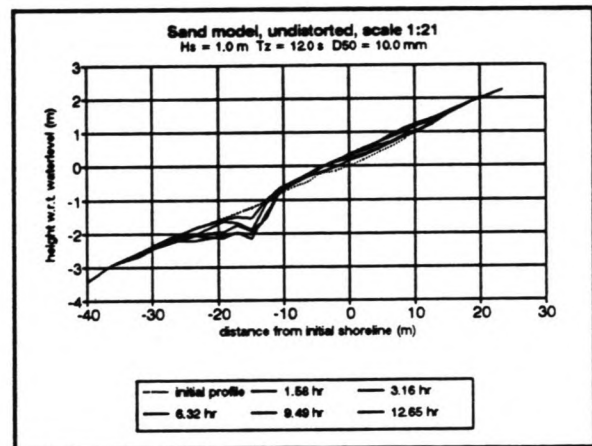
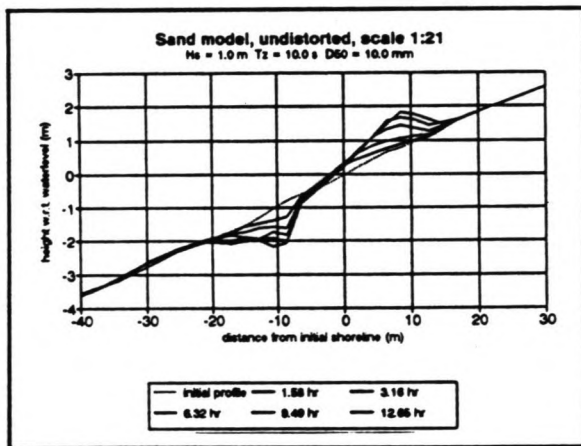
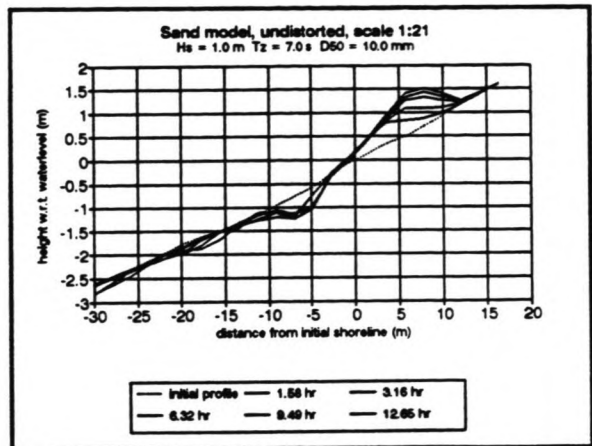
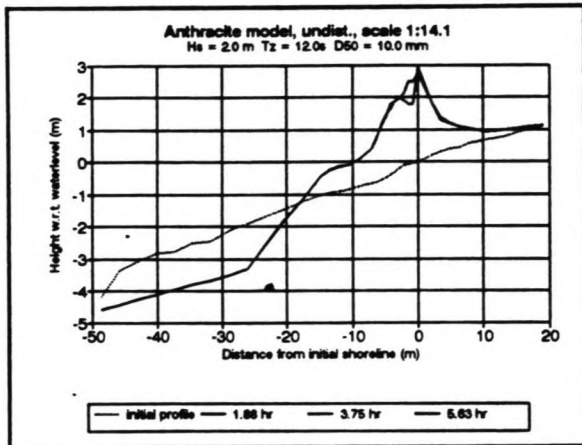
Sand model scale 1:21								
File (.COL)	Input data	zero (volts)	calibration factor (cm/V *10 ⁻²)	MWL (volts)	No. of zero crossings	H _{mean} (cm)	T _z (s)	H _z (cm)
M047152A	H _z = 1.0 m T _z = 7.0 s	2020	2.003	2023	408	2.548	1.470	4.112
M047152F	H _z = 1.0 m T _z = 7.0 s	2020	2.003	2023	412	2.509	1.459	4.052
M047217C	H _z = 1.0 m T _z = 10.0 s	2031	1.994	2030	322	2.580	1.863	4.217
M047217H	H _z = 1.0 m T _z = 10.0 s	2031	1.994	2028	325	2.530	1.846	4.224
M047260A	H _z = 1.0 m T _z = 12.0 s	2031	1.994	2028	277	2.446	2.168	3.882
M047260C	H _z = 1.0 m T _z = 12.0 s	2040	2.003	2038	267	2.534	2.245	3.951
M0705152	H _z = 1.5 m T _z = 7.0 s	1969	2.116	1958	408	3.805	1.472	6.182
M705152C	H _z = 1.5 m T _z = 7.0 s	1968	2.127	1958	410	3.816	1.461	6.226
M705217A	H _z = 1.5 m T _z = 10.0 s	1968	2.127	2015	310	4.365	1.929	6.951
M705217G	H _z = 1.5 m T _z = 10.0 s	2020	2.003	2026	307	4.149	1.955	6.608
M705260A	H _z = 1.5 m T _z = 12.0 s	1968	2.003	2015	285	3.849	2.105	6.270
M705260E	H _z = 1.5 m T _z = 12.0 s	1968	2.003	2013	279	3.970	2.151	6.395
M94152A	H _z = 2.0 m T _z = 7.0 s	2025	2.164	2196	417	6.130	1.441	10.11
M94152F	H _z = 2.0 m T _z = 7.0 s	2025	2.164	2187	408	6.257	1.470	10.12
M94217B	H _z = 2.0 m T _z = 10.0 s	2025	2.164	2016	318	5.461	1.886	8.882
M94217G	H _z = 2.0 m T _z = 10.0 s	2025	2.164	2015	319	5.455	1.882	8.884
M94260A	H _z = 2.0 m T _z = 12.0 s	2025	2.164	2016	275	5.243	2.173	8.397
M94260E	H _z = 2.0 m T _z = 12.0 s	2038	2.151	2026	279	5.182	2.145	8.391

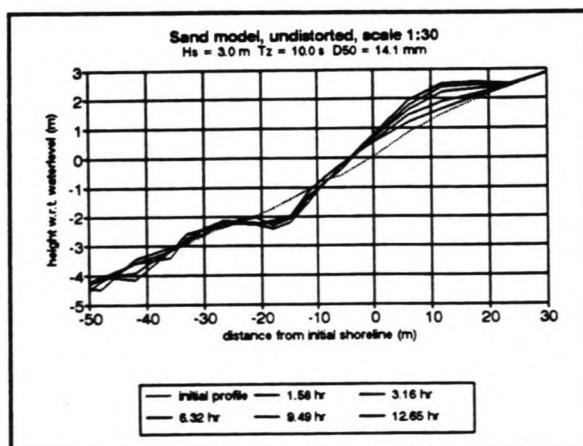
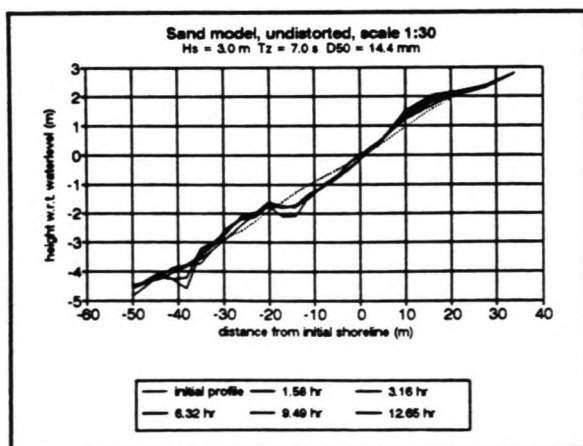
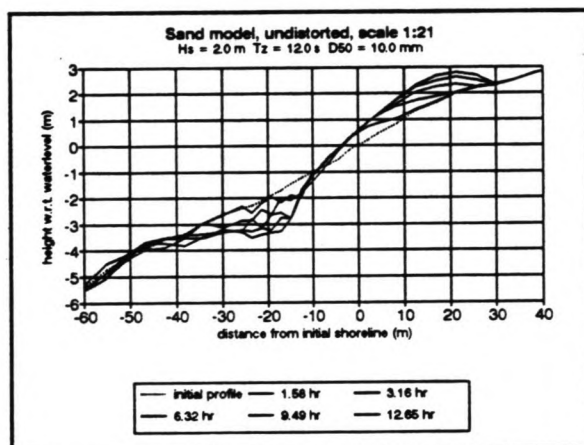
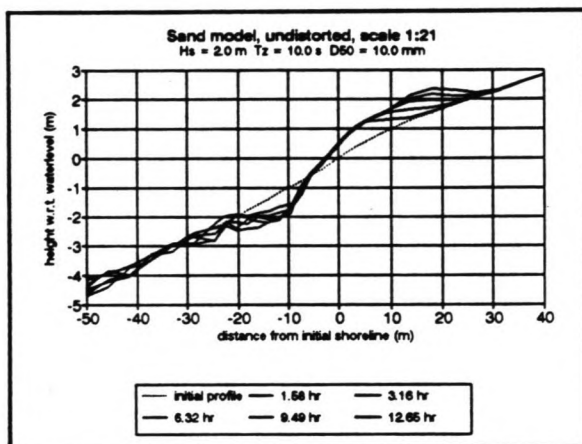
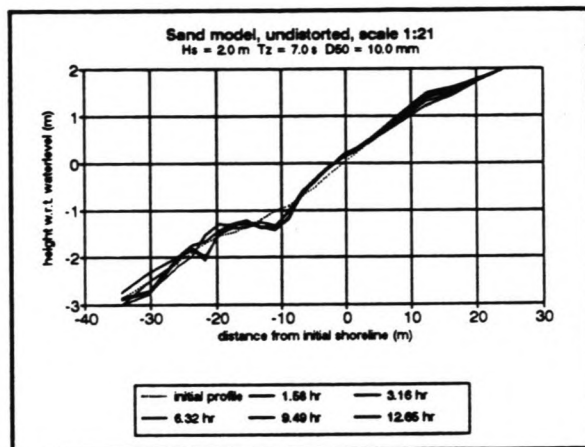
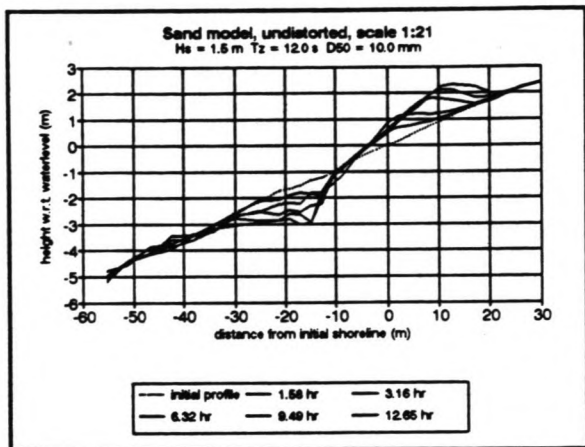
Appendix C Beach profile graphs.

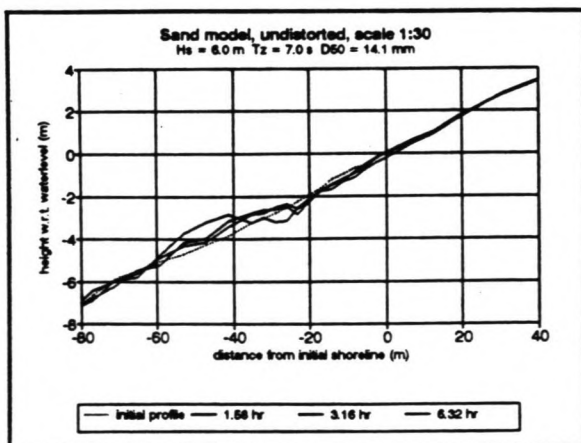
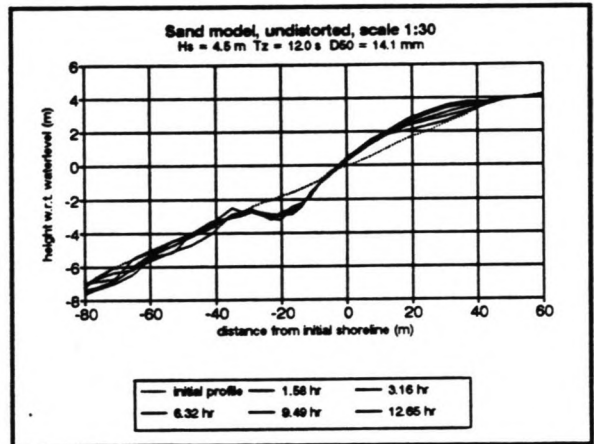
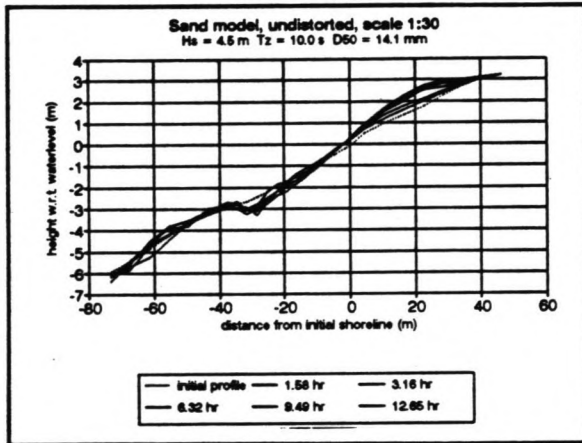
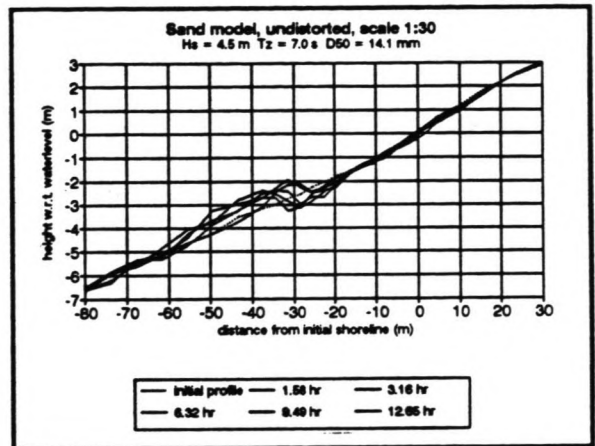
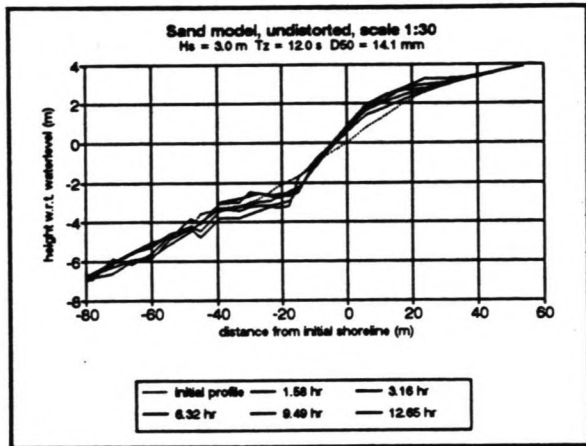












Appendix D

Data on the berm and the step of the beach profile.

D1 Elevation of the berm height and deepening of the step from the initial profile.

Change in berm height. (Calculated from initial profile).				Sand model $D_{50} = 10.0$ mm		
t (hrs)	Hs = 1.0 m Tz = 7.0 s		Hs = 1.0 m Tz = 10.0 s		Hs = 1.0 m Tz = 12.0 s	
	1:10 model	1:21 model	1:10 model	1:21 model	1:10 model	1:21 model
	Δh (m)	Δh (m)	Δh (m)	Δh (m)	Δh (m)	Δh (m)
0	0	0	0	0	0	0
1.58	0.09	0.45	0.26	0.28	0.19	0.15
3.16	0.21	0.60	0.28	0.43	0.24	0.26
6.32	0.38	1.74	0.46	0.68	0.27	0.32
9.49	0.48	0.83	0.80	0.92	0.27	0.34
12.65	0.58	0.92	1.03	1.04	0.35	0.36

Change in berm height. (Calculated from initial profile).				Sand model $D_{50} = 10.0$ mm		
t (hrs)	Hs = 1.5 m Tz = 7.0 s		Hs = 1.5 m Tz = 10.0 s		Hs = 1.5 m Tz = 12.0 s	
	1:10 model	1:21 model	1:10 model	1:21 model	1:10 model	1:21 model
	Δh (m)	Δh (m)	Δh (m)	Δh (m)	Δh (m)	Δh (m)
0	0	0	0	0	0	0
1.58	0.28	0.38	0.26	0.34	0.27	0.53
3.16	0.29	0.55	0.37	0.34	0.34	0.96
6.32	0.48	0.66	0.49	0.62	0.34	1.11
9.49	0.73	0.74	0.75	0.79	0.39	1.21
12.65	0.83	0.81	0.96	0.89	0.55	1.30

Change in berm height. (Calculated from initial profile).			Sand model $D_{50} = 10.0$ mm			
t (hrs)	Hs = 2.0 m Tz = 7.0 s		Hs = 2.0 m Tz = 10.0 s		Hs = 2.0 m Tz = 12.0 s	
	1:10 model	1:21 model	1:10 model	1:21 model	1:10 model	1:21 model
	Δh (m)	Δh (m)	Δh (m)	Δh (m)	Δh (m)	Δh (m)
0	0	0	0	0	0	0
1.58	0.28	0.043	0.34	0.66	0.30	0.53
3.16	0.22	0.11	0.39	0.70	0.34	0.72
6.32	0.34	0.19	0.62	0.70	0.42	0.75
9.49	0.53	0.23	0.83	0.75	0.59	0.92
12.65	0.79	0.30	1.15	0.87	0.81	1.02

Change in berm height. (Calculated from initial profile).			Anthracite model, scale 1:14 Prototype $D_{50} = 10.0$ mm.		
t (hrs)	Hs = 1.0 m Tz = 7.0 s	Hs = 1.0 m Tz = 10.0 s	Hs = 1.0 m Tz = 12.0 s	Hs = 1.5 m Tz = 7.0 s	Hs = 1.5 m Tz = 10.0 s
	Δh (m)	Δh (m)	Δh (m)	Δh (m)	Δh (m)
0	0	0	0	0	0
1.88	1.85	1.79	1.68	1.92	2.42
3.75	2.13	1.89	2.12	2.28	3.00
5.63	2.21	1.96	2.24	2.41	3.19

Change in berm height. (Calculated from initial profile).			Anthracite model, scale 1:14 Prototype $D_{50} = 10.0$ mm.	
t (hrs)	Hs = 1.5 m Tz = 12.0 s	Hs = 2.0 m Tz = 7.0 s	Hs = 2.0 m Tz = 10.0 s	Hs = 2.0 m Tz = 12.0 s
	Δh (m)	Δh (m)	Δh (m)	Δh (m)
0	0	0	0	0
1.88	2.12	2.02	3.02	2.76
3.75	2.52	2.43	3.33	2.94
5.63	2.93	2.59		

Change in berm height. (Calculated from initial profile).				Sand model, scale 1:30 Prototype $D_{50} = 14.1$ mm.	
t (hrs)	Hs = 3.0 m Tz = 7.0 s	Hs = 3.0 m Tz = 10.0 s	Hs = 3.0 m Tz = 12.0 s	Hs = 4.5 m Tz = 7.0 s	Hs = 4.5 m Tz = 10.0 s
	Δh (m)	Δh (m)	Δh (m)	Δh (m)	Δh (m)
0	0	0	0	No berm !	0
1.58	0.24	0.48	0.63		0.24
3.16	0.30	0.60	0.87		0.45
6.32	0.36	0.78	1.17		0.75
9.49	0.48	0.93	1.08		0.81
12.65	0.54	1.02	0.93		0.93

Change in berm height. (Calculated from initial profile).				Sand model, scale 1:30 Prototype $D_{50} = 14.1$ mm.	
t (hrs)	Hs = 4.5 m Tz = 12.0 s	Hs = 6.0 m Tz = 7.0 s	Hs = 6.0 m Tz = 10.0 s	Hs = 6.0 m Tz = 12.0 s	
	Δh (m)	Δh (m)	Δh (m)	Δh (m)	
0	0	No berm !	No measurements !		
1.58	0.90				
3.16	0.75				
6.32	0.84				
9.49	1.02				
12.65	1.17				

Change in depth at step. (Calculated from initial profile).				Anthracite model, scale 1:14 Prototype $D_{50} = 10.0$ mm.	
t (hrs)	Hs = 1.0 m Tz = 7.0 s	Hs = 1.0 m Tz = 10.0 s	Hs = 1.0 m Tz = 12.0 s	Hs = 1.5 m Tz = 7.0 s	Hs = 1.5 m Tz = 10.0 s
	Δh (m)	Δh (m)	Δh (m)	Δh (m)	Δh (m)
0	0	0	0	0	0
1.88	-0.76	-0.89	-0.61	-0.80	-1.04
3.75	-0.80	-0.88	-0.80	-0.93	-1.37
5.63	-0.86	-0.94	-0.91	-0.97	-1.40

Change in depth at step. (Calculated from initial profile).				Anthracite model, scale 1:14 Prototype $D_{50} = 10.0$ mm.	
t (hrs)	Hs = 1.5 m Tz = 12.0 s	Hs = 2.0 m Tz = 7.0 s	Hs = 2.0 m Tz = 10.0 s	Hs = 2.0 m Tz = 12.0 s	
	Δh (m)	Δh (m)	Δh (m)	Δh (m)	
0	0	0	0	0	
1.88	-1.03	-0.89	-1.31	-1.41	** Bottom reached !
3.75	-1.31	-1.14	-1.42		
5.63	-1.33	-1.28			

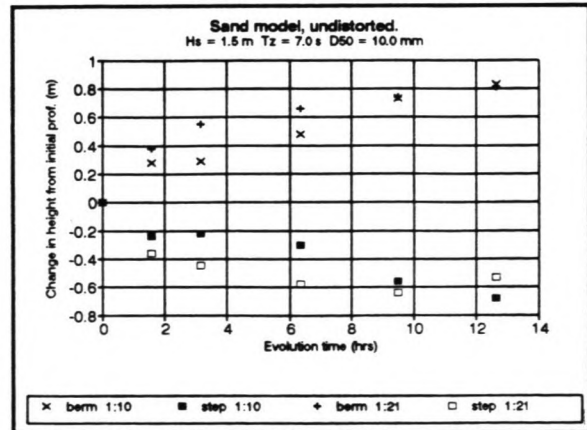
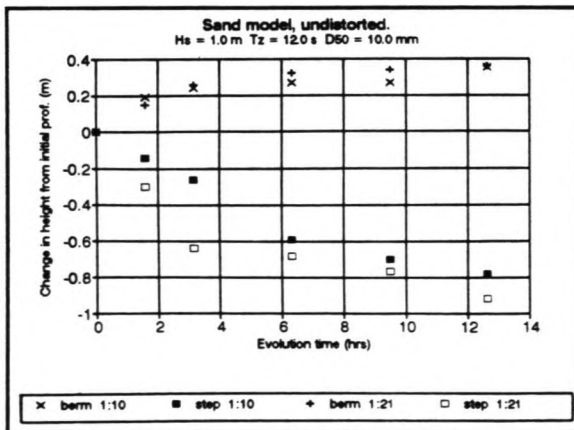
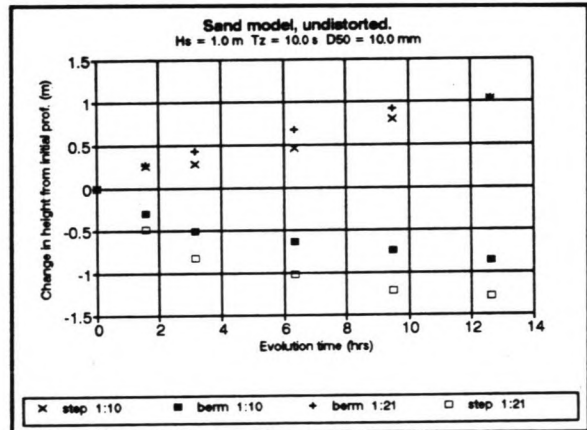
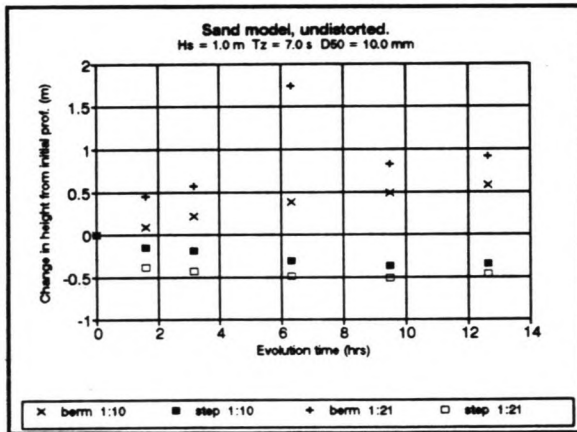
Change in depth at step. (Calculated from initial profile).				Sand model, scale 1:30 Prototype $D_{50} = 14.1$ mm.	
t (hrs)	Hs = 3.0 m Tz = 7.0 s	Hs = 3.0 m Tz = 10.0 s	Hs = 3.0 m Tz = 12.0 s	Hs = 4.5 m Tz = 7.0 s	Hs = 4.5 m Tz = 10.0 s
	Δh (m)	Δh (m)	Δh (m)	Δh (m)	Δh (m)
0	0	0	0	0	0
1.58	-0.45	-0.57	-0.63	-0.24	-0.45
3.16	-0.48	-0.66	-0.66	-0.48	-0.33
6.32	-0.42	-0.78	-0.84	-0.60	-0.57
9.49	-0.48	-0.66	-1.05	-0.63	-0.66
12.65	-0.81	-0.78	-1.32	-0.60	-0.84

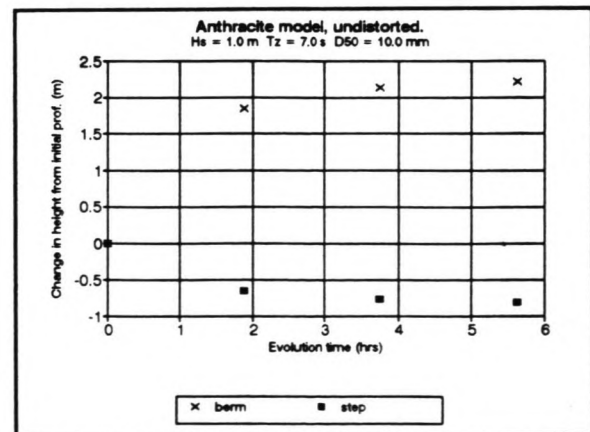
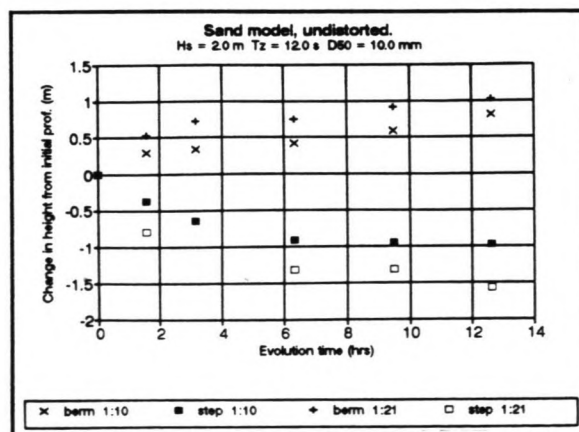
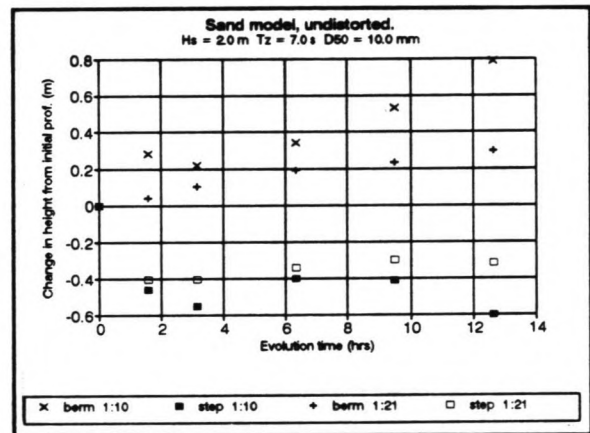
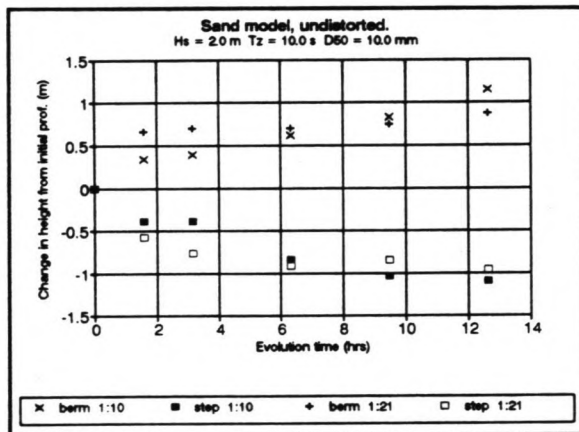
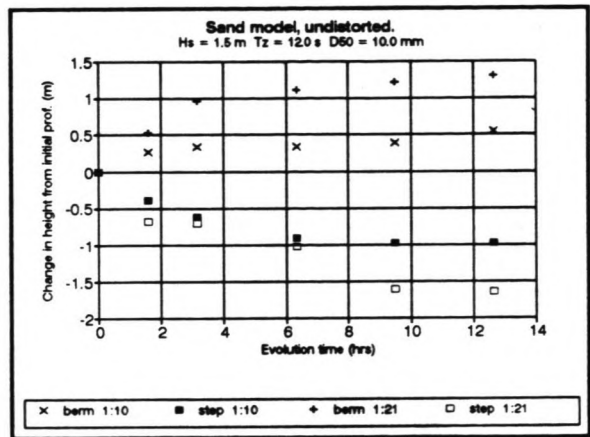
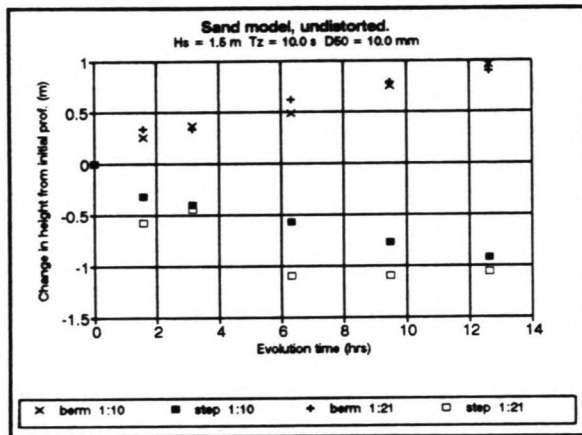
Change in depth at step. (Calculated from initial profile).				Sand model, scale 1:30 Prototype $D_{50} = 14.1$ mm.	
t (hrs)	Hs = 4.5 m Tz = 12.0 s	Hs = 6.0 m Tz = 7.0 s	Hs = 6.0 m Tz = 10.0 s	Hs = 6.0 m Tz = 12.0 s	
	Δh (m)	Δh (m)	Δh (m)	Δh (m)	
0	0	0			
1.58	-1.08	-0.36	No measurements !		
3.16	-1.17	-0.60			
6.32	-1.08	-0.66			
9.49	-1.41				
12.65	-1.14				

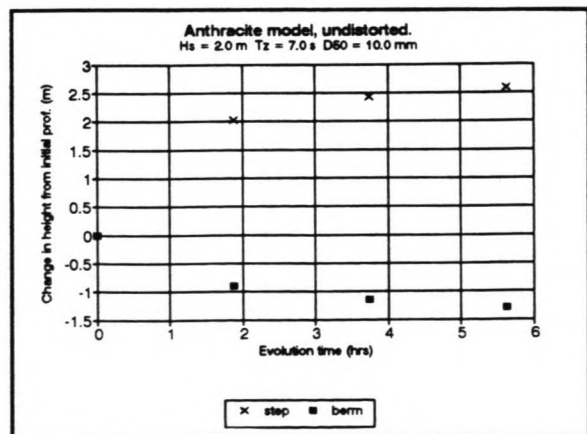
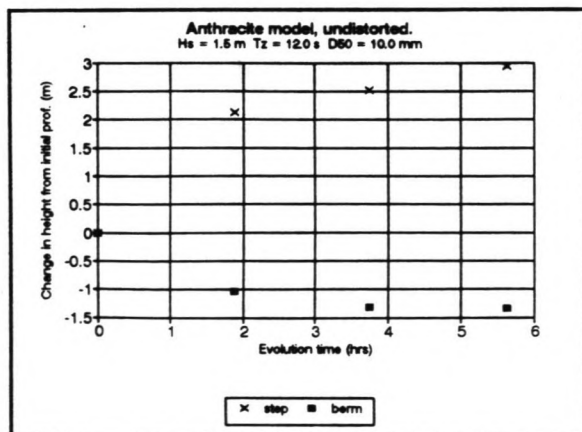
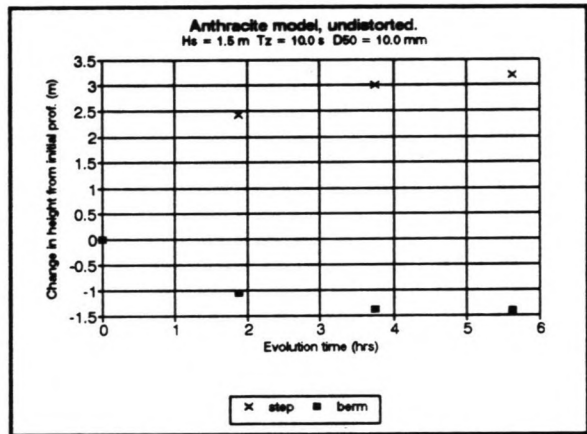
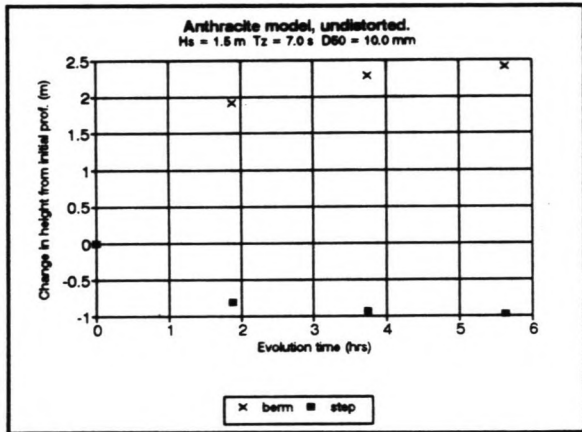
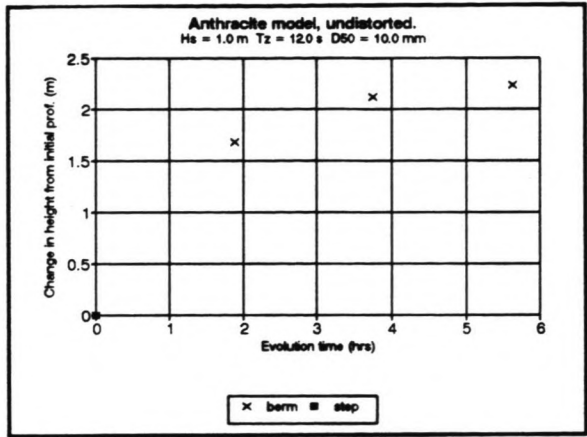
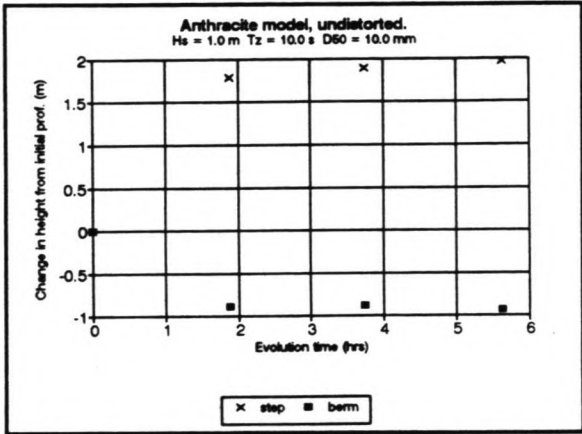
Change in depth at the step. (Calculated from initial profile).				Sand model $D_{50} = 10.0 \text{ mm}$		
t (hrs)	Hs = 1.0 m Tz = 7.0 s		Hs = 1.0 m Tz = 10.0 s		Hs = 1.0 m Tz = 12.0 s	
	1:10 model	1:21 model	1:10 model	1:21 model	1:10 model	1:21 model
	Δh (m)	Δh (m)	Δh (m)	Δh (m)	Δh (m)	Δh (m)
0	0	0	0	0	0	0
1.58	-0.15	-0.38	-0.30	-0.49	-0.14	-0.30
3.16	-0.19	-0.43	-0.51	-0.83	-0.26	-0.64
6.32	-0.31	-0.49	-0.64	-1.02	-0.59	-0.68
9.49	-0.37	-0.51	-0.74	-1.21	-0.70	-0.77
12.65	-0.35	-0.47	-0.86	-1.28	-0.78	-0.92

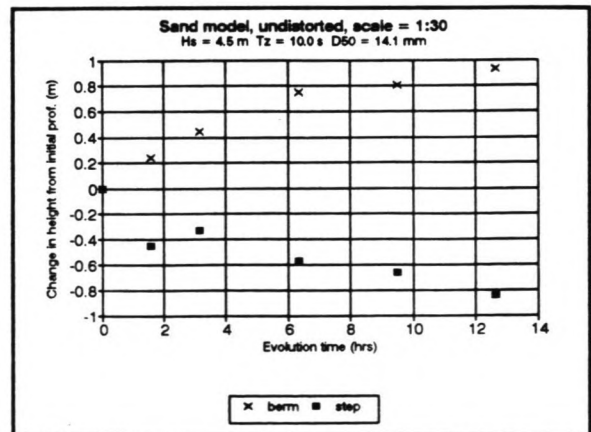
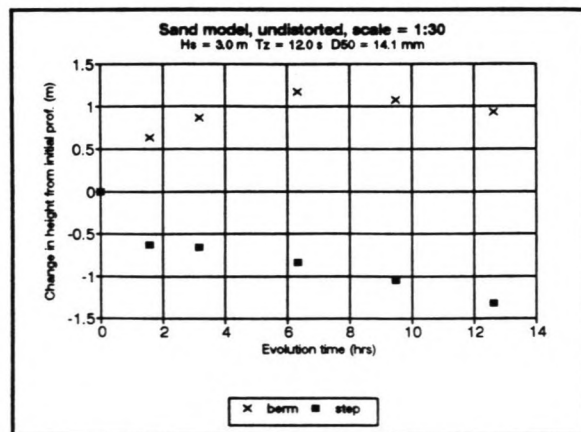
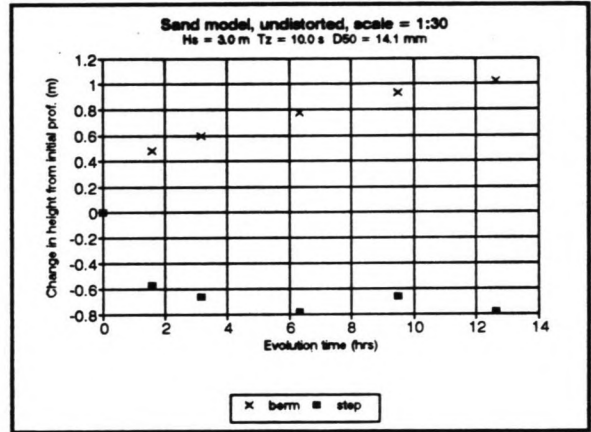
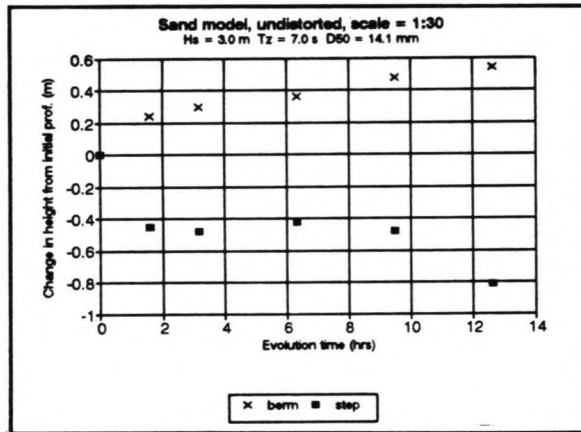
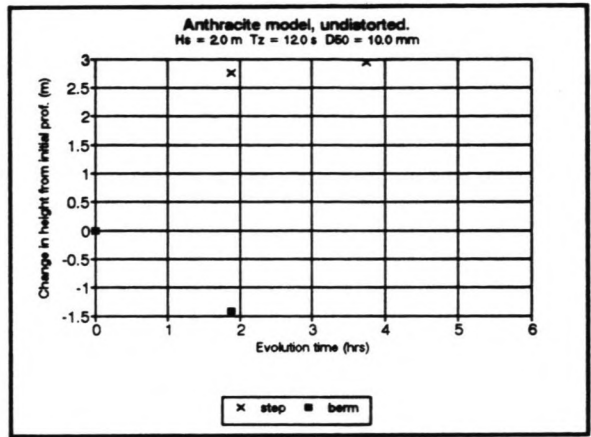
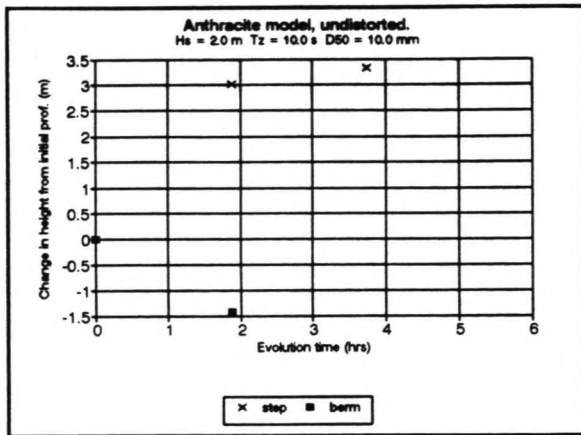
Change in depth at the step. (Calculated from initial profile).				Sand model $D_{50} = 10.0 \text{ mm}$		
t (hrs)	Hs = 1.5 m Tz = 7.0 s		Hs = 1.5 m Tz = 10.0 s		Hs = 1.5 m Tz = 12.0 s	
	1:10 model	1:21 model	1:10 model	1:21 model	1:10 model	1:21 model
	Δh (m)	Δh (m)	Δh (m)	Δh (m)	Δh (m)	Δh (m)
0	0	0	0	0	0	0
1.58	-0.24	-0.36	-0.32	-0.58	-0.39	-0.68
3.16	-0.22	-0.45	-0.40	-0.45	-0.62	-0.70
6.32	-0.30	-0.58	-0.57	-1.09	-0.91	-1.02
9.49	-0.56	-0.64	-0.77	-1.09	-0.98	-1.60
12.65	-0.68	-0.53	-0.92	-1.06	-0.97	-1.64

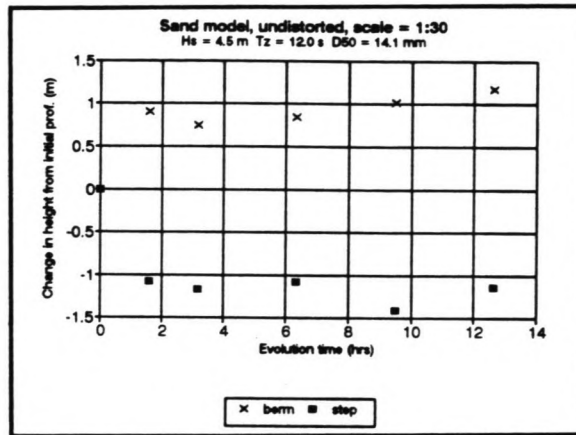
Change in depth at the step. (Calculated from initial profile).		Sand model $D_{50} = 10.0$ mm				
t (hrs)	Hs = 2.0 m Tz = 7.0 s		Hs = 2.0 m Tz = 10.0 s		Hs = 2.0 m Tz = 12.0 s	
	1:10 model	1:21 model	1:10 model	1:21 model	1:10 model	1:21 model
	Δh (m)	Δh (m)	Δh (m)	Δh (m)	Δh (m)	Δh (m)
0	0	0	0	0	0	0
1.58	-0.46	-0.40	-0.39	-0.56	-0.37	-0.79
3.16	-0.55	-0.40	-0.39	-0.77	-0.64	-0.64
6.32	-0.40	-0.34	-0.84	-0.92	-0.92	-1.32
9.49	-0.41	-0.30	-1.04	-0.85	-0.95	-1.32
12.65	-0.60	-0.32	-1.10	-0.96	-0.97	-1.57











D2 Revised values for elevation of the berm and deepening of the step related to H/wT .

Elevation of the berm related to H/wT						
	sand model 1:10		sand model 1:21		sand model 1:30	
H/wT	Δh (m) (best)	Δh (m) (variation)	Δh (m) (best)	Δh (m) (variation)	Δh (m) (best)	Δh (m) (variation)
0.198	0.35	0.31 - 0.39	0.36	0.36 - 0.72		
0.238	1.03	0.97 - 1.03	1.04	0.98 - 1.04		
0.298	0.47	0.40 - 0.55	1.15	1.15 - 1.21		
0.340	0.58	0.56 - 0.58	0.91	0.86 - 0.91		
0.357	1.01	0.96 - 1.01	0.83	0.83 - 0.87		
0.397	0.69	0.60 - 0.81	0.88	0.79 - 1.00		
0.476	0.96	0.85 - 1.13	0.81	0.76 - 0.87		
0.501					1.04	0.93 - 1.08
0.510	0.79	0.79 - 0.83	0.63	0.63 - 0.68		
0.601					1.16	1.02 - 1.16
0.680	0.72	0.70 - 0.75	0.30	0.28 - 0.32		
0.751					1.17	0.99 - 1.17
0.859					0.60	0.54 - 0.60
0.902					0.90	0.90 - 0.97

Deepening of the step related to H/wT.						
	sand model 1:10		sand model 1:21		sand model 1:30	
H/wT	Δh (m) (best)	Δh (m) (variation)	Δh (m) (best)	Δh (m) (variation)	Δh (m) (best)	Δh (m) (variation)
0.198	-0.61	0.61 - 0.78	-0.88	0.81 - 0.92		
0.238	-0.68	0.61 - 0.75	-1.05	0.98 - 1.05		
0.298	-0.87	0.78 - 1.17	-1.59	1.42 - 1.63		
0.340	-0.32	0.32 - 0.39	-0.52	0.48 - 0.52		
0.357	-0.87	0.68 - 0.98	-0.81	0.71 - 0.89		
0.397	-1.10	1.10 - 1.70	-1.50	1.47 - 1.64		
0.476	-1.20	1.00 - 1.30	-0.68	0.65 - 0.77		
0.501					-1.15	0.98 - 1.38
0.510	-0.68	0.68 - 0.76	-0.63	0.53 - 0.66		
0.601					-0.77	0.71 - 0.82
0.680	-0.55	0.55 - 0.68	-0.27	0.27 - 0.41		
0.751					-0.68	0.64 - 0.71
0.859					-0.69	0.47 - 0.78
0.902					-0.81	0.79 - 0.83

Appendix E Data on the position of the shoreline.

E1 Advancement of the shoreline as a function of the evolution time.

Advancement of shoreline. (A positive value indicates a wider beach)				Sand model $D_{50} = 10.0$ mm		
t (hrs)	Hs = 1.0 m Tz = 7.0 s		Hs = 1.0 m Tz = 10.0 s		Hs = 1.0 m Tz = 12.0 s	
	1:10 model	1:21 model	1:10 model	1:21 model	1:10 model	1:21 model
	Δy (m)	Δy (m)	Δy (m)	Δy (m)	Δy (m)	Δy (m)
0	0	0	0	0	0	0
1.58	1.29	0.73	2.53	2.43	0.40	1.66
3.16	1.62	0.92	2.67	2.38	0.82	3.65
6.32	1.77	0.54	2.33	2.00	2.00	3.78
9.49	2.21	0.54	2.10	1.63	2.73	3.72
12.65	2.57	0.90	1.90	1.63	3.18	3.40

Advancement of shoreline. (A positive value indicates a wider beach)				Sand model $D_{50} = 10.0$ mm		
t (hrs)	Hs = 1.5 m Tz = 7.0 s		Hs = 1.5 m Tz = 10.0 s		Hs = 1.5 m Tz = 12.0 s	
	1:10 model	1:21 model	1:10 model	1:21 model	1:10 model	1:21 model
	Δy (m)	Δy (m)	Δy (m)	Δy (m)	Δy (m)	Δy (m)
0	0	0	0	0	0	0
1.58	0.143	2.13	2.62	1.94	1.60	4.26
3.16	0.124	1.75	3.08	1.35	2.50	3.98
6.32	0.168	1.50	3.15	1.63	2.90	3.88
9.49	0.142	1.46	3.12	1.76	2.82	3.95
12.65	0.149	1.46	3.17	2.08	2.58	3.65

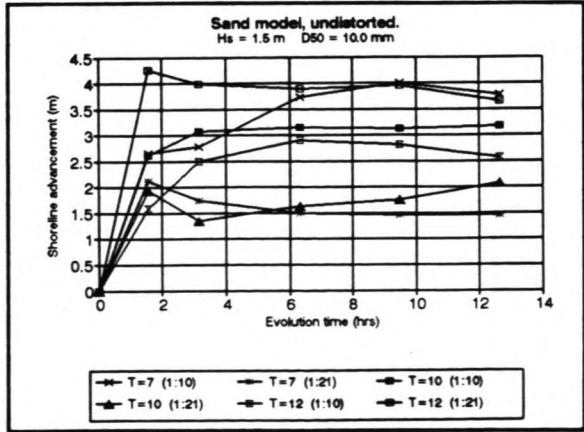
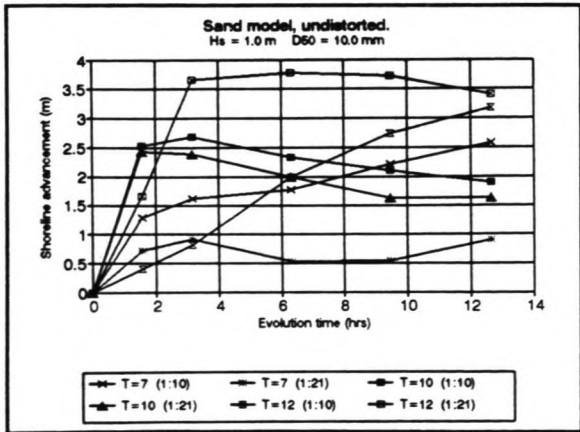
Advancement of shoreline. (A positive value indicates a wider beach)				Sand model $D_{50} = 10.0$ mm		
t (hrs)	Hs = 2.0 m Tz = 7.0 s		Hs = 2.0 m Tz = 10.0 s		Hs = 2.0 m Tz = 12.0 s	
	1:10 model	1:21 model	1:10 model	1:21 model	1:10 model	1:21 model
	Δy (m)	Δy (m)	Δy (m)	Δy (m)	Δy (m)	Δy (m)
0	0	0	0	0	0	0
1.58	1.93	1.84	2.27	3.67	2.33	3.25
3.16	1.52	1.70	2.35	3.62	3.10	3.14
6.32	1.64	1.59	2.50	3.62	2.57	3.50
9.49	2.33	1.49	2.58	3.97	1.69	3.63
12.65	2.43	1.84	1.80	4.15	1.00	3.59

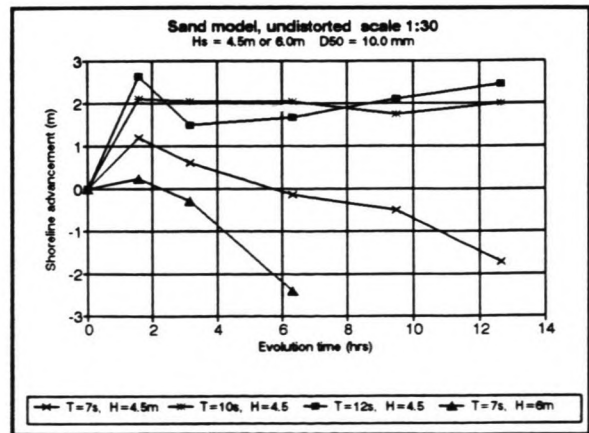
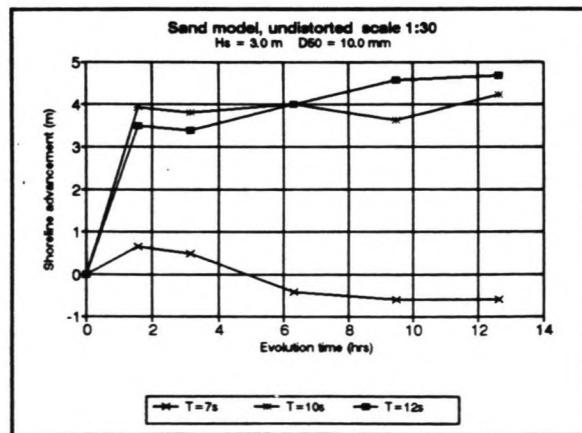
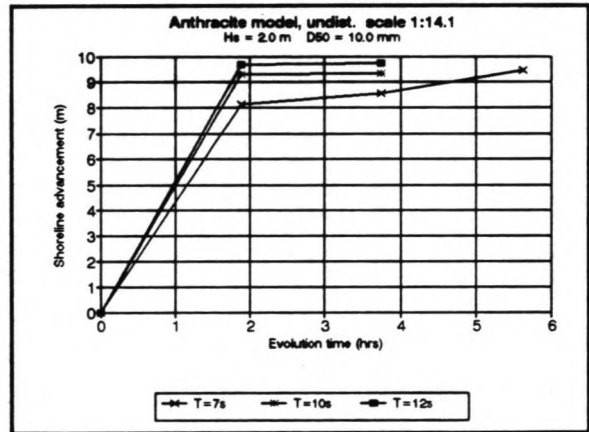
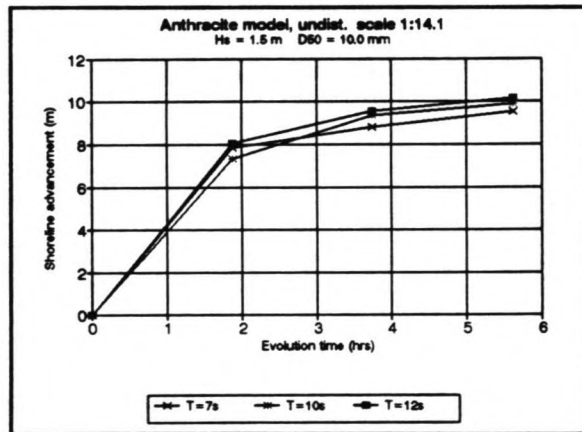
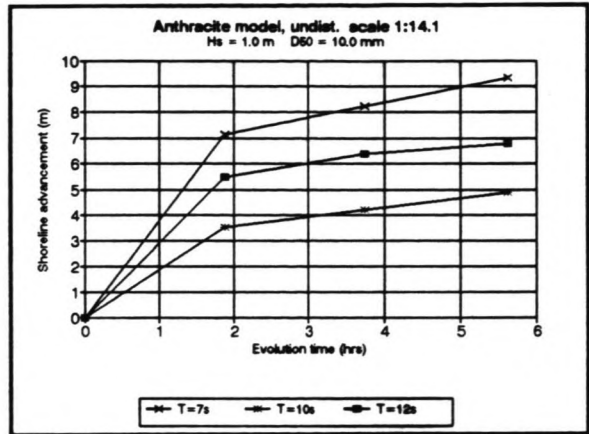
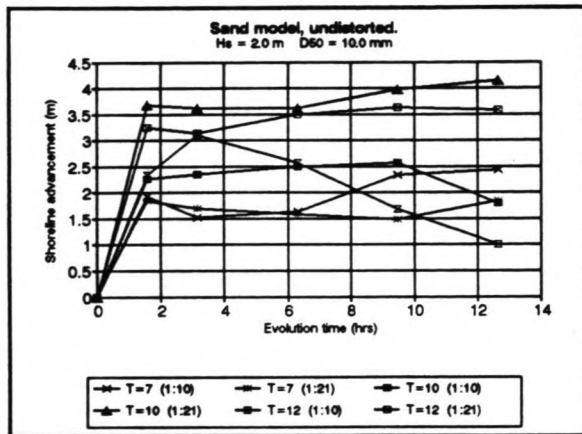
Advancement of shoreline. (A positive value indicates a wider beach.)				Anthracite model, scale 1:14 Prototype $D_{50} = 10.0$ mm.	
t (hrs)	Hs = 1.0 m Tz = 7.0 s	Hs = 1.0 m Tz = 10.0 s	Hs = 1.0 m Tz = 12.0 s	Hs = 1.5 m Tz = 7.0 s	Hs = 1.5 m Tz = 10.0 s
	Δy (m)	Δy (m)	Δy (m)	Δy (m)	Δy (m)
0	0	0	0	0	0
1.88	7.12	3.53	5.48	7.84	7.33
3.75	8.23	4.20	6.38	8.81	9.33
5.63	9.33	4.87	6.80	9.52	9.87

Advancement of shoreline. (A positive value indicates a wider beach.)				Anthracite model, scale 1:14 Prototype $D_{50} = 10.0$ mm.	
t (hrs)	Hs = 1.5 m Tz = 12.0 s	Hs = 2.0 m Tz = 7.0 s	Hs = 2.0 m Tz = 10.0 s	Hs = 2.0 m Tz = 12.0 s	
	Δy (m)	Δy (m)	Δy (m)	Δy (m)	
0	0	0	0	0	
1.88	8.04	8.14	9.31	9.68	
3.75	9.56	8.58	9.34	9.75	
5.63	10.15	9.45			

Advancement of shoreline. (A positive value indicates a wider beach).		Sand model, scale 1:30 Prototype $D_{50} = 14.1$ mm.			
t (hrs)	Hs = 3.0 m Tz = 7.0 s	Hs = 3.0 m Tz = 10.0 s	Hs = 3.0 m Tz = 12.0 s	Hs = 4.5 m Tz = 7.0 s	Hs = 4.5 m Tz = 10.0 s
	Δy (m)	Δy (m)	Δy (m)	Δy (m)	Δy (m)
0	0	0	0	0	0
1.58	0.66	3.92	3.50	1.20	2.10
3.16	0.49	3.80	3.38	0.60	2.05
6.32	-0.41	4.00	4.00	-0.136	2.05
9.49	-0.59	3.63	4.58	-0.50	1.75
12.65	-0.59	4.22	4.67	-1.72	2.00

Advancement of shoreline. (A positive value indicates a wider beach).		Sand model, scale 1:30 Prototype $D_{50} = 14.1$ mm.		
t (hrs)	Hs = 4.5 m Tz = 12.0 s	Hs = 6.0 m Tz = 7.0 s	Hs = 6.0 m Tz = 10.0 s	Hs = 6.0 m Tz = 12.0 s
	Δy (m)	Δy (m)	Δy (m)	Δy (m)
0	0	0		
1.58	2.63	0.225	No measurements !	
3.16	1.50	-0.3		
6.32	1.67	-2.4		
9.49	2.10			
12.65	2.45			





E2 Revised data on the position of the shoreline, related to H/wT .

H/wT	sand model 1:10		sand model 1:21		sand model 1:30	
	Δy (m) (best)	Δy (m) (variation)	Δy (m) (best)	Δy (m) (variation)	Δy (m) (best)	Δy (m) (variation)
0.198	3.18	3.10 - 3.25	3.40	3.40 - 3.78		
0.238	1.90	1.90 - 2.10	1.63	1.63 - 2.00		
0.298	2.58	2.58 - 2.90	3.65	3.65 - 4.00		
0.340	2.57	2.50 - 2.65	0.90	0.80 - 0.95		
0.357	3.17	3.10 - 3.25	2.08	1.97 - 2.15		
0.397	3.10	2.50 - 3.50	3.59	3.57 - 3.65		
0.476	2.58	2.25 - 2.70	4.15	4.05 - 4.25		
0.501					4.67	4.50 - 4.75
0.510	3.77	3.75 - 4.00	1.46	1.46 - 1.75		
0.601					4.22	4.15 - 4.30
0.680	2.43	2.35 - 2.50	1.84	1.78 - 1.92		
0.751					2.45	2.32 - 2.62
0.859					-0.59	0.50 - 0.65
0.902					2.00	1.75 - 2.10
1.29					-1.72	1.60 - 1.80

Appendix F Data on the mean beach slope.

F1 Mean beach slope as a function of evolution time.

Beach slope between highest point of step and lowest point of berm.				Sand model $D_{50} = 10.0$ mm		
t (hrs)	Hs = 1.0 m Tz = 7.0 s		Hs = 1.0 m Tz = 10.0 s		Hs = 1.0 m Tz = 12.0 s	
	1:10 model	1:21 model	1:10 model	1:21 model	1:10 model	1:21 model
	$\tan\beta$	$\tan\beta$	$\tan\beta$	$\tan\beta$	$\tan\beta$	$\tan\beta$
0						
1.58	0.0992	0.182	0.136	0.18	0.111	0.114
3.16	0.112	0.178	0.152	0.212	0.142	0.157
6.32	0.134	0.173	0.124	0.191	0.167	0.151
9.49	0.146	0.171	0.154	0.216	0.134	0.159
12.65	0.146	0.184	0.181	0.209	0.138	0.159

Beach slope between highest point of step and lowest point of berm.				Sand model $D_{50} = 10.0$ mm		
t (hrs)	Hs = 1.5 m Tz = 7.0 s		Hs = 1.5 m Tz = 10.0 s		Hs = 1.5 m Tz = 12.0 s	
	1:10 model	1:21 model	1:10 model	1:21 model	1:10 model	1:21 model
	$\tan\beta$	$\tan\beta$	$\tan\beta$	$\tan\beta$	$\tan\beta$	$\tan\beta$
0						
1.58	0.143	0.148	0.146	0.170	0.129	0.173
3.16	0.124	0.123	0.148	0.130	0.139	0.196
6.32	0.168	0.156	0.141	0.171	0.136	0.170
9.49	0.142	0.174	0.124	0.141	0.126	0.183
12.65	0.149	0.153	0.154	0.148	0.127	0.179

Beach slope between highest point of step and lowest point of berm.				Sand model $D_{50} = 10.0$ mm		
t (hrs)	Hs = 2.0 m Tz = 7.0 s		Hs = 2.0 m Tz = 10.0 s		Hs = 2.0 m Tz = 12.0 s	
	1:10 model	1:21 model	1:10 model	1:21 model	1:10 model	1:21 model
	$\tan\beta$	$\tan\beta$	$\tan\beta$	$\tan\beta$	$\tan\beta$	$\tan\beta$
0						
1.58	0.156	0.114	0.157	0.187	0.173	0.183
3.16	0.163	0.116	0.147	0.169	0.171	0.170
6.32	0.130	0.108	0.1	0.127	0.154	0.129
9.49	0.119	0.117	0.159	0.137	0.128	0.131
12.65	0.148	0.111	0.165	0.139	0.139	0.141

Beach slope between highest point of berm and lowest point of step			Anthracite model, scale 1:14 Prototype $D_{50} = 10.0$ mm.		
t (hrs)	Hs = 1.0 m Tz = 7.0 s	Hs = 1.0 m Tz = 10.0 s	Hs = 1.0 m Tz = 12.0 s	Hs = 1.5 m Tz = 7.0 s	Hs = 1.5 m Tz = 10.0 s
	$\tan\beta$	$\tan\beta$	$\tan\beta$	$\tan\beta$	$\tan\beta$
0					
1.88	0.250	0.204	0.160	0.248	0.171
3.75	0.276	0.206	0.192	0.257	0.219
5.63	0.264	0.219	0.202	0.228	bottom!

Beach slope between highest point of berm and lowest point of step			Anthracite model, scale 1:14 Prototype $D_{50} = 10.0$ mm.	
t (hrs)	Hs = 1.5 m Tz = 12.0 s	Hs = 2.0 m Tz = 7.0 s	Hs = 2.0 m Tz = 10.0 s	Hs = 2.0 m Tz = 12.0 s
	$\tan\beta$	$\tan\beta$	$\tan\beta$	$\tan\beta$
0				
1.88	0.179	0.157	0.187	bottom!
3.75	0.205	0.183	0.243	bottom!
5.63	0.235	0.195	bottom!	bottom!

Beach slope between highest point of berm and lowest point of step			Sand model, scale 1:30 Prototype $D_{50} = 14.1$ mm.		
t (hrs)	Hs = 3.0 m Tz = 7.0 s	Hs = 3.0 m Tz = 10.0 s	Hs = 3.0 m Tz = 12.0 s	Hs = 4.5 m Tz = 7.0 s	Hs = 4.5 m Tz = 10.0 s
	$\tan\beta$	$\tan\beta$	$\tan\beta$	$\tan\beta$	$\tan\beta$
0					
1.58	0.123	0.166	0.156	No berm!	0.0963
3.16	0.126	0.137	0.144		0.100
6.32	0.126	0.169	0.150		0.107
9.49	0.140	0.133	0.128		0.112
12.65	0.150	0.138	0.187		0.110

Beach slope between highest point of berm and lowest point of step			Sand model, scale 1:30 Prototype $D_{50} = 14.1$ mm.		
t (hrs)	Hs = 4.5 m Tz = 12.0 s	Hs = 6.0 m Tz = 7.0 s	Hs = 6.0 m Tz = 10.0 s	Hs = 6.0 m Tz = 12.0 s	
	$\tan\beta$	$\tan\beta$	$\tan\beta$	$\tan\beta$	
0					
1.58	0.152	No berm !	No measurements !		
3.16	0.141				
6.32	0.132				
9.49	0.119				
12.65	0.117				

F2 Revised beach slopes related to H/wT .

	sand model 1:10		sand model 1:21		sand model 1:30	
H/wT	tan β (best)	tan β (variation)	tan β (best)	tan β (variation)	tan β (best)	tan β (variation)
0.198	0.106	0.106 - 0.121	0.157	0.104 - 0.164		
0.238	0.152	0.122 - 0.181	0.197	0.179 - 0.209		
0.298	0.125	0.118 - 0.132	0.157	0.137 - 0.179		
0.340	0.136	0.117 - 0.127	0.171	0.160 - 0.184		
0.357	0.138	0.127 - 0.142	0.134	0.133 - 0.166		
0.397	0.143	0.129 - 0.156	0.149	0.139 - 0.162		
0.476	0.135	0.123 - 0.165	0.132	0.122 - 0.139		
0.501					0.155	0.139 - 0.163
0.510	0.131	0.120 - 0.143	0.153	0.145 - 0.162		
0.601					0.164	0.155 - 0.181
0.680	0.131	0.119 - 0.148	0.116	0.105 - 0.125		
0.751					0.139	0.127 - 0.149
0.859					0.141	0.133 - 0.150
0.902					0.116	0.108 - 0.119

Appendix G Computer program for eigenfunction analysis and results.

The subroutines in this program, which reduces the matrices to their tridiagonal form and derive the eigenvalues and eigenvectors of the matrices are taken from:

Press, W. H. (1986) *Numerical Recipes: The art of scientific computing (Fortran version)*, Cambridge University Press.

```

C*****
PROGRAM EIGENVALUE
C
C
C*****
C   This program generates the spatial and
C   temporal correlation matrices from data
C   for the depth of the beach profile. It also
C   calculates the eigenvalues and eigenvectors
C   of these matrices.
C*****
C
C   INTEGER NX,NT,X,T,I,J
C   REAL H,HELP,A,B,MA,MB,DA,EA,DB,EB
C   REAL PERX,PERT,PARTX,PARTT,SUM
C   PARAMETER (NP = 50)
C   DIMENSION DA(NP),DB(NP),EA(NP),EB(NP)
C   DIMENSION H(50,50),HELP(50,50)
C   DIMENSION A(NP,NP),MA(NP,NP)
C   DIMENSION B(NP,NP),MB(NP,NP)
C   DIMENSION PERX(NP),PERT(NP),PARTX(NP),PARTT(NP)
C
C   OPEN (100, FILE = 'data1-7.dat')
C   OPEN (200, FILE = 'neig1-7.dat')
C
C*****
C   Read the values for the depth or
C   elevation of the beach profile,
C   h(xt) as a function of distance
C   from the shoreline and time, and
C   count the number of points along
C   the profile (nx) and the number
C   of recorded profiles (nt)
C*****
C
C   X = 0
C   T = 0
C   NX = 0
C   NT = 0
5   T = T+1
6   X = X+1

```

```

READ (100,10) HELP(X,T)
IF (HELP(X,T).NE.100) THEN
  IF (HELP(X,T).NE.1000) THEN
    NX = NX+1
    H(X,T) = HELP(X,T)
    GO TO 6
  ELSE
    NT = NT+1
  END IF
ELSE
  NT = NT+1
  X = 0
  NX = 0
  GO TO 5
END IF

10  FORMAT (F12.2)
C
WRITE (200,30) NX
WRITE (200,40) NT
C
30  FORMAT ('The number of points along the profile, nx = ',I2)
40  FORMAT ('The number of profiles recorded, ',8X,'nt = ',I2)
C
C*****
C  Calculate the spatial and temporal
C  correlation matrices and the sum of
C  the diagonal elements of each matrix
C  which is equal to the sum of all the
C  eigenvalues and represents the total
C  mean square value of the data.
C*****
C
C
DO I = 1,NX
  DO J = 1,NX
    A(I,J) = 0.0
    DO T = 1,NT
      A(I,J) = A(I,J) + (H(I,T)*H(J,T))
    END DO
    A(I,J) = A(I,J)/(NX*NT)
    MA(I,J) = A(I,J)
  END DO
END DO
C
SUM = 0.0
DO I = 1,NX
  SUM = SUM + A(I,I)
END DO
WRITE (200,*)
WRITE (200,*)
WRITE (200,20) SUM
C
20  FORMAT ('The total mean square value of the data is ',F8.3)
C
C*****

```

```

DO I = 1,NT
  DO J = 1,NT
    B(I,J) = 0.0
    DO X = 1,NX
      B(I,J) = B(I,J) + (H(X,I)*H(X,J))
    END DO
    B(I,J) = B(I,J)/(NX*NT)
    MB(I,J) = B(I,J)
  END DO
END DO

```

C
C

C*****

C In order to calculate the eigenvalues
C and eigenvectors of the matrices
C the matrices are reduced to a
C tridiagonal form.

C*****

C
C

```

CALL TRED2(MA,NX,NP,DA,EA)
CALL TRED2(MB,NT,NP,DB,EB)

```

C
C

C*****

C Calculate the eigenvalues and eigen-
C vectors of matrices A and B by using
C the tridiagonal matrices, just generated
C and calculate for each eigenvalue the
C percentage of the mean square value of
C the data and the percentage of the largest
C eigenvalue representing the variance from
C the mean (beach) function.

C
C

C Write the 5 largest eigenvalues of the
C spatial correlation matrix to a file.
C (The eigenvalues of the temporal
C correlation matrix are the same). Write
C the corresponding eigenvectors to a file.

C*****

C

```

CALL TQLI(DA,EA,NX,NP,MA)

```

C
C

C*****

```

DO I = NX,NX-4,-1
  PERX(I) = (DA(I)/SUM)*100
  IF (I.NE.NX) THEN
    PARTX(I) = 100*PERX(I)/(100-PERX(NX))
  END IF
END DO

```

C
C

C*****

```

WRITE (200,*)
WRITE (200,50)

```

```

WRITE (200,*)
DO I = NX,NX-4,-1
  WRITE (200,*)
  WRITE (200,60) I,DA(I),PERX(I)
  IF (I.NE.NX) THEN
    WRITE (200,65) PARTX(I)
  END IF
END DO
C
C*****
C
DO I = NX,NX-4,-1
  WRITE (200,*)
  WRITE (200,80)
  WRITE (200,85) I,DA(I)
  WRITE (200,*)
  DO J = 1,NX
    WRITE (200,90) MA(J,I)
  END DO
END DO
C
C
C*****
C
CALL TQLI(DB,EB,NT,NP,MB)
C
C*****
C
DO I = NT,NT-4,-1
  PERT(I) = (DB(I)/SUM)*100
  IF (I.NE.NT) THEN
    PARTT(I) = 100*PERT(I)/(100-PERT(NT))
  END IF
END DO
C
C*****
C
DO I = NT,NT-4,-1
  WRITE (200,*)
  WRITE (200,80)
  WRITE (200,85) I,DB(I)
  WRITE (200,*)
  DO J = 1,NT
    WRITE (200,90) MB(J,I)
  END DO
END DO
C
C*****
C
50 FORMAT ('The eigenvalues of the spatial correlation matrix are:')
60 FORMAT ('Lambda(',I2,')',10X,'= ',F9.4,4X,F8.4,'%')
65 FORMAT ('Percentage of rest = ',13X,F6.2,'%')
70 FORMAT ('The eigenvalues of the temporal correlation matrix are:')
80 FORMAT ('The eigenvector corresponding to the')
85 FORMAT (I2,'th eigenvalue, lambda = ',F9.4,' is:')
90 FORMAT (F9.4)

```

END

C
C#####
C
C
C
C
C
C
C
C
C
C
C
C
C

SUBROUTINE TRED2(A,N,NP,D,E)

This subroutine reduces the matrices
to their tri-diagonal form.

```
REAL A,D,E
PARAMETER (NP = 50)
DIMENSION A(NP,NP),D(NP),E(NP)
IF (N.GT.1) THEN
  DO 18 I = N,2,-1
    L = I-1
    H = 0.
    SCALE = 0.
    IF (L.GT.1) THEN
      DO 11 K = 1,L
        SCALE = SCALE + ABS(A(I,K))
11      CONTINUE
      IF (SCALE.EQ.0.) THEN
        E(I) = A(I,L)
      ELSE
        DO 12 K = 1,L
          A(I,K) = A(I,K)/SCALE
          H = H+A(I,K)**2
12      CONTINUE
        F = A(I,L)
        G = -SIGN(SQRT(H),F)
        E(I) = SCALE*G
        H = H-F*G
        A(I,L) = F-G
        F = 0.
        DO 15 J = 1,L
          A(J,I) = A(I,J)/H
          G = 0.
          DO 13 K = 1,J
            G = G+A(J,K)*A(I,K)
13          CONTINUE
          IF (L.GT.J) THEN
            DO 14 K = J+1,L
              G = G+A(K,J)*A(I,K)
14            CONTINUE
          END IF
          E(J) = G/H
          F = F+E(J)*A(I,J)
15        CONTINUE
        HH = F/(H+H)
        DO 17 J = 1,L
          F = A(I,J)
          G = E(J)-HH*F
          E(J) = G
```

```

        DO 16 K = 1,J
          A(J,K) = A(J,K)-F*E(K)-G*A(I,K)
16      CONTINUE
17      CONTINUE
        END IF
        ELSE
          E(I) = A(I,L)
        END IF
        D(I) = H
18      CONTINUE
    END IF
    D(1) = 0.
    E(1) = 0.
    DO 23 I = 1,N
      L = I-1
      IF (D(I).NE.0.) THEN
        DO 21 J = 1,L
          G = 0.
          DO 19 K = 1,L
            G = G+A(I,K)*A(K,J)
19          CONTINUE
          DO 20 K = 1,L
            A(K,J) = A(K,J)-G*A(K,I)
20          CONTINUE
21          CONTINUE
        END IF
        D(I) = A(I,I)
        A(I,I) = 1.
        IF (L.GE.1) THEN
          DO 22 J = 1,L
            A(I,J) = 0
            A(J,I) = 0
22          CONTINUE
        END IF
23      CONTINUE
    RETURN
    END

```

C

C#####

C

 SUBROUTINE TQLI(D,E,N,NP,Z)

C

C*****

C This subroutine calculates the
C eigenvalues and the corresponding
C eigenvectors of the matrices.

C*****

C

 REAL D,E,Z
 PARAMETER (NP = 50)
 DIMENSION D(NP),E(NP),Z(NP,NP)

C

 IF (N.GT.1) THEN
 DO 11 I = 2,N
 E(I-1) = E(I)
11 CONTINUE

```

E (N) = 0
DO 15 L = 1,N
  ITER = 0
1  DO 12 M = L,N-1
    DD = ABS(D(M))+ABS(D(M+1))
    IF (ABS(E(M))+DD.EQ.DD) GO TO 2
12  CONTINUE
    M = N
2  IF (M.NE.L) THEN
    IF (ITER.EQ.30)PAUSE 'too many iterations'
    ITER = ITER+1
    G = (D(L+1)-D(L))/(2.*E(L))
    R = SQRT(G**2+1.)
    G = D(M)-D(L)+E(L)/(G+SIGN(R,G))
    S = 1.
    C = 1.
    P = 0.
    DO 14 I = M-1,L,-1
      F = S*E(I)
      B = C*E(I)
      IF (ABS(F).GE.ABS(G)) THEN
        C = G/F
        R = SQRT(C**2+1.)
        E(I+1) = F*R
        S = 1./R
        C = C*S
      ELSE
        S = F/G
        R = SQRT(S**2+1.)
        E(I+1) = G*R
        C = 1./R
        S = S*C
      END IF
      G = D(I+1)-P
      R = (D(I)-G)*S+2.*C*B
      P = S*R
      D(I+1) = G+P
      G = C*R-B
      DO 13 K = 1,N
        F = Z(K,I+1)
        Z(K,I+1) = S*Z(K,I)+C*F
        Z(K,I) = C*Z(K,I)-S*F
13      CONTINUE
14      CONTINUE
      D(L) = D(L)-P
      E(L) = G
      E(M) = 0
      GO TO 1
    END IF
15  CONTINUE
  END IF
  RETURN
END

```

The number of points along the profile, $n_x = 41$
 The number of profiles recorded, $n_t = 9$

The total mean square value of the data is 178.234

The eigenvalues of the spatial correlation matrix are:

Lambda(41)	=	177.7915	99.7520%
Lambda(40)	=	0.3056	0.1714%
Percentage of rest	=		69.11%
Lambda(39)	=	0.0701	0.0393%
Percentage of rest	=		15.85%
Lambda(38)	=	0.0235	0.0132%
Percentage of rest	=		5.32%
Lambda(37)	=	0.0136	0.0076%
Percentage of rest	=		3.08%

The spatial eigenvectors are:

e(41)	e(40)	e(39)	e(38)	e(37)
0.1706	0.1506	0.0476	0.0112	0.0087
0.1533	0.1507	0.0456	-0.0005	-0.0065
0.1382	0.1315	0.0254	-0.0013	0.0341
0.1293	0.1006	0.0364	0.0201	0.0081
0.1133	0.0854	0.0339	-0.0139	0.0031
0.1010	0.0285	-0.0287	0.0088	0.0168
0.0991	-0.2467	-0.0201	-0.0577	-0.0292
0.0983	-0.4504	0.0356	-0.0308	-0.0435
0.0781	-0.3753	0.0984	-0.0624	-0.0162
0.0480	-0.3273	0.0795	-0.0364	-0.0413
0.0246	-0.2642	0.0441	-0.0547	-0.0718
-0.0019	-0.1885	-0.0251	0.0225	-0.1504
-0.0298	-0.1010	-0.1078	0.0088	-0.2173
-0.0487	-0.0261	-0.0989	0.0320	-0.1327
-0.0745	0.0394	-0.6260	-0.2709	-0.1982
-0.0954	0.2527	-0.1442	-0.1794	0.0756
-0.0969	0.2010	-0.1129	-0.0152	0.0965
-0.0949	0.0861	0.0038	0.0037	0.1204
-0.0962	0.0650	0.0306	0.0957	0.0511
-0.1018	-0.0151	-0.0929	-0.2797	-0.0737
-0.1093	-0.0422	0.2175	0.0755	0.2741
-0.1137	0.0139	0.3083	-0.1762	-0.2237
-0.1236	-0.0483	-0.0774	0.1257	0.2216
-0.1374	0.0830	0.3958	-0.0788	-0.0807
-0.1408	0.0034	0.1313	0.1282	0.2892
-0.1535	0.1170	0.2235	0.2286	-0.6645

-0.1656	0.1704	0.3084	-0.3055	0.0614
-0.1744	0.1078	-0.1005	0.5316	-0.1506
-0.1797	0.0593	0.0820	-0.4980	-0.0624
-0.1915	0.0594	-0.1178	0.0278	-0.1471
-0.1912	0.0928	0.0523	-0.0185	-0.1155
-0.1996	-0.0083	-0.0242	0.0760	0.0789
-0.2047	0.0056	-0.0150	0.0369	0.0371
-0.2113	-0.0428	-0.0452	0.1373	0.1302
-0.2196	-0.0551	-0.0733	-0.0297	-0.0382
-0.2265	-0.1445	-0.0041	0.0141	-0.0204
-0.2315	-0.1363	-0.0160	0.0010	-0.0141
-0.2379	-0.1237	-0.0402	-0.0308	0.0772
-0.2469	-0.0772	-0.0608	0.0007	0.0700
-0.2614	-0.0536	0.0006	-0.0752	0.0765
-0.2701	-0.1544	-0.0209	0.0756	0.0979

The temporal eigenvectors are:

e(9)	e(8)	e(7)	e(6)	e(5)
-0.3141	0.6256	0.3310	-0.1431	-0.3016
-0.3194	0.4092	0.2442	0.5213	0.4618
-0.3247	0.2101	-0.1648	-0.5374	-0.2200
-0.3293	0.0591	-0.4278	-0.1818	0.0734
-0.3335	-0.0269	-0.4318	-0.0493	0.4002
-0.3372	-0.1222	-0.3208	0.3819	-0.1202
-0.3434	-0.2757	0.0673	0.3845	-0.6249
-0.3462	-0.3599	0.1356	-0.0906	0.0619
-0.3504	-0.4152	0.5553	-0.2857	0.2703

Appendix H

Data on measurement errors in wave height and period.

Variation in H/T due to differences between input data and recorded values								
Input	Recorded values.							
	1:10 sand	error (%)	1:21 sand	error (%)	1:14 anthr.	error (%)	1:30 sand	error (%)
0.083	0.084 0.085	2.00	0.083 0.081	-2.58	0.091 0.095	14.28		
0.100	0.089 0.089	-11.05	0.101 0.106	5.50	0.109 0.107	8.80		
0.125	0.135	8.16	0.137 0.137	9.92	0.147 0.146	17.44		
0.143	0.152 0.157	9.73	0.129 0.128	-10.36	0.149 0.146	3.92		
0.150	0.164 0.167	11.53	0.166 0.156	10.80	0.160 0.171	14.07		
0.167	0.192 0.194	16.58	0.178 0.181	8.82	0.189 0.191	14.78		
0.200	0.246 0.244	22.8	0.217 0.218	8.85	0.217	8.35		
0.214	0.241 0.237	12.27	0.194 0.197	-9.61	0.218 0.221	2.94		
0.250							0.240 0.265	-4.16 5.96
0.286	0.329 0.334	17.01	0.324 0.293	13.27	0.296 0.302	5.71		
0.300							0.278 0.281	-7.33
0.375							0.416 0.387	10.96
0.429							0.350 0.320	-25.24
0.450							0.460 0.464	3.02
0.643							0.5121 0.4752	-26.08
0.857							0.624 0.620	-27.66

Appendix I Porosity of the sediment.

Measurements of the porosity were performed, using a small container with a content of 2.24 litre. The results are presented in the following tables.

Sand BS 14/25		
Total volume (l)	Volume of water (l)	porosity (%)
2.24	0.881	39.3
2.24	0.831	37.1
2.24	0.891	39.8
average:		38.7

Sand BS 22/60		
Total volume (l)	Volume of water (l)	porosity (%)
2.24	0.853	37.3
2.24	0.832	37.1
2.24	0.831	37.1
average:		37.2

Anthracite Grade 3		
Total volume (l)	Volume of water (l)	porosity (%)
2.24	1.044	46.6
2.24	1.005	44.9
2.24	1.018	45.4
average:		45.6

